H. B. ROBINSON STEAM ELECTRIC PLANT, UNIT NO. 2

REQUEST FOR TECHNICAL
SPECIFICATIONS CHANGE REGARDING
STEAM GENERATOR ALTERNATE REPAIR CRITERIA

WCAP-16627-NP

Steam Generator Alternate Repair Criteria for Tube Portion Within the Tubesheet at H. B. Robinson Unit 2

August 2006

Non-Proprietary Version

WCAP-16627-NP

August 2006

Steam Generator Alternate Repair Criteria for
Tube Portion Within the Tubesheet at H.B. Robinson Unit 2

Westinghouse

WCAP-16627-NP

Steam Generator Alternate Repair Criteria for Tube Portion Within the Tubesheet at H.B. Robinson Unit 2

Gary Whiteman
Regulatory Compliance and Plant Licensing

August 2006

Reviewer: *_____

C. D. Cassino
Steam Generator Design and Analysis

Approved: *_____

Earl Morgan, Manager
Chemistry Diagnostics & Materials Engineering

Approved: *_____

Gordon Bischoff, Programs Manager
Power Water Reactor Owners Group

This work was performed under PWROG Project Number PA-MSC-0272

*Electronically Approved Records Are Authenticated In the Electronic Document Management System.

**Pressurized Water Reactor Owners Group
Member Participation* for PWROG Project PA-MSC-0272**

Utility Member	Plant Site(s)	Participant Yes	No
AmerenUE	Callaway (W)		X
American Electric Power	D.C. Cook 1& 2 (W)		X
Arizona Public Service	Palo Verde Unit 1, 2, & 3 (CE)		X
Constellation Energy Group	Calvert Cliffs 1 & 2 (CE)		X
Constellation Energy Group	Ginna (W)		X
Dominion Connecticut	Millstone 2 (CE)		X
Dominion Connecticut	Millstone 3 (W)	X	
Dominion Kewaunee	Kewaunee (W)		X
Dominion VA	Surry 1 & 2 (W)		X
Dominion VA	North Anna Unit 1 & 2 (W)		X
Duke Energy	Catawba 1 & 2, McGuire 1 & 2 (W)		X
Entergy Nuclear Northeast	Indian Point 2 & 3 (W)		X
Entergy Operations South	Arkansas 2, Waterford 3 (CE)		X
Exelon Generation Co. LLC	Braidwood 1 & 2, Byron 1 & 2 (W)		X
FirstEnergy Nuclear Operating Co	Beaver Valley 1 & 2 (W)		X
Florida Power & Light Group	St. Lucie 1 & 2 (CE)		X
Florida Power & Light Group	Turkey Point 3 & 4 (W)		X
Florida Power & Light Group	Seabrook (W)		X
Nuclear Management Company	Prairie Island 1 & 2, Point Beach 2 (W)		X
Nuclear Management Company	Point Beach 1 (W)	X	
Nuclear Management Company	Palisades (CE)		X
Omaha Public Power District	Fort Calhoun (CE)		X
Pacific Gas & Electric	Diablo Canyon 1 & 2 (W)		X
Progress Energy	H.B. Robinson (W)	X	
Progress Energy	Shearon Harris (W)		X
PSEG – Nuclear	Salem 1 (W)	X	
PSEG - Nuclear	Salem 2 (W)		X
Southern California Edison	SONGS 2 & 3 (CE)		X
South Carolina Electric & Gas	V.C. Summer (W)		X
South Texas Project Nuclear Operating Co.	South Texas Project 1 & 2 (W)		X
Southern Nuclear Operating Co.	Farley 1 & 2, Vogtle 1 & 2 (W)		X
Tennessee Valley Authority	Sequoyah 1 & 2, Watts Bar (W)		X
TXU Power	Comanche Peak 1 (W)		X
TXU Power	Comanche Peak Unit 2 (W)	X	
Wolf Creek Nuclear Operating Co.	Wolf Creek (W)		X

* Project participants as of the date the final deliverable was completed. On occasion, additional members will join a project. Please contact the PWROG Program Management Office to verify participation before sending this document to participants not listed above.

Pressurized Water Reactor Owners Group
International Member Participation* for PWROG Project PA-MSC-0272

Utility Member	Plant Site(s)	Participant Yes	Participant No
British Energy	Sizewell B		X
Electrabel (Belgian Utilities)	Doel 1, 2 & 4, Tihange 1 & 3		X
Kansai Electric Co., LTD	Mihama 1, Ohi 1 & 2, Takahama 1 (W)		X
Korea Hydro & Nuclear Power Corp.	Kori 3 & 4 Yonggwang 2 (W)		X
Korea Hydro & Nuclear Power Corp.	Kori 1, 2 Yonggwang 1 (W)	X	
Korea Hydro & Nuclear Power Corp.	Yonggwang 3, 4, 5 & 6 Ulchin 3, 4 & 5 (CE)		X
Nuklearna Electrarna KRSKO	Krsko (W)		X
Nordostschweizerische Kraftwerke AG (NOK)	Beznau 1 & 2 (W)		X
Ringhals AB	Ringhals 2, 3 & 4 (W)		X
Spanish Utilities	Asco 1 & 2, Vandellos 2, Almaraz 1 & 2 (W)		X
Taiwan Power Co.	Maanshan 1 & 2 (W)		X
Electricite de France	54 Units		X

* This is a list of participants in this project as of the date the final deliverable was completed. On occasion, additional members will join a project. Please contact the PWROG Program Management Office to verify participation before sending documents to participants not listed above.

TABLE OF CONTENTS

LIST OF TABLES

LIST OF FIGURES

1.0 EXECUTIVE SUMMARY

Nondestructive examination indications of primary water stress corrosion cracking were found in the Westinghouse Model D5 Alloy 600 thermally treated steam generator tubes at the Catawba 2 nuclear power plant in the fall of 2004. Most of the indications were located in the tube-to-tubesheet welds with a few of the indications being reported as extending into the parent tube. In addition, a small number of tubes were reported with indications about 3/4 inch above the bottom of the tube within a region referred to as the tack-expansion, and multiple indications were reported in one tube at internal bulge locations in the upper third of the tubesheet. The tube end weld indications were dominantly axial in orientation and almost all of the indications were concentrated in one steam generator. Circumferential cracks were also reported at internal bulge locations in two of the Alloy 600 thermally treated steam generator tubes at the Vogtle 1 plant site in the spring of 2005. Internal tube bulges within the tubesheet are created in a number of locations as an artifact of the manufacturing process. Based on interpretations of requirements published by the NRC staff in GL 2004-01 and IN 2005-9, Progress Energy requested that a recommendation be developed for future examinations of the tubesheet regions of the steam generator tubes at H.B. Robinson Unit 2. An evaluation was performed that considered the requirements of the ASME Code, Regulatory Guides, NRC Generic Letters, NRC Information Notices, the Code of Federal Regulations, NEI 97-06, and additional industry requirements. The conclusions of the technical evaluation are that:

1) the structural integrity of the primary-to-secondary pressure boundary is unaffected by tube degradation of any magnitude below a tube location-specific depth ranging from 4.78 to 8.34 inches depending on the tube leg and bundle zone being considered, designated as H*, and,

2) that the accident condition leak rate integrity can be bounded by a factor of 2 times the normal operation leak rate from degradation at or below a calculated distance of 8.01 in., designated as B*, from the top of the 21.81 inch thick tubesheet, including degradation of the tube end welds.

These results follow from analyses demonstrating that the tube-to-tubesheet hydraulic joints make it extremely unlikely that any operating or faulted condition loads are transmitted below the H* elevation, and the contact pressure dependent leak rate resistance increases below the B* elevation within the tubesheet. The possibility of degradation at such locations in the H.B. Robinson Unit 2 steam generator tubes exists based on the reported degradation at Catawba 2 and previously at Vogtle 1. The determination of the required engagement depth was based on results from finite element model structural analyses and a steam line break to normal operation comparative leak rate evaluation. It was also concluded that the evaluation of the conditions on the hot leg would always bound those for the cold leg with regard to leak rate performance. The cold leg requirements are greater than the hot leg requirements with regard to pullout resistance (the above numbers bound both). The structural length is slightly greater than that needed to restrict leak resistance to be the same during accident conditions at the center of the bundle. Application of the structural analysis and leak rate evaluation results to eliminate inspection and/or repair of tube indications in the region of the tube below the H* or B* elevation is interpreted to constitute a redefinition of the primary-to-secondary pressure boundary relative to the original design of the SG and requires the approval of the NRC staff through a license amendment. Using a maximum depth of 9.00 inches as the governing inspection length is sufficient to address all hot leg and cold leg considerations for both structural and leak rate integrity. This report also supports the implementation of a more

conservative 17" inspection length permanent alternate repair criteria for H.B. Robinson Unit 2 by providing responses to several NRC requests for additional information for another plant.

2.0 BACKGROUND

There has been extensive experience associated with the operation of SGs wherein it was believed, based on NDE, that throughwall tube indications were present within the tubesheet. The installation of the SG tubes usually involves the development of a short interference fit, referred to as the tack expansion, at the bottom of the tubesheet. The tack expansion was usually effected by a hard rolling process through October of 1979 and thereafter, in most instances, by the Poisson expansion of a urethane plug inserted into the tube end and compressed in the axial direction. The rolling process by its very nature is considered to be more intensive with regard to metalworking at the inside surface of the tube and would be expected to lead to higher residual surface stresses. A urethane expansion process was used during fabrication of the H.B. Robinson Unit 2 SGs. The tube-to-tubesheet weld was then performed to create the ASME Code pressure boundary between the tube and the tubesheet.[1]

The development of the F* alternate repair criterion (ARC) in 1985-1986 for tubes hard rolled into the tubesheet was prompted by the desire to account for the inherent strength of the tube-to-tubesheet joint away from the weld and to allow tubes with degradation within the tubesheet to remain in service, Reference 1. The result of the development activity was the demonstration that the tube-to-tubesheet weld was superfluous with regard to the structural and leakage integrity of the rolled joint between the tube and the tubesheet. Once the plants were in operation, the structural and leakage resistance requirements for the joints were based on the plant Technical Specifications, and a means of demonstrating joint integrity that was acceptable to the NRC staff was delineated in Reference 1. License amendments were sought and granted for several plants with hard rolled tube-to-tubesheet joints to omit the inspection of the tube below a depth of about 1.5 inches from the top of the tubesheet. Similar criteria, designated as W*, were developed for explosively expanded tube-to-tubesheet joints in Westinghouse designed SGs in the 1991-1992 timeframe, Reference 2. The W* criteria were first applied to operating SGs in 1999 based on a generic evaluation for Model 51 SGs, Reference 3, and the subsequent safety evaluation by the NRC staff, Reference 4. However, the required engagement length to meet structural and leakage requirements was on the order of 5.2 to 7 inches because an explosively expanded joint does not have the same level of residual interference fit as that of a rolled joint. It is noted that the length of joint necessary to meet the structural requirements is not the same as, and is frequently shorter than, that needed to meet the leakage integrity requirements.

The post-weld expansion of the tubes into the tubesheet in the H.B. Robinson Unit 2 SGs was effected by a hydraulic expansion of the tube instead of rolling or explosive expansion. The hydraulically formed joints do not exhibit the level of interference fit that is present in rolled or explosively expanded joints. However, when the thermal and internal pressure expansion of the tube is considered during normal operation and postulated accident conditions, appropriate conclusions regarding the need for the weld similar to those for the other two types of joint can be made. Evaluations were performed in 1996 of the effect of tube-to-tubesheet weld damage that occurred from an object in the bowl of a SG with tube-to-tubesheet joints similar to those in the H.B. Robinson Unit 2 SGs, on the structural and leakage integrity of the joint, Reference 5. It was concluded in that evaluation that the strength of the tube-to-tubesheet joint is sufficient to prevent pullout in accordance with the requirements of the performance criteria of

---

[1] The actual weld is between the Alloy 600 tube and weld buttering, a.k.a. cladding, on the bottom of the carbon steel tubesheet.

Reference 6 and that a significant number of tubes could be damaged without violating the performance criterion related to the primary-to-secondary leak rate during postulated accident conditions.

3.0 INTRODUCTION

Indications of cracking were reported based on the results from the nondestructive, eddy current examination of the steam generator (SG) tubes during the fall 2004 outage at the Catawba 2 nuclear power plant operated by the Duke Power Company, References 7, 8, and 9. The tube indications at Catawba were reported about 7.6 inches from the top of the tubesheet in one tube, and just above the tube-to-tubesheet welds in a region of the tube known as the tack expansion (TE) in several other tubes. Finally, indications were also reported in the tube-end welds (TEWs), also known as tube-to-tubesheet welds, joining the tube to the tubesheet. The spatial distribution by row and column number is shown on Figure 3-1 for SG A, Figure 3-2 for SG B, and Figure 3-3 for SG D at Catawba 2. There were no indications in SG C. The Catawba 2 plant has Westinghouse designed, Model D5 SGs fabricated with Alloy 600TT (thermally treated) tubes. Another plant with Westinghouse Model D5 steam generators, which belongs to another utility, has inspected 3% of the tubes in the hot leg of all steam generators from 3 inches above to 21 inches below the top of the tubesheet during 2R08 and has reported no indications. There is the potential for additional tube indications similar to those already reported at Catawba 2 within the tubesheet region to be reported during future inspections.

It was subsequently noted that an indication was reported in SG tubes at the Vogtle Unit 1 plant operated by the Southern Nuclear Operating Company (Reference 10). The Vogtle SGs are of the Westinghouse Model F design with slightly smaller, diameter and thickness, A600TT tubes.

> Note: No indications of this type were found during the planned inspections of the Braidwood 2 SG (Model D5 SGs) tubes in April 2005, a somewhat similar inspection of the tubes in two SGs at Wolf Creek (Model F SGs) in April 2005, or an inspection of the tubes at Comanche Peak 2 (Model D5 SGs) in the spring of 2005. Also, no indications of this type were found uring similar inspections at Byron 2 (Model D5 SGs) and Vogtle 2 (Model F SGs) in the fall of 2005.

The SGs for all four Model D5 plant sites were fabricated in the 1978 to 1980 timeframe using similar manufacturing processes with a few exceptions. For example, the fabrication technique used for the installation of the SG tubes at Braidwood 2 would be expected to lead to a much lower likelihood for crack-like indications to be present in the region known as the tack expansion relative to Catawba 2 because a lower stress urethane expansion process for effecting the tack expansions was adopted prior to the time of the fabrication of the Braidwood 2 SGs. The tack expansions in the steam generator tubes at H.B. Robinson Unit 2 were completed by a urethane expansion process as they were shipped in 1983.

The findings in the Catawba 2 and Vogtle 1 SG tubes present three distinct issues with regard to future inspections of A600TT SG tubes which have been hydraulically expanded into the tubesheet:

1) indications in internal bulges within the tubesheet,

2) indications at the elevation of the tack expansion transition, and

3) indications in the tube-to-tubesheet welds, including some extending into the tube.

The scope of this document is to:

a) address the applicable requirements, including the original design basis, Reference 11, and regulatory issues, Reference 12, and

b) provide analysis support for technical arguments to limit inspection of the tubesheet region to a distance of 9 inches below the top of the tubesheet below which degradation of any extent would not adversely affect SG performance criteria

These results follow from analyses demonstrating that the tube-to-tubesheet hydraulic joints make it extremely unlikely that any operating or faulted condition loads are transmitted below the H* elevation, and that the tube-to-tubesheet contact leak rate resistance increases below the B* elevation within the tubesheet. The determination of the required engagement depth was based on the use of finite element model structural analyses and of a bounding leak rate evaluation based on the change in contact pressure between the tube and the tubesheet between normal operation and postulated accident conditions. The results provide the technical rationale to eliminate inspection of the region of the tube below the H* or B* elevation. Such an approach is interpreted to constitute a redefinition of the primary-to-secondary pressure boundary relative to the original design of the SG and requires the approval of the NRC staff through a license amendment.

A similar type of Technical Specification change was approved, on a one-time basis, to limit inspections of the Wolf Creek Model F and Braidwood 2 Model D5 SGs during the spring 2005 inspection campaigns, for example see References 13 and 14 respectively. Subsequent approvals were also obtained for use at Byron 2 and Vogtle 2 for their fall 2005 inspection campaigns, Reference 15 for example for the latter. This report was prepared to justify the specialized probe, e.g., RPC (rotating probe coil), exclusion zone to the portion of the tube below specific elevations from the top of the tubesheet based on meeting the structural and leak rate performance criteria for both the hot and cold leg, and to provide the necessary information for a detailed NRC staff review of the technical basis for that request. The major difference between the current evaluation of the H.B. Robinson Unit 2 SGs and prior applications is the identification of an inspection length that is above the neutral plane instead of simply using an arbitrary, bounding value of 17 inches from the top of the tubesheet.

The H* values were determined to assure meeting the structural performance criteria for the operating SG tubes as delineated in NEI 97-06, Revision 2, Reference 6. The B* values were determined based on meeting the accident condition leak rate performance criteria. Compliance is based on demonstrating both structural and leakage integrity during normal operation and postulated accident conditions. The structural model was based on standard analysis techniques and finite element models as used for the original design of the SGs and documented in numerous submittals for the application of criteria to deal with tube indications within the tubesheet of other models of Westinghouse designed SGs with tube-to-tubesheet joints fabricated by other techniques, e.g., explosive expansion.

All full depth expanded tube-to-tubesheet joints in Westinghouse-designed SGs have a residual radial preload between the tube and the tubesheet. Early vintage SGs involved hard rolling which resulted in the largest magnitude of the residual interface pressure. Hard rolling was replaced by explosive expansion which resulted in a reduced magnitude of the residual interface pressure. Finally, hydraulic expansion replaced explosive expansion for the installation of SG tubes, resulting in a further reduction in the

residual interface pressure. In general, it was found that the leak rate through the joints in hard rolled tubes is insignificant. Subsequent testing demonstrated that the leak rate resistance of explosively expanded tubes was not as great as that of hard rolled tubes and prediction methods based on empirical data to support theoretical models were developed to deal with the potential for leakage. The same approach was followed to develop a prediction methodology for hydraulically expanded tubes. However, the model has been under review since its inception, with the intent of verifying its accuracy because it involved analytically combining the results from independent tests of leak rate through cracks with the leak rate through the tube-to-tubesheet crevice. The leak rate model associated with the initial development of H* to meet structural performance criteria is such a model; technical acceptance could be time consuming since it has not been previously reviewed by the NRC staff. An alternative approach, provided in this report, was developed for application at H.B. Robinson Unit 2 from engineering expectations of the relative leak rate between normal operation and postulated accident conditions based on a first principles engineering evaluation.

An executive summary, background and introduction discussion are provided in Sections 1.0, 2.0 and 3.0 of this report. A summary discussion is provided in Section 4.0. Section 5.0 addresses plant operating conditions at H.B. Robinson Unit 2. Section 6.0 discusses the tube pullout and leakage test programs that are applicable to the Model 44F SGs at H.B. Robinson Unit 2. A summary of the conclusions from the structural analysis of the joint is provided in Section 7.0. The leak rate analysis is provided in Section 8.0. A determination of the requisite inspection depth based on leak rate considerations is provided in Section 9.0. A review of the qualitative arguments used by the NRC Staff for the tube joint inspection length approved for other plants is discussed in Section 10.0. Finally, conclusions from the structural and leak rate evaluations are contained in Section 11.0 of this report.

SG - 2A   +Point Indications Within the Tubesheet

Catawba EOC13   DDP D5

E 1 INDICATION WITHIN 0.25" OF HOT
        LEG TUBE END

□ 66 PLUGGED TUBE
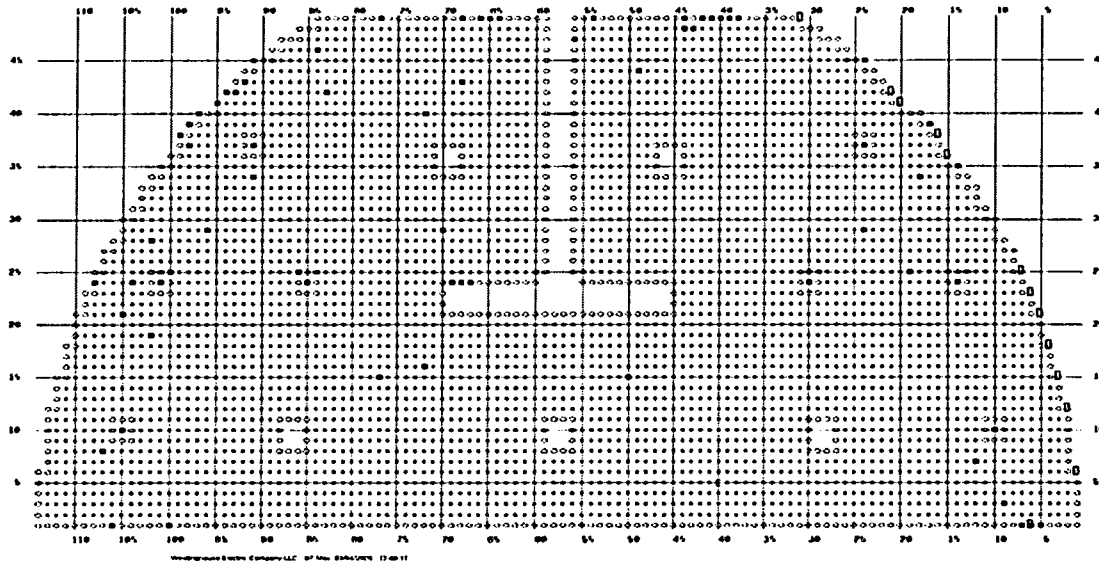
Figure 3-1. Distribution of Indications in SG A at Catawba 2

SG - 2B   +Point Indications Within the Tubesheet

Catawba EOC13   DDP D5

Z 1 MULTIPLE INDICATIONS AT
     APPROXIMATELY 7" BELOW HOT
     LEG TOP OF TUBESHEET

W 1 INDICATIONS WITHIN 0.25" AND
     BETWEEN 0.26" AND 0.80" OF
     HOT LEG TUBE END

B 0 INDICATION BETWEEN 0.26" AND
     0.80" OF HOT LEG TUBE END

E 192 INDICATION WITH 0.25" OF HOT
        LEG TUBE END
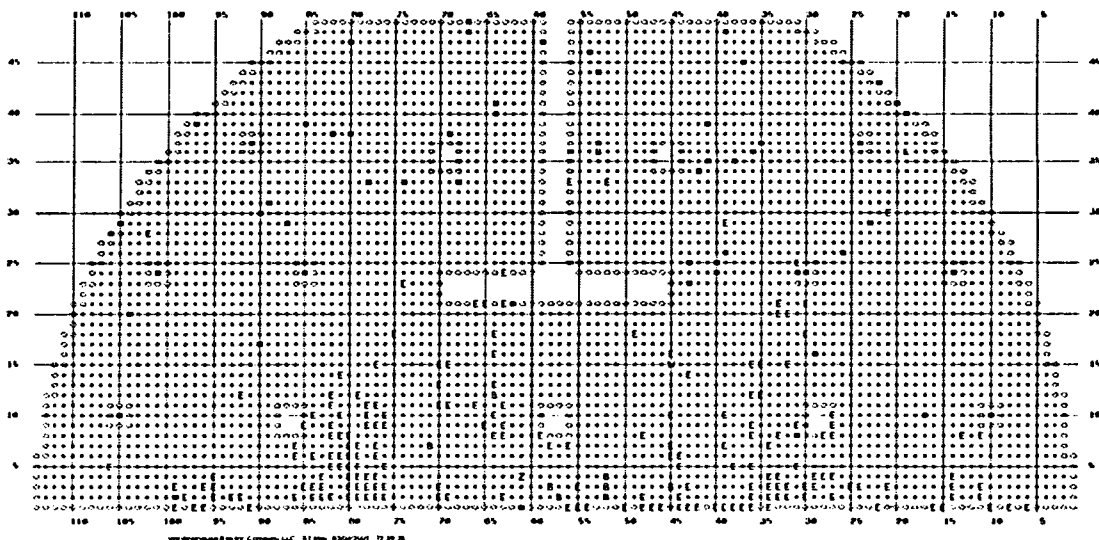
□ 68 PLUGGED TUBE

Figure 3-2. Distribution of Indications in SG B at Catawba 2

SG - 2D +Point Indications Within the Tubesheet

Catawba EOC13   DDP D5

E 7 INDICATION WITHIN 0.25" OF
   HOT LEG TUBE END

o 85 PLUGGED TUBE
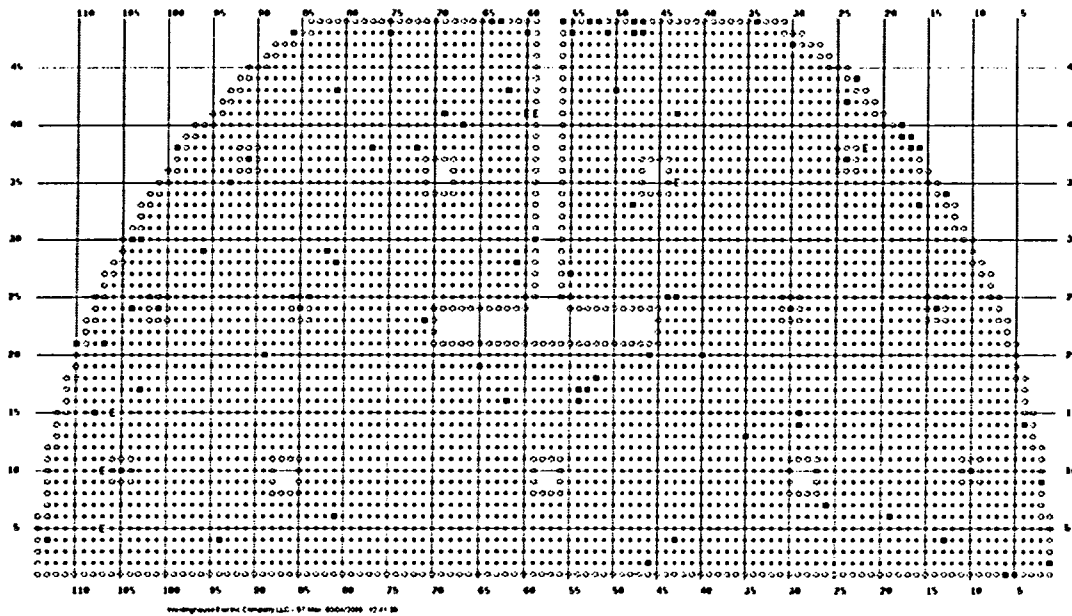
Figure 3-3. Distribution of Indications in SG D at Catawba 2

4.0   SUMMARY DISCUSSION

An evaluation has been performed that considered the requirements of the ASME Code, Regulatory Guides, NRC Generic Letters, NRC Information Notices, the Code of Federal Regulations, NEI 97-06, and additional industry requirements. The conclusion of the technical evaluation is that:

1)   the structural integrity of the primary-to-secondary pressure boundary is unaffected by tube degradation of any magnitude below a tube location-specific depth ranging from 4.78 to 8.34 inches, designated as H*, and,

2)   that the accident condition leak rate integrity can be bounded by twice the normal operation leak rate from degradation of any magnitude below 9 inches from the top of the nominally 21.81 inch thick tubesheet, including degradation of the tube end welds.

These results follow from analyses demonstrating that the tube-to-tubesheet hydraulic joints make it extremely unlikely that any operating or faulted condition loads that adversely impact structural integrity are transmitted below the H* elevation.

However, the leak rate during postulated accident conditions would be expected to be less than that during normal operation for indications near the bottom of the tubesheet (including indications in the tube end welds) based on the observation that while the driving pressure increases by about a factor of almost two, the flow resistance increases because the tube-to-tubesheet contact pressure also increases. Depending on the depth within the tubesheet, the relative increase in resistance could easily be larger than that of the pressure potential. Therefore, the leak rate under normal operating conditions could exceed its allowed value before the accident condition leak rate would be expected to exceed its allowed value. This approach is termed an application of the "bellwether principle." The evaluations were performed to specifically determine relative changes in the leak rate resistance as a function of tube location from the center of the tubesheet and degradation distance from the top of the tubesheet. The assessment envelopes postulated circumferential cracking of the tube or the tube-to-tubesheet weld that is 100% deep by 360° in extent because it is based on the premise that the tube and weld are not present below the analyzed elevations.

Based on the information summarized above, no inspection of the tube-to-tubesheet welds, tack roll region or bulges below the distance determined to have the potential for safety significance as specified in Reference 16, i.e., the H* depths, would be considered to be the minimum distance to be necessary to assure compliance with the structural requirements for the SGs. In addition, based on the results from consideration of application of the bellwether principle regarding potential leakage during postulated accident conditions, inspection depths as a function of tube location can be established using the results from these analyses but are not planned to be used by Progress Energy.

The length determined for structural compliance purposes may or may not bound the required length for leak rate compliance as discussed in Sections 8.0 and 9.0 of this report. For example, compare the results in Table 7-12 to those in Table 9-2. The application of the bellwether approach to the leak rate analysis as described in Section 8.1 of this report negates the need to consider specific leak rates because it relies only on the relative magnitude of the joint contact pressures between the tube and the tubesheet.

5.0 OPERATING CONDITIONS

H.B. Robinson Unit 2 is a three-loop nuclear power plant with Westinghouse designed and fabricated Model 44F SGs; there are 3214 tubes in each SG. The design of these SGs includes Alloy 600 thermally treated (A600TT) tubing, full-depth hydraulically expanded tubesheet joints, and broached hole quatrefoil tube support plates constructed of stainless steel.

5.1 BOUNDING OPERATING CONDITIONS

Values that bound the current H.B. Robinson Unit 2 SG thermal and hydraulic parameters during normal operation are tabulated below:

Parameter and Units		Bounding Operating Conditions [1,2]	MUR Operating Conditions [3]
Power – NSSS	MWt	2300	2339
Reactor Vessel Outlet Temperature	°F	604.5	604.1
Reactor Coolant System Pressure	psig	2235	2235
SG Steam Temperature	°F	518.2	521.4
SG Steam Pressure	psig	785	806.2
Steam Line Break Pressure	psig ·	2560	· 2560

(1) Reference 17

(2) For determining H*/B* Values, bounding normal operating conditions are generally lower steam pressure and lower primary/secondary side fluid temperature. However, the limiting condition for determining the maximum H* value for H.B. Robinson Unit 2 is the postulated SLB event.

(3) The plant operating conditions are defined in EC 47160, Rev. 3, NSSS and BOP Analysis to Support Appendix K Uprate, 3/31/2003

5.2 FAULTED CONDITIONS

In addition to the RG 1.121 criteria, it is necessary to satisfy the updated final safety analysis report (UFSAR) accident condition assumptions for primary-to-secondary leak rates. Calculated primary-to-secondary side leak rate during postulated events should: 1) not exceed the total charging pump capacity of the primary coolant system, and 2) be such that the off-site radiological dose consequences do not exceed Title 10 of the Code of Federal Regulations (10 CFR) Part 100 guidelines.

The accident condition primary-to-secondary leakage must be limited to acceptable values established by plant specific UFSAR evaluations. Pressure differentials associated with a postulated accident condition event can result in leakage from a throughwall crack through the interface between a hydraulically

expanded tube in the tubesheet and the tube hole surface. Therefore, a steam generator leakage evaluation for faulted conditions is provided in this report. The accidents that are affected by primary-to-secondary leakage are those that include, in the activity release and off-site dose calculation, modeling of leakage and secondary steam release to the environment. Steamline break (SLB) is the limiting condition; the reasons that the SLB is limiting are:

1) the SLB primary-to-secondary leak rate in the faulted loop is assumed to be greater than the operating leak rate because of the sustained increase in differential pressure, and

2) leakage in the faulted steam generator is assumed to be released directly to the environment.

For evaluating the radiological consequences due to a postulated SLB, the activity released from the affected SG (which is connected to the broken steam line) is released directly to the environment. The unaffected steam generators are assumed to continually discharge steam and entrained activity via the safety and relief valves up to the time when initiation of the RHR system can be accomplished. The radiological consequences evaluated, based on meteorological conditions, usually assume that all of this flow goes to the affected SG. With the analytically determined level of leakage, the resultant doses are expected to be within the guideline values of 10 CFR 50.67.

6.0 STEAM GENERATOR TUBE LEAKAGE AND PULLOUT TEST PROGRAM DISCUSSION

While the tube material and tube installation into the tubesheet technique are similar between the Westinghouse Model F and Model D5 SGs, there are also differences between the designs with regard to the tube size, thickness, number of tubes and tube pitch. Data are available with regard to pullout and leak rate testing for each of the SG geometries. The original testing of Reference 17 was performed to investigate postulated extreme effects on the tube-to-tubesheet weld from a loose part on the primary side of one Model F SG. These data were also used to support the model specific development of the required H* length and to characterize the leak rate from throughwall tube indications within the tubesheet as a function of the contact pressure between the tube and the tubesheet, e.g., Reference 19 was originally written for the Wolf Creek SGs. The testing also provides valuable information regarding the calculation of the 9 inch inspection length once a relative SLB to NOp leak rate has been identified. Pullout and leak rate data were also available from similar testing performed using Model D5 specific geometry, Reference 20. The data from both sets of testing programs were combined to support the development of the inspection criteria delineated in this report for Model 44F SGs.

- The results from strength tests were used to establish the joint lengths needed to meet the structural performance criteria during normal operation and postulated accident conditions, the required engagement length being designated as H*. The inherent strength of the joint coupled with the results from a finite element model of the loading conditions is used to calculate the required H* values for Model D5 and Model F SGs. The information is provided as a consistency check for the Model 44F SGs tube pullout results and to provide a discussion of the basis for the SLB leakage results.

- The results from leak rate tests were used to support the methodology to quantify the leak rate during postulated accident conditions as a function of the leak rate during normal operation. The required engagement length to meet a specific leak rate objective is 8.01 inches so that the leak rate expected during a postulated accident event is no more than twice that during normal operation.

Data from the test programs for the Model F SGs, Reference 21, directly supports the determination of both the H* and the 9 inch inspection length values for the SG tubes. The testing programs had two purposes:

1) To characterize the strength of the tube-to-tubesheet joints in Model F SGs during normal operation, e.g., 600°F, and under postulated accident conditions, and,

2) To characterize the leak resistance of the tube-to-tubesheet joints in Model F SGs during normal operation and under postulated accident conditions.

Similar testing was performed using specimens designed to simulate installed tubes in Model D5 SGs to develop parallel criteria for other plants. The independent testing programs that were conducted to characterize the joint strength and leak rate characteristics for Model F and Model D5 SGs are discussed separately in the following sections.

6.1 TUBE PULLOUT RESISTANCE PROGRAMS

The purpose of the tube pullout testing discussed below was to determine the resistance of the simulated Model F, D5 and 44F tube-to-tubesheet joints to pullout at temperatures ranging from [
]^{a,c,e}.

6.1.1 Model F Tube Pullout Test Program and Results

Mechanical loading, [

]^{a,c,e}. All of the test results are listed in Table 6-5.

[

]^{a,c,e}.

6.1.2 Model D5 Tube Pullout Test Program and Results

The Model D5 pullout test samples were fabricated with the same processes as used for the leakage tests, refer to Figure 6-5, and described later in this section. The tube expansion tool used in the program was a factory device, modified to achieve an expansion ranging of from three to seven inches.

Model D5 hydraulic expansion joints with nominal axial lengths of [
]^{a,c,e} The range of joints tested approximated the range of H* values expected for a plant with Model D5 SGs. Since the strength can be characterized as a resistance force per unit length, a strict correlation between laboratory specimen joint length and plant length is unnecessary.

Joint strength, based on the recorded load-deflection curve is typically taken as anywhere from the [

]^{a,c,e} Generally, but not always, the larger-deflection load value is greater than the knee value. In this program [
]^{a,c,e} was used to obtain the input information for calculation of the H* values for the plants (see Table 6-7). The pullout load from these plots simply provides one of the inputs used to calculate H*. The other variables include tubesheet bending (causing the tubesheet hole to dilate and/or contract depending on the distance of a certain point below the tubesheet top), the thermal growth mismatch effect (owing to the differential thermal growth between the Alloy 600TT tube and the carbon steel tubesheet and the "differential pressure tightening" of the tube within the tubesheet.

Mechanical loading, or pullout, tests on samples of the tube joints were run [

$]^{a,c,c}$

[

$]^{a,c,c}$

6.1.3   Model 44F Tube Pullout Test Program and Results

Mechanical loading (pullout) tests on samples of the tube joints were run on a mechanical testing machine, configured so that the tube could be pulled out of the simulated tubesheet (however, it is pulled through a limited range for testing purposes). In this test series, the testing was run with non-pressurized tubes. In some previous similar testing, pressurized tubes were also included in the test matrix. Typically the resistive force for the pressurized case is so high that the tube would yield and break rather than being able to obtain data on pullout forces. Therefore, for this test series, just the non-pressurized tubes were used.

Three tests were conducted at room temperature, three at 400°F, and three at 600°F. Each of the groupings of three tests consisted of one test with an engagement length of 3 inches, one at 5 inches, and one at 7 inches (all values nominal). Following expansion of the non-welded Alloy 600 tubes at a pressure of 31 ksi (expansions for the H.B. Robinson Unit 2 SGs were in the range of 31 to 34 ksi), the samples were subject to a high temperature soak to simulate the stress relief of the channel head –to-tubesheet weld. The specimens were then subjected to pull testing to determine the load required to effect a displacement of 0.25 inch of the tube in the tubesheet. The average force per inch required to produce a 0.25 inch displacement was 1172 lb per inch with a standard deviation of 558 lb per inch. Using the average value results in a calculated pullout force of 614 lb per inch. Refer to Reference 24 for data from several samples.

In the 600°F pullout tests, the lowest value for small displacement was 1310 lbs. The average small displacement load for these 600°F samples was 2044 lbs. The maximum load at 0.25 inch displacement for these three 600°F samples was 7687 lbs, the minimum load was 6248 lbs. The results are analyzed in Section 7.0 of this report.

6.2   LEAK RATE TESTING PROGRAMS

The purpose of the testing programs was to provide quantified data with which to determine the [

$]^{a,c,c}$ As discussed in detail in Section 8.0, the analytical model for the leak rate is referred to as the Darcy or Hagen-Poiseuille formulation. The volumetric flow is a function of the pressure potential, the inverse of the crevice length, the inverse of the

fluid viscosity, and the inverse of an resistance term characteristic of the geometry of the tube-to-tubesheet joint and referred to as the loss coefficient. Thus, the purpose of the testing programs is to obtain data with which to determine the loss coefficient. Data were available from leak rate test programs that independently addressed the Model F and the Model D5 tube-to-tubesheet joints:

    a. The Model F tube joint leakage resistance program involved tests at [

        $]^{a,c,e}$.

    b. The Model D5 tube joint leakage resistance program involved tests at [

        $]^{a,c,e}$.

The Model F program and results are described in Section 6.2.1, followed by the description and results of the Model D5 program in Section 6.2.4.

6.2.1 Model F Tube Joint Leakage Resistance Program

A total of [

$]^{a,c,e}$ The leakage resistance data were calculated for the test conditions listed in Table 6-1.

6.2.1.1 Model F Test Specimen Configuration

The intent of the test samples was to model key features of the Model F tube-to-tubesheet joint for [$]^{a,c,e}$. The following hardware was used:

A Model F tubesheet simulating collar which mimicked the radial stiffness of a Model F tubesheet unit cell with an outside diameter of approximately [$]^{a,c,e}$. The length of the test collars was [$]^{a,c,e}$ thickness of the steam generator tubesheet. This allowed for the introduction and collection of leakage in unexpanded sections of the tube, while retaining conservative or typical hydraulic expansion lengths. The collars were drilled to the nominal design value inside diameters with the surface finish based on drawing tolerances. In addition, the run-out tolerance for the collar drilling operation was held to within [$]^{a,c,e}$.

[

]^{a,c,e}.

Model F A600TT tubing with a yield strength approximately the same as that of the tubes in the operating plants, which ranges from [   ]^{a,c,e} was used. The tubing used was from a certified heat and lot conforming to ASME SB163, Section III Class 1 and was maintained in a Quality Systems-controlled storeroom prior to use.

The intent of the leakage portion of the test program was to determine the leakage resistance of simulated Model F tube-to-tubesheet joints, disregarding the effect of the tube-to-tubesheet weld and the [

]^{a,c,e}, see Figure 6-1. The welds were a feature of the test specimen design and made no contribution to the hydraulic resistance.

6.2.1.2 Model F Test Sample Assembly

The SG factory tube installation drawing specifies a [

]^{a,c,e}, to facilitate the tube weld to the cladding on the tubesheet face and it was omitted from the test. Following welding of the tube to the tubesheet, a full-length hydraulic expansion of the tube into the tubesheet is performed. The hydraulic expansion pressure range for the Model F SGs was approximately [   ]^{a,c,e} The majority of the test samples were expanded using a specified pressure of [   ]^{a,c,e} to conservatively bound the lower expansion pressure limit used for SG fabrication.

The tube expansion tool used in the factory consisted of a pair of seals, spaced by a tie rod between them. The hydraulically expanded zone was positioned relative to the lower surface of the tubesheet, overlapping the upper end of the tack expanded region. It extended to within a short distance of the upper surface of the tubesheet. This produced a hydraulically expanded length of approximately [

]^{a,c,e} inch nominal tubesheet thickness. The majority of the test specimens were fabricated using [

]^{a,c,e} Previous test programs which employed a segmented approach to expansion confirmed the expectation that uniform results from one segment to the next would result. This approach produced the desired expansion pressures for a conservative length of [   ]^{a,c,e} inch-expanded length being simulated. The remaining length of tube was expanded to the pressure at which the expansion bladder failed, usually between [   ]^{a,c,e}. These samples are described as "Segmented Expansion" types. A tube expansion schematic is shown on Figure 6-2.

Data were also available from a small group of the test samples that had been previously fabricated using a [   ]^{a,c,e} tool which had been fabricated expressly for such tests. These samples were described as "Full Depth Expansion" types. The expansion method with regard to the segmented or full length aspect does not have a bearing on the test results.

6.2.2   Model F Leakage Resistance Tests

The testing reported herein was performed according to a test procedure which outlined two types of leak tests as follows:

1) Model F elevated temperature primary-to-secondary leak tests were performed using an [

]^{a,c,e} These tests were performed following the room temperature primary-to-secondary side leak tests on the chosen samples. The test results showed a [

]$.^{a,c,e}$

Model F room temperature primary-to-secondary side leak tests were performed on all test samples, [

]$.^{a,c,e}$ These tests were performed following the elevated temperature primary-to-secondary side leak tests on the chosen samples.

6.2.2.1 Model F Leak Test Results

The leak tests on segmented expansion collars averaged [

]^{a,c,e}. (As a point of reference, there are approximately 75,000 drops in one gallon.)
Leakage data were also recorded at room temperature conditions to provide input for the low contact
pressure portion of the flow loss coefficient-versus-contact pressure correlation.

6.2.3 Model D5 Tube Joint Leakage Resistance Program

A total of [

]^{a,c,e}

The lower bound leakage resistance distribution for the collars with the nominal tubesheet hole diameter
was used in the present leakage evaluation. This lower bound leakage resistance was made using data for
the test conditions shown in Table 6-2 below combined with the Model F leak test results discussed in
Section 6.1.

6.2.3.1 Model D5 Test Specimen Configuration

The intent of the test samples was to model key features of the Model D5 tube-to-tubesheet joint for
[   ]^{a,c,e}. The following hardware was used:

A Model D5 tubesheet simulating collar matching the radial stiffness of a Model D5 tubesheet unit
cell, utilizing an appropriate outside diameter of approximately [

]^{a,c,e}.

Model D5 Tubing with an average yield strength for the SG Alloy 600 tubing in the Model D plants is
[   ]^{a,c,e}. The Alloy 600 tubing used for these tests was from heats conforming to ASME SB163,
Section III Class 1. It was obtained from a Quality Systems-controlled Storeroom.

The intent of the leakage portion of the test program was to determine the leakage resistance of simulated Model D5 tube-to-tubesheet joints, disregarding the effect of the [

]^{a,c,e}.

Tube-to-tubesheet stimulant samples of the Model D5 configuration were designed and fabricated. The steam generator factory tubing drawing specifies a [

]^{a,c,e}.

The hydraulic expansion pressure range for the Model D5 steam generators was [

]^{a,c,e}. This value conservatively bounds the lower expansion pressure limit used for the Model D5 steam generators. Refer to Figure 6-3 for the details of the configuration for the leak test. The test equipment consisted of a make-up tank (MUT), primary water autoclave (AC1) and a secondary autoclave (AC2) connected by insulated pressure tubing. Two specimens were installed into the secondary autoclave to minimize setup time and variability across test runs. AC1 was run with deoxygenated primary water containing specified amounts of boron, lithium and dissolved hydrogen. The primary chemistry conditions were controlled in the MUT and a pump and backpressure system allowed the primary water to re-circulate from the MUT to the AC1. The primary autoclave had the normal controls for heating, monitoring pressure and safety systems including rupture discs. Figure 6-4 shows the entire test system with key valves and pressure transducers identified. In addition to the normal controls for heating, monitoring pressure and maintaining safety, the secondary autoclave was outfitted water cooled condensers that converted any steam escaping from the specimens into room temperature water. The pressure in the secondary side (in the main body of AC2, was monitored by pressure transducers. For most tests, the leakage was collected in a graduated cylinder on a digital balance connected to a computer so that the amount of water could be recorded as a function of time. For some normal operating tests, the leakage was calculated based on changes in the secondary side pressure. All relevant autoclave temperatures and pressures were recorded with an automatic data acquisition system at regular time intervals.

6.2.3.2 Model D5 Test Sample Assembly

The assumption that pull-out resistance is distributed uniformly through the axial extent of the joint is an adequate technical approach. The pullout resistance is asymptotic to some large value, the form of the relation is one minus an exponential to a negative multiple of the length of engagement. For short engagement lengths, say up to 5 to 8 inches, the linear approximation is sufficient. Extrapolations to higher pullout resistance for longer lengths could be non-conservative except for the fact that the pullout strength of the shorter lengths exceeds the structural performance criteria.

6.2.4 Model D5 Leakage Resistance Tests

For the Model D5 testing, primary-to-secondary leak tests were performed on all test samples, using simulated primary water as a pressurizing medium. Refer to Figure 6-3. [

]^{a,c,e}

[

$]^{a,c,e}$, to simulate a perforation of the tube wall due to corrosion cracking. All of the elevated temperature primary-to-secondary side leak tests were performed using an [

$]^{a,c,e}$ as the pressurizing/leakage medium. In the case of 800 psid back pressure tests, the leakage was collected in the autoclave as it issued from the tube-to-collar crevice. In the remainder of the autoclave tests, the leakage was collected in the autoclave as it issued from the tube-to-collar crevice but it was piped to a condenser/cooler and weighed on an instrumented scale.

6.2.4.1 Model D5 Leak Test Results

The leakage rates for the Model D5 600°F normal operating and accident pressure differential conditions were similar to the respective Model F values. Leakage ranged from [

$]^{a,c,e}$. Leakage data were also recorded at room temperature conditions to provide input for the low contact pressure portion of the flow loss coefficient-versus-contact pressure correlation.

6.3   LOSS COEFFICIENT ON CONTACT PRESSURE REGRESSION

A logarithmic-linear (log-linear) regression and an uncertainty analysis were performed for the combined Model F and D5 SG data. Figure 6-6 provides a plot of the loss coefficient versus contact pressure with the linear regression trendline for the combined data represented as a thick, solid black line. The regression trendline is represented by the log-linear relation,

$$\ln(K) = b_0 + b_1 P_c \qquad (1)$$

where b_0 = the $\ln(K)$ intercept of the log-linear regression trendline, and,

b_1 = the slope of the log-linear regression trendline.

In conclusion, the log-linear fit to the combined Model F and Model D5 loss coefficient data follow a relation of the form,

$$K = e^{b_0 + b_1 P_c}, \qquad (2)$$

where the Model D5 data were adjusted to correspond to the diameter of an installed Model F tube. The absolute leak rates *per se* are not used in the determination the 17 inch inspection length and the confidence curve on the charts is provided for information only. Since the 17 inspection length criteria is

based on the ratio of the SLB leak rate to the NOp leak rate it is not significantly sensitive to changes in the correlation slope or intercept. No additional leakage testing was conducted for the Model 44F steam generators (see Section 9.2.1 of this report for further discussion).

Table 6-1. Model F Leak Test Program Matrix			a,c,e

*   The loss coefficient for leakage analyses is treated as an empirical parameter and is obtained by correlating the elevated temperature test data, which is representative of normal operation and accident conditions. The single set of room temperature data used at the low end of the contact pressure range conservatively extends the elevated temperature data to low contact pressure conditions.

Table 6-2. Model D5 Leak Test Program Matrix

a,c,e

Table 6-3. Model F Leak Rate Testing Data					a,c,e

Table 6-4. Model D5 Experimental Loss Coefficients					a,c,e

Table 6-4. Model D5 Experimental Loss Coefficients (Cont.)					a,c,e

Table 6-5. Model F 0.25 Inch Displacement Pullout Test Data							a,c,e

Table 6-6. Model F Small Displacement Data at 600°F				a,c,e

Table 6-7. Model D5 0.25 Inch Displacement Pullout Test Data									a,c,e

a,c,e

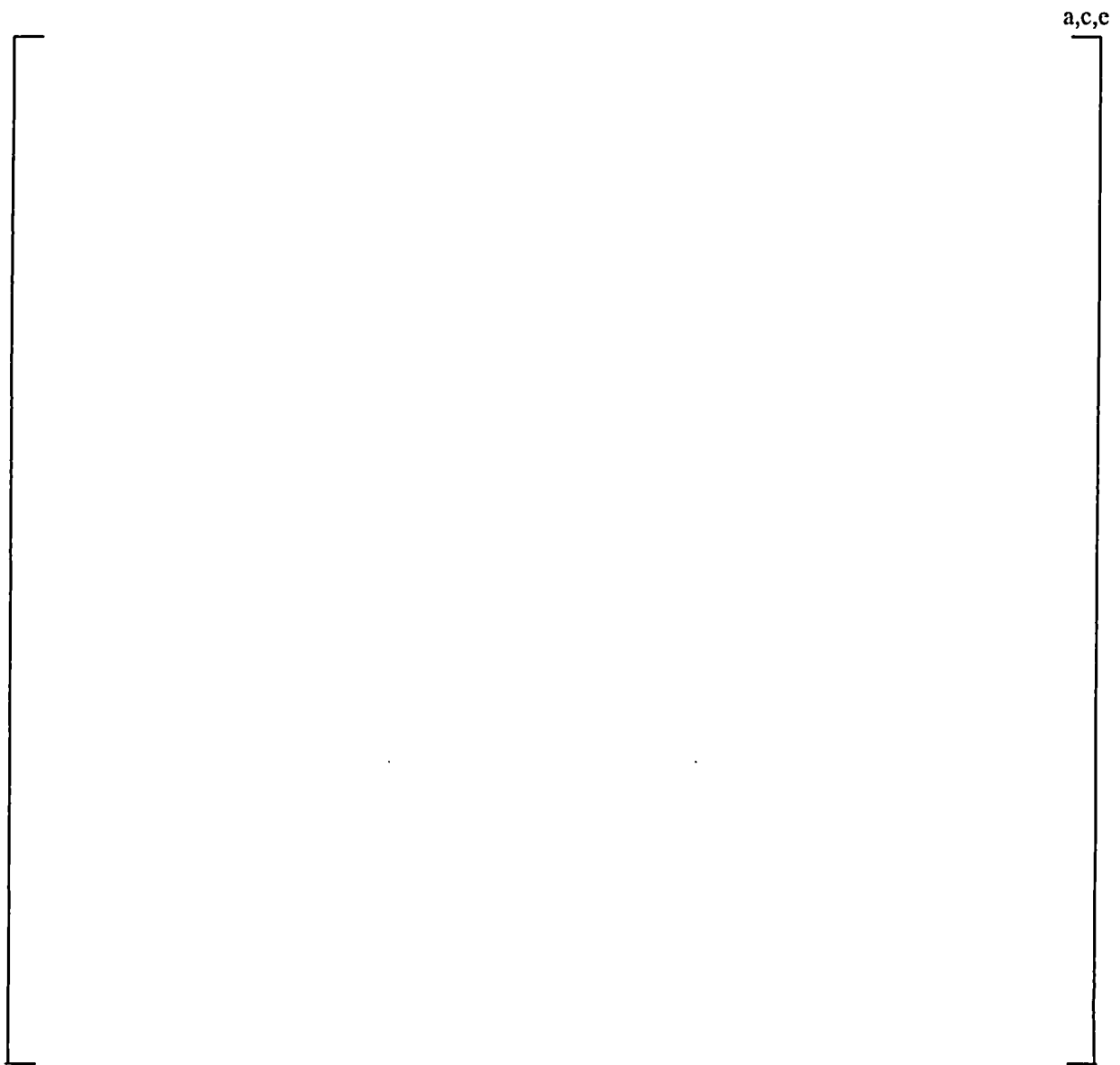Figure 6-1. Example Leakage Test Schematic

a,c,e
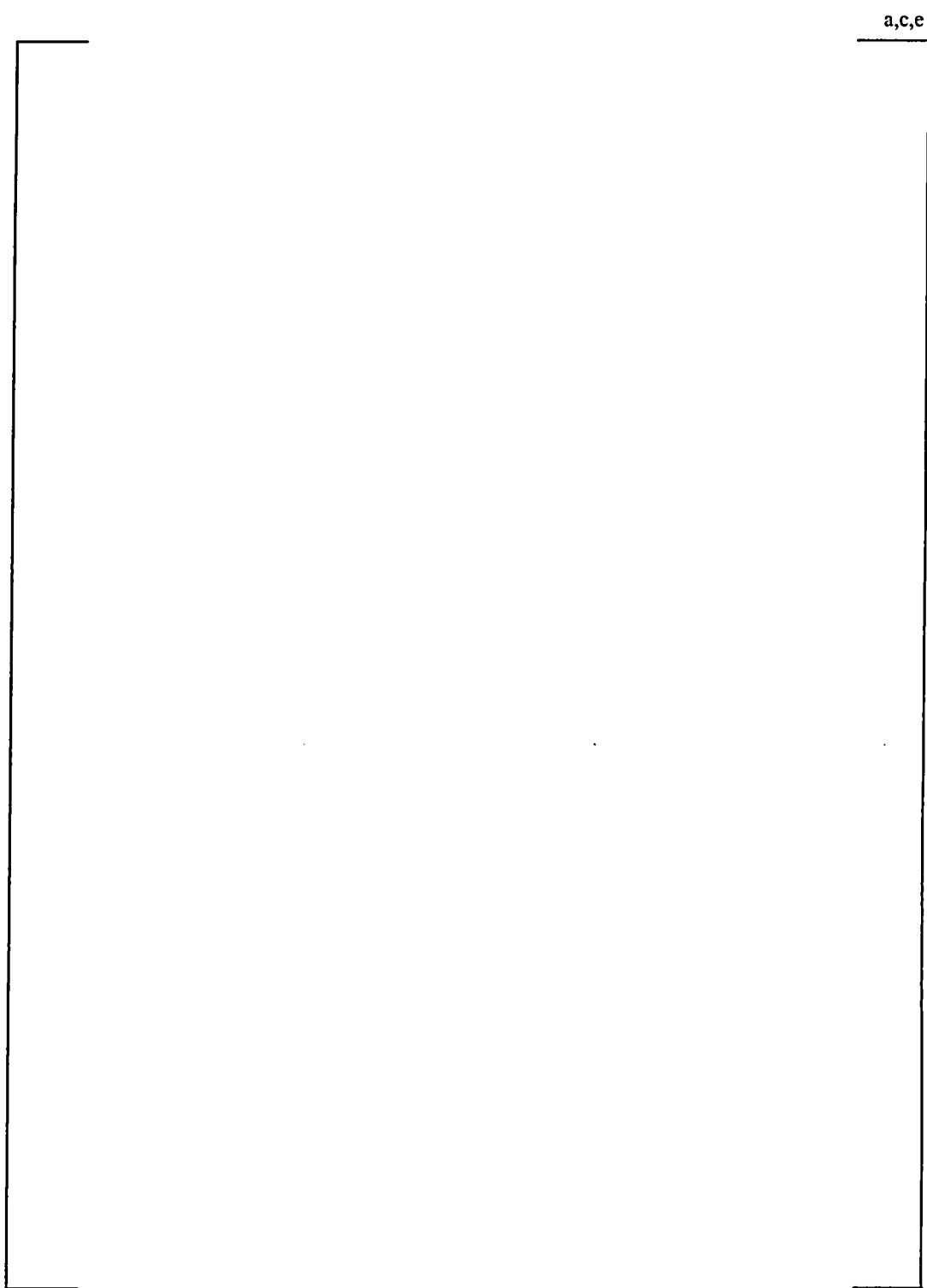
Figure 6-2. Example Tube Hydraulic Expansion Process Schematic

a,c,e
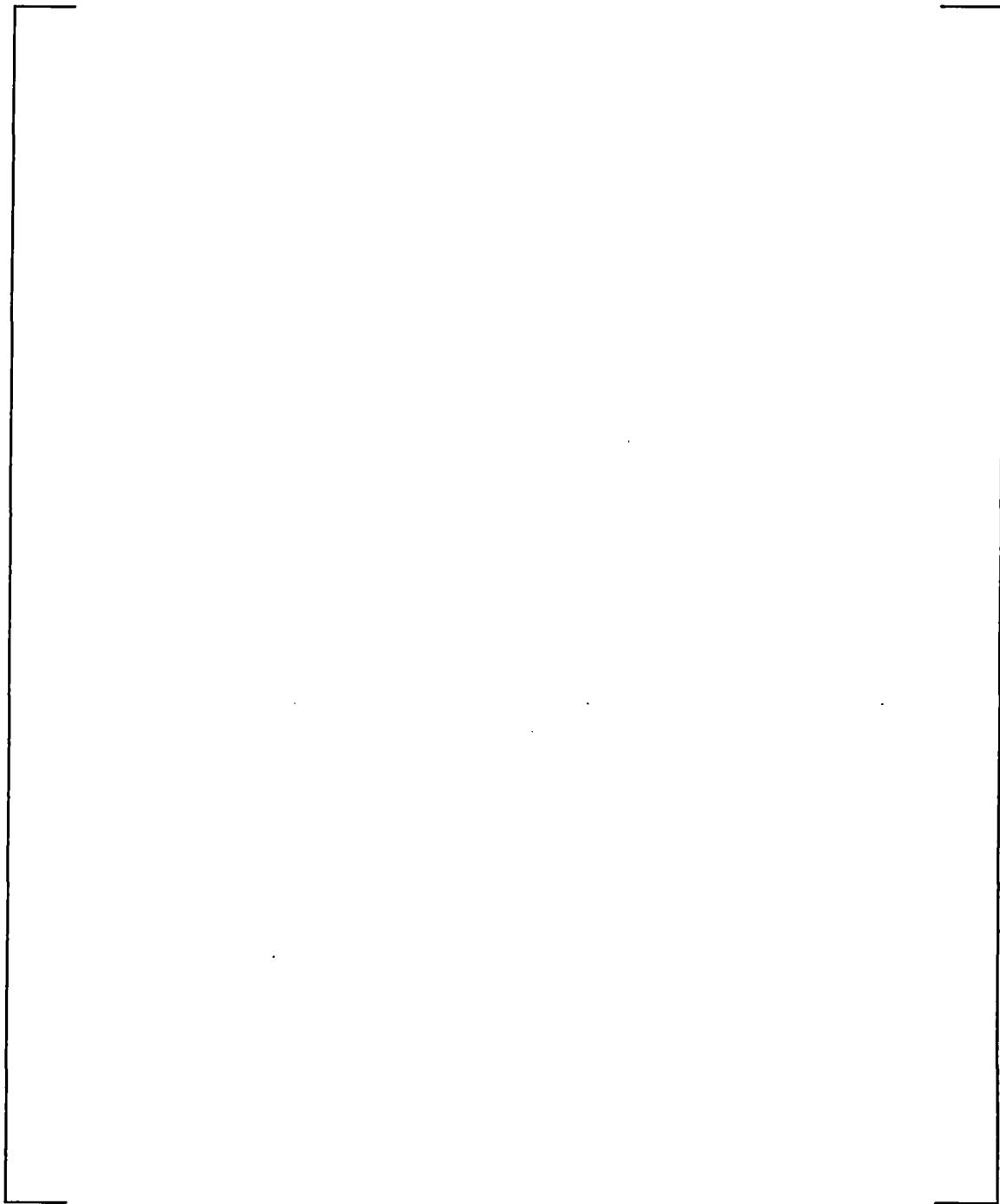
Figure 6-3. Example Tube Joint Leakage Test Configuration

a, c, e

Figure 6-4. Schematic for the Test Autoclave Systems for Leak Rate Testing

a,c,e
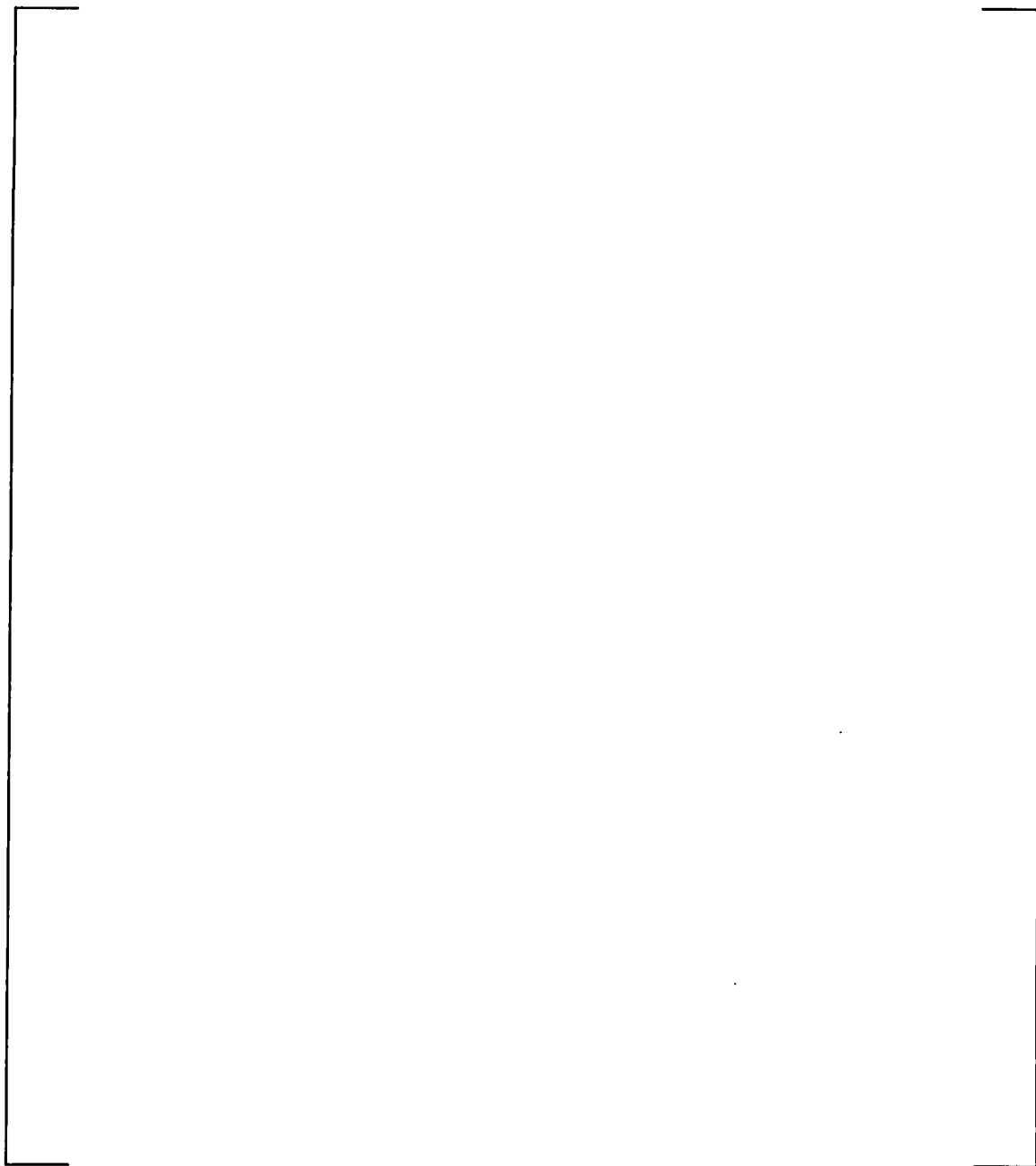
Figure 6-5. Example Tube Joint Sample Pullout Test Configuration

a,c,e

Figure 6-6. Loss Coefficient Values for Model F & D5 Leak Rate Analysis

7.0 STRUCTURAL ANALYSIS OF TUBE-TO-TUBESHEET JOINT

This section summarizes the structural aspects and analysis of the entire tube-to-tubesheet joint region. The tube end weld was originally designed as a pressure boundary structural element in accordance with the requirements of Section III of the ASME (American Society of Mechanical Engineers) Boiler and Pressure Vessel Code, Reference 11. The construction code for the H.B. Robinson Unit 2 replacement SGs was the 1965 edition with the Summer 1966 addenda. This means that there were no strength considerations made with regard to the expansion joint between the tube and the tubesheet, including the tack expansion regardless of whether it was achieved by rolling or Poisson expansion of a urethane plug.

An extensive empirical and analytical evaluation of the structural capability of the as-installed tube-to-tubesheet joints based on considering the weld to be absent was performed specifically for the H.B. Robinson Unit 2 Model 44F SGs and the results are reported below. Typical Model 44F hydraulic expansion joints with lengths comparable to those being proposed in what follows for limiting inspection examination requirements were tested for pullout resistance strength at temperatures ranging from 70 to 600°F. The results of the tests coupled with those from finite element evaluations of the effects of temperature and primary-to-secondary pressure on the tube-to-tubesheet interface loads have been used to demonstrate that engagement lengths of approximately 4.78 to 8.34 inches were sufficient to equilibrate the axial loads resulting from consideration of 3 times the normal operating and 1.4 times the limiting accident condition pressure differences. The variation in required engagement length is a function of tube location, i.e., row and column, and decreases away from the center of the SG where the maximum value applies. The tubesheet bows, i.e., deforms, upward from the primary-to-secondary pressure difference and results in the tube holes becoming dilated above the neutral plane of the tubesheet, which is slightly below the mid-plane because of the effect of the tensile membrane stress from the pressure loading. The amount of dilation is a maximum near the radial center of the tubesheet (restricted by the divider plate) and diminishes radially with increasing radius outward. Moreover, the tube-to-tubesheet joint becomes tighter below the neutral axis and is a maximum at the bottom of the tubesheet[1]. In conclusion, the need for the weld is obviated by the interference fit between the tube and the tubesheet. Axial loads are not transmitted to the portion of the tube below the H* distance during operation or faulted conditions, by factors of safety of at least 3 and 1.4 respectively. Inspection of the tube below the H* distance including the tube-to-tubesheet weld is not technically necessary. Also, if the expansion joint were not present, there would be no effect on the strength of the weld from axial cracks, and tubes with circumferential cracks up to about 180° by 100% deep would have sufficient strength to meet the nominal ASME Code structural requirements, based on the margins of safety reported in Reference 25.

An examination of Table 7-7 through 7-9 illustrates that the holding power of the tube-to-tubesheet joint at a depth of 9 inches below the top of the tubesheet. Note that the radii reported in these tables were picked to conservatively represent the entire radial zones of consideration as defined on Figure 7-1. For example, Zone C has a maximum radius of 23.2 inches, however, in order to establish an H* value that was conservative throughout the zone, the tube location for which the analysis results were reported, is at a radius of 3.73 inches. Likewise for tubes in Zone B under the heading 34.4 inches the basis for the calculation was a tube at a radius of 23.2 inches. The purpose of this discussion is to illustrate the conservatism associated with the holding power of the joint above the neutral surface of the tubesheet,

---

[1] There is a small reversal of the bending stress beyond a radius of about 50 inches because the support ring prevents rotation and the hole dilation is at the bottom of the tubesheet.

and to identify the proper tube radii for consideration. In the center of the tubesheet the cumulative holding strength in the 3.56 inch range from 5.44 to 9.00 inches below the top of the tubesheet is 3345.26 lbf during normal operation, which meets the performance criterion of 3.0 ΔP within the first 2.9 inch of engagement above 9 inches. The performance criterion for 1.4·SLB ΔP is met by the first 2.45 inch of engagement above 9 inches. At a radius of 45.5 inches the corresponding length of engagement needed is 2.01 inches above 9 inches.

7.1 EVALUATION OF TUBESHEET DEFLECTION EFFECTS FOR TUBE-TO-TUBESHEET CONTACT PRESSURE

A finite element model was developed for the Model 44F tubesheet, channel head, and shell region to determine the tubesheet hole dilations in the H.B. Robinson Unit 2 steam generators. [

]^{a,c,e} loads in the tube.

7.1.1 Material Properties and Tubesheet Equivalent Properties

The tubes in the H.B. Robinson Unit 2 SGs were fabricated of A600TT material. Summaries of the applicable mechanical and thermal properties for the tube material are provided in Table 7-1. The tubesheets were fabricated from SA-508, Class 2a, material for which the properties are listed in Table 7-2. The shell material is SA-533 Grade A Class 2, and its properties are in Table 7-3. Finally, the channel head material is SA-216 Grade WCC, and its properties are in Table 7-4. The material properties are from Reference 26, and match the properties listed in the ASME Code.

The perforated tubesheet in the Model 44F channel head assembly is treated as an equivalent solid plate in the global finite element analysis. An accurate model of the overall plate behavior was achieved by using the concept of an equivalent elastic material with anisotropic properties. For square tubesheet hole patterns, the equivalent material properties depend on the orientation of loading with respect to the symmetry axes of the pattern. An accurate approximation was developed (Reference 27), where energy principles were used to derive effective average isotropic elasticity matrix coefficients for the in-plane loading. The average isotropic stiffness formulation gives results that are consistent with those using the Minimum Potential Energy Theorem, and the elasticity problem thus becomes axisymmetric. The solution for strains is sufficiently accurate for design purposes, except in the case of very small ligament efficiencies, which are not of issue for the evaluation of the SG tubesheet.

The stress-strain relations for the axisymmetric perforated part of the tubesheet are given by:

$$\begin{bmatrix} \sigma_R^* \\ \sigma_0^* \\ \sigma_Z^* \\ \tau_{RZ}^* \end{bmatrix} = \begin{bmatrix} D_{11} & D_{12} & D_{13} & 0 \\ D_{21} & D_{22} & D_{23} & 0 \\ D_{31} & D_{32} & D_{33} & 0 \\ 0 & 0 & 0 & D_{44} \end{bmatrix} \begin{bmatrix} \varepsilon_R^* \\ \varepsilon_0^* \\ \varepsilon_Z^* \\ \gamma_{RZ}^* \end{bmatrix}$$

where the elasticity coefficients are calculated as:

$$D_{11} = D_{22} = \frac{\overline{E}_p^*}{f(1+\overline{v}_p^*)}\left[1 - \frac{\overline{E}_p^*}{E_z^*}v^2\right] + \frac{1}{2}\left[\overline{G}_p^* - \frac{\overline{E}_p^*}{2(1+\overline{v}_p^*)}\right]$$

$$D_{21} = D_{12} = \frac{\overline{E}_p^*}{f(1+\overline{v}_p^*)}\left[\overline{v}_p^* + \frac{\overline{E}_p^*}{E_z^*}v^2\right] - \frac{1}{2}\left[\overline{G}_p^* - \frac{\overline{E}_p^*}{2(1+\overline{v}_p^*)}\right]$$

$$D_{13} = D_{23} = D_{31} = D_{32} = \frac{\overline{E}_p^*v}{f}$$

$$D_{33} = \frac{E_z^*(1-\overline{v}_p^*)}{f} \text{ and } D_{44} = \overline{G}_z^*$$

$$\text{where } f = 1 - \overline{v}_p^* - 2\frac{\overline{E}_p^*}{E_z^*}v^2 \text{ and } \overline{G}_p^* = \frac{\overline{E}_d^*}{2(1+\overline{v}_d^*)}.$$

Here,

$\overline{E}_p^*$ = Effective elastic modulus for in-plane loading in the pitch direction,

E_z^* = Effective elastic modulus for loading in the thickness direction,

$\overline{v}_p^*$ = Effective Poisson's ratio for in-plane loading in the pitch direction,

$\overline{G}_p^*$ = Effective shear modulus for in-plane loading in the pitch direction,

$\overline{G}_z^*$ = Effective modulus for transverse shear loading,

$\overline{E}_d^*$ = Effective elastic modulus for in-plane loading in the diagonal direction,

$\overline{v}_d^*$ = Effective Poisson's ratio for in-plane loading in the diagonal direction, and,

v = Poisson's ratio for the solid material.

The tubesheet is a thick plate and the application of the pressure load results in a generalized plane strain condition. The pitch of the square, perforated hole pattern is 1.2344 inches and nominal hole diameters are 0.893 inch. The ID of the tube after expansion into the tubesheet is taken to be 0.794 inch based on an assumption of 1% thinning during installation. Equivalent properties of the tubesheet are calculated without taking credit for the stiffening effect of the tubes.

$$\text{Ligament Efficiency, } \eta = \frac{h_{nominal}}{P_{nominal}}$$

where: $h_{nominal}$ = $P_{nominal} - d_{maximum}$

$P_{nominal}$ = 1.2344 inches, the pitch of the square hole pattern

$d_{maximum}$ = .893 inches, the tube hole diameter

Therefore, $h_{nominal}$ = 0.3414 inches (1.2344-0.893), and η = 0.2766 when the tubes are not included. From Slot, Reference 28, the in-plane mechanical properties for Poisson's ratio of 0.3 are:

Property	Value
E*p/E	0.3945
v*p	0.1615
G*p/G	0.1627
E*z/E	0.5890
G*z/G	0.4137

where the subscripts p and d refer to the pitch and diagonal directions, respectively. These values are substituted into the expressions for the anisotropic elasticity coefficients given previously. In the global model, the X-axis corresponds to the radial direction, the Y-axis to the vertical or tubesheet thickness direction, and the Z-axis to the hoop direction. The directions assumed in the derivation of the elasticity coefficients were X- and Y-axes in the plane of the tubesheet and the Z-axis through the thickness. In addition, the order of the stress components in the WECAN/Plus (Reference 28) elements used for the global model is σ_{xx}, σ_{yy}, τ_{xy}, and σ_{zz}. The mapping between the Reference 27 equations and WECAN/+ is therefore:

Coordinate Mapping	
Reference 27	WECAN/+
1	1
2	4
3	2
4	3

Table 7-2 gives the modulus of elasticity, E, of the tubesheet material at various temperatures. Using the equivalent property ratios calculated above in the equations presented at the beginning of this section gives the elasticity coefficients for the equivalent solid plate model in the perforated region of the tubesheet. These elasticity coefficients are listed in Table 7-5 for the tubesheet, without accounting for the effect of the tubes. The values for 600°F were used for the finite element unit load runs. The material properties of the tubes are not utilized in the finite element model, but are listed in Table 7-1 for use in the calculations of the tube/tubesheet contact pressures.

7.1.2 Finite Element Model

The analysis of the contact pressures utilizes conventional (thick shell equations) and finite element analysis techniques. A finite element model was developed for the Model 44F SG channel head/tubesheet/shell region (which includes the H.B. Robinson Unit 2 steam generators) in order to determine the tubesheet rotations. The elements used for the models of the channel head/tubesheet/shell region were the quadratic version of the 2-D axisymmetric isoparametric elements STIF53 and STIF56 of WECAN/Plus (Reference 28). The model for the Model 44F steam generator is shown in Figure 7-2.

The unit loads applied to this model are listed below:

Unit Load	Magnitude
Primary Side Pressure	1000 psi
Secondary Side Pressure	1000 psi
Tubesheet Thermal Expansion	500°F
Shell Thermal Expansion	500°F
Channel Head Thermal Expansion	500°F

The three temperature loadings consist of applying a uniform thermal expansion to each of the three component members, one at a time, while the other two remain at ambient conditions. The boundary conditions imposed for all five cases are: UX=0 at all nodes on the centerline, and UY=0 at one node on the lower surface of the tubesheet support ring. In addition, an end cap load is applied to the top of the secondary side shell for the secondary side pressure unit load equal to:

$$P_{endcap} = -\left[\frac{(R_i)^2}{(R_o)^2 - (R_i)^2}\right]P = -7742.5 \text{ psi}^{\#}$$

[#]Negative sign denotes direction of load in WECAN/PLUS

where, R_i = Inside radius of secondary shell in finite element model = 60.845in.

R_o = Outside radius of secondary shell in finite element model = 64.655 in.

P = Secondary pressure unit load = 1000 psi.

This yielded displacements throughout the tubesheet for the unit loads.

7.1.3 Tubesheet Rotation Effects

Loads are imposed on the tube as a result of tubesheet rotations under pressure and temperature conditions. Previous calculations performed showed that the displacements at the center of the tubesheet when the divider plate is included are [

$]^{a,c,e}$.

The radial deflection at any point within the tubesheet is found by scaling and combining the unit load radial deflections at that location according to:

a,c,e

]

This expression is used to determine the radial deflections along a line of nodes at a constant axial elevation (e.g. top of the tubesheet) within the perforated area of the tubesheet. The expansion of a hole of diameter D in the tubesheet at a radius R is given by:

$$\left[\right]^{a,c,e}$$

UR is available directly from the finite element results. dUR/dR may be obtained by numerical differentiation.

The maximum expansion of a hole in the tubesheet is in either the radial or circumferential direction.
[

$$]^{a,c,e}$$

Where SF is a scale factor between zero and one. For the eccentricities typically encountered during tubesheet rotations, [   ]^{a,c,e}. These values are listed in the following table:

a,c,e	

The data were fit to the following polynomial equation:

[   ]^{a,c,e}

The hole expansion calculation as determined from the finite element results includes the effects of tubesheet rotations and deformations caused by the system pressures and temperatures. It does not include the local effects produced by the interactions between the tube and tubesheet hole. Standard thick shell equations, including accountability for the end cap axial loads in the tube (Reference 30), in combination with the hole expansions from above are used to calculate the contact pressures between the tube and the tubesheet.

The unrestrained radial expansion of the tube OD due to thermal expansion is calculated as:

$$\Delta R_t^{th} = c\,\alpha_t\,(T_t - 70)$$

and from pressure acting on the inside and outside of the tube as,

$$\Delta R_{to}^{pr} = \frac{P_i c}{E_t}\left[\frac{(2-v)b^2}{c^2 - b^2}\right] - \frac{P_o c}{E_t}\left[\frac{(1-2v)c^2 + (1+v)b^2}{c^2 - b^2}\right],$$

where: P_i = Internal primary side pressure, P_{pri} psi

P_o = External secondary side pressure, P_{sec} psi

b = Inside radius of tube = 0.397 in.

c = Outside radius of tube = 0.4465 in.

α_t = Coefficient of thermal expansion of tube, in/in/°F

E_t = Modulus of Elasticity of tube, psi

T_t = Temperature of tube, °F ,and,

v = Poisson's Ratio of the material.

The thermal expansion of the hole ID is included in the finite element results and does not have to be expressly considered in the algebra, however, the expansion of the hole ID produced by pressure is given by:

$$\Delta R_{TS}^{pr} = \frac{P_i c}{E_{TS}}\left[\frac{d^2 + c^2}{d^2 - c^2} + v\right],$$

where: E_{TS} = Modulus of Elasticity of tubesheet, psi

d = Outside radius of cylinder which provides the same radial stiffness as the tubesheet, that is, [   ]^{a,c,c}.

If the unrestrained expansion of the tube OD is greater than the expansion of the tubesheet hole, then the tube and the tubesheet are in contact. The inward radial displacement of the outside surface of the tube produced by the contact pressure is given by: (Note: The use of the term δ in this section is unrelated its potential use elsewhere in this report.)

$$\delta_t = \frac{P_2 c}{E_t}\left[\frac{c^2 + b^2}{c^2 - b^2} - v\right]$$

The radial displacement of the inside surface of the tubesheet hole produced by the contact pressure between the tube and hole is given by:

$$\delta_{TS} = \frac{P_2 c}{E_{TS}}\left[\frac{d^2 + c^2}{d^2 - c^2} + v\right]$$

The equation for the contact pressure P_2 is obtained from:

$$\delta_{to} + \delta_{TS} = \Delta R_{to} - \Delta R_{TS} - \Delta R_{ROT}$$

where ΔR_{ROT} is the hole expansion produced by tubesheet rotations obtained from finite element results. The ΔR's are:

$$\Delta R_{to} = c\alpha_t (T_t - 70) + \frac{P_{pri}c}{E_t}\left[\frac{(2-v)b^2}{c^2-b^2}\right] - \frac{P_{sec}c}{E_t}\left[\frac{(1-2v)c^2+(1+v)b^2}{c^2-b^2}\right]$$

$$\Delta R_{TS} = \frac{P_{sec}c}{E_{TS}}\left[\frac{d^2+c^2}{d^2-c^2}+v\right]$$

The resulting equation is:

$$\left[\qquad\qquad\qquad\qquad \right]^{a,c,e}$$

For a given set of primary and secondary side pressures and temperatures, the above equation is solved for selected elevations in the tubesheet to obtain the contact pressures between the tube and tubesheet as a function of radius. The elevations selected ranged from the top to the bottom of the tubesheet. Negative "contact pressure" indicates a gap condition.

The OD of the tubesheet cylinder is equal to that of the cylindrical (simulate) collars (2.25 inches) designed to provide the same radial stiffness as the tubesheet, which was determined from a finite element analysis of a section of the tubesheet (References 31 and 20).

The tube inside and outside radii within the tubesheet are obtained by assuming a nominal diameter for the hole in the tubesheet (0.893 inch) and wall thinning in the tube equal to the average of that measured during hydraulic expansion tests. The final wall thickness is 0.0495 inch for the tube. The following table lists the values used in the equations above, with the material properties evaluated at 600°F. (Note that the properties in the following sections are evaluated at the primary fluid temperature).

Thick Cylinder Equations Parameter	Value
b, inside tube radius, in.	0.397
c, outside tube radius, in.	0.4465
d, outside radius of cylinder w/ same radial stiffness as TS, in.	$[\quad]^{a,c,e}$
α_t, coefficient of thermal expansion of tube, in/in °F	$7.82 \cdot 10^{-6}$
E_t, modulus of elasticity of tube, psi	$28.7 \cdot 10^{6}$
α_{TS}, coefficient of thermal expansion of tubesheet, in/in °F	$7.42 \cdot 10^{-6}$
E_{TS}, modulus of elasticity of tubesheet, psi	$26.4 \cdot 10^{6}$

7.1.4 H.B. Robinson Unit 2 Contact Pressures

7.1.4.1 Bounding Operating Conditions

The loadings considered in the analysis are based on an umbrella set of conditions as defined in References 17 and 32. The current operating parameters from Reference 17 are used. The temperatures and pressures for normal operating conditions at H.B. Robinson Unit 2 are bracketed by the following case:

Loading	Bounding Operating Conditions (See Section 5.1)
Primary Pressure	2235 psig
Secondary Pressure	785 psig
Primary Fluid Temperature (T_{hot})	604.5°F
Secondary Fluid Temperature	518.2°F

The primary pressure [

]^{a,c,e}.

.

7.1.4.2 Faulted Conditions

Of the faulted conditions, Steamline Break (SLB) is the most limiting.

Previous analyses have shown that SLB is the limiting faulted condition, with tube lengths required to resist push out during a postulated loss of coolant accident (LOCA) typically less than one-fourth of the tube lengths required to resist pull out during SLB (References 30, 20 and 21). Therefore LOCA was not considered in this analysis.

7.1.4.3 Steam Line Break

As a result of SLB, the faulted SG will rapidly blow down to atmospheric pressure, resulting in a large ΔP across the tubes and tubesheet. The entire flow capacity of the auxiliary feedwater system would be delivered to the dry, hot shell side of the faulted SG. The primary side re-pressurizes to the pressurizer safety valve set pressure. The hot leg temperature decreases throughout the transient, reaching a minimum temperature of 212°F at approximately 2000 seconds for three loop plants. The pertinent parameters are listed below. The combination of parameters yielding the most limiting results is used.

Primary Pressure	=	2560 psig
Secondary Pressure	=	0 psig
Primary Fluid Temperature (T_{hot})	=	212°F
Secondary Fluid Temperature	=	212°F

For this set of primary and secondary side pressures and temperatures, the equations derived in Section 7.2 below are solved for the selected elevations in the tubesheet to obtain the contact pressures between the tube and tubesheet as a function of tubesheet radius for the hot leg.

7.1.4.4 Summary of FEA Results for Tube-to-Tubesheet Contact Pressures

For H.B. Robinson Unit 2, the contact pressures between the tube and tubesheet for various plant conditions are listed in Table 7-6 and plotted versus radius on Figure 7-3 through Figure 7-5. The application of these values to the determination of the required engagement length is discussed in Section 7.2.

7.2 DETERMINATION OF REQUIRED ENGAGEMENT LENGTH OF THE TUBE IN THE TUBESHEET

The elimination of a portion of the tube (i.e., a portion of the pressure boundary) within the tubesheet from the in-service inspection requirement constitutes a change in the pressure boundary. The required length of engagement of the tube in the tubesheet to resist performance criteria tube end cap loads is designated by the variable H*. This length is based on structural requirements only and does not include any connotation associated with leak rate, except perhaps in a supporting role with regard to the leak rate expectations relative to normal operating conditions. The contact pressure is used for estimating the magnitude of the anchorage of the tube in the tubesheet over the H* length.

To take advantage of the tube-to-tubesheet joint anchorage, it is necessary to demonstrate that the [

]. ^{a,c,e}

The end cap loads for Normal and Faulted conditions are:

Normal (maximum): $\pi \cdot (2235\text{-}785) \cdot (0.893)^2 /4 = 908$ lbs.

Faulted (SLB): $\pi \cdot 2560 \cdot (0.893)^2 /4 = 1603$ lbs.

Seismic loads have also been considered, but they are not significant in the tube joint region of the tubes.

A key element in estimating the strength of the tube-to-tubesheet joint during operation or postulated accident conditions is the residual strength of the joint stemming from the expansion preload due to the manufacturing process, i.e., hydraulic expansion. During operation the preload increases because the thermal expansion of the tube is greater than that of the tubesheet and because a portion of the internal pressure in the tube is transmitted to the interface between the tube and the tubesheet. However, the tubesheet bows upward leading to a dilation of the tubesheet holes at the top of the tubesheet and a contraction at the bottom of the tubesheet when the primary-to-secondary pressure difference is positive. The dilation of the holes acts to reduce the contact pressure between the tubes and the tubesheet. The H*

lengths are based on the pullout resistance associated with the net contact pressure during normal or accident conditions. The calculation of the residual strength involves a conservative approximation that the strength is uniformly distributed along the entire length of the tube. This leads to a lower bound estimate of the strength and relegates the contribution of the preload to having a second order effect on the determination of H*.

A series of tests were performed to determine the residual strength of the joint. The data from this series of pullout tests are listed in Reference 24 and in Table 7-10. Three (3) each of the tests were performed at room temperature, 400°F, and 600°F. [

]^{a,c,e}

[

$]^{a,c,e}$

The force resisting pullout acting on a length of a tube between elevations h_1 and h_2 is given by:

$$F_i = (h_2 - h_1)F_{HE} + \mu\pi d \int_{h_1}^{h_2} P dh$$

where: F_{HE} = Resistance to pull out due to the initial hydraulic expansion = 614.18 lb/inch,

P = Contact pressure acting over the incremental length segment dh, and,

μ_f = Coefficient of friction between the tube and tubesheet, conservatively assumed to be 0.2 for the pullout analysis to determine H*.

The contact pressure is assumed to vary linearly between adjacent elevations in the top part of Table 7-7 through Table 7-9, so that between elevations L1 and L2,

$$P = P_1 + \frac{(P_2 - P_1)}{(L_2 - L_1)}(h - L_1)$$

or,

$$\left[\qquad\qquad\qquad\qquad \right]^{a,c,e}$$

so that,

$$\left[\qquad\qquad\qquad\qquad \right]^{a,c,e}$$

where u_f is the coefficient of friction. This equation was used to accumulate the force resisting pullout from the top of the tubesheet to each of the elevations listed in the lower parts of Table 7-7 through Table 7-9. The above equation is also used to find the minimum contact lengths needed to meet the pullout force requirements. In Zone C (See Figure 7-1), the length calculated was 7.07 inches for the 3 times the normal operating pressure performance criterion which corresponds to a pullout force of 2724 lbf in the Cold Leg .

The top part Table 7-9 lists the contact pressures through the thickness at each of the radial sections for Faulted (SLB) condition. The last row, "h(0)," of this part of the table lists the maximum tubesheet elevation at which the contact pressure is greater than or equal to zero. The above equation is used to calculate the force resisting pull out from the top of the tubesheet for each of the elevations listed in the lower part of Table 7-9. In Zone C, this length is 8.04 inches for the 1.4 times the accident pressure performance criterion which corresponds to a pullout force of 2245 lbs in the Hot Leg for the Faulted

(SLB) condition. The H* calculations for each loading condition at each of the radii considered are summarized in Reference 26. The H* results for each zone are summarized in Table 7-12.

Therefore, the bounding condition for the determination of the H* length is the SLB performance criterion for Zones A, B and C. The minimum contact length for the SLB faulted condition is 8.04 inches in Zone C. In Zone B, the minimum contact length is 6.82 inches. In Zone A, the minimum contact length is calculated to be 4.48 inches.

7.3 NDE UNCERTAINTY DISCUSSION

Application of alternate repair criteria for axial and circumferential cracks requires that a provision be made in the engineering evaluations for the uncertainties inherent in the measurement of NDE parameters. For H* these include the distance between the BET and the uppermost crack tip and the H* length. The following uncertainties are considered in the determination of the proposed inspection length and are based on a study conducted for determining similar parameters in the development of a W* criteria for several other plants (Reference 3):

Measurement	Plus Point Probe (300 kHz) Uncertainty (Inches)	
	Measurement Uncertainty	Applied Error
BET- Flaw Tip	0.00 ± 0.17	0.28
H* Length	-0.11 ± 0.14	0.12

The BET-to-crack-tip uncertainty is used to decrease the distance between the BET and the upper most crack tip below the BET. The applied error value of 0.28 inch assures a one-sided 95% upper bound on the actual distance and the net sum of the average error plus 1.65 times the standard deviation.

The H* length of uncertainty of 0.12 inch is applied directly to the H* value.

Table 7-1. Summary of Material Properties Alloy 600 Tube Material							
Property	Temperature (°F)						
	70	200	300	400	500	600	700
Young's Modulus (psi·10^6)	31.00	30.20	29.90	29.50	29.00	28.70	28.20
Thermal Expansion (in/in/°F·10^{-6})	6.90	7.20	7.40	7.57	7.70	7.82	7.94
Density (lb-sec^2/in^4·10^{-4})	7.94	7.92	7.90	7.89	7.87	7.85	7.83
Thermal Conductivity (Btu/sec-in-°F·10^{-4})	2.01	2.11	2.22	2.34	2.45	2.57	2.68
Specific Heat (Btu-in/lb-sec^2-°F)	41.2	42.6	43.9	44.9	45.6	47.0	47.9

Table 7-2. Summary of Material Properties for SA-508 Class 2a Tubesheet Material							
Property	Temperature (°F)						
	70	200	300	400	500	600	700
Young's Modulus (psi·10^6)	29.20	28.50	28.00	27.40	27.00	26.40	25.30
Thermal Expansion (in/in/°F·10^{-6})	6.50	6.67	6.87	7.07	7.25	7.42	7.59
Density (lb-sec^2/in^4·10^{-4})	7.32	7.30	7.29	7.27	7.26	7.24	7.22
Thermal Conductivity (Btu/sec-in-°F·10^{-4})	5.49	5.56	5.53	5.46	5.35	5.19	5.02
Specific Heat (Btu-in/lb-sec^2-°F)	41.9	44.5	46.8	48.8	50.8	52.8	55.1

Table 7-3. Summary of Material Properties SA-533 Grade A Class 2 Shell Material							
Property	Temperature (°F)						
	70	200	300	400	500	600	700
Young's Modulus (psi·10^6)	29.20	28.50	28.00	27.40	27.00	26.40	25.30
Thermal Expansion (in/in/°F·10^{-6})	7.06	7.25	7.43	7.58	7.70	7.83	7.94
Density (lb-sec^2/in^4·10^{-4})	7.32	7.30	7.283	7.265	7.248	7.23	7.211

Table 7-4. Summary of Material Properties SA-216 Grade WCC Channelhead Material							
Property	Temperature (°F)						
	70	200	300	400	500	600	700
Young's Modulus (psi·10^6)	29.50	28.80	28.30	27.70	27.30	26.70	25.50
Thermal Expansion (in/in/°F·10^{-6})	5.53	5.89	6.26	6.61	6.91	7.17	7.41
Density (lb-sec²/in⁴·10^{-4})	7.32	7.30	7.29	7.27	7.26	7.24	7.22

Table 7-5. Equivalent Solid Plate Elasticity Coefficients for 44F Perforated TS
SA-508 Class 2a Tubesheet Material (psi)

a,c,e

Table 7-6. Tube/Tubesheet Maximum & Minimum Contact Pressures & H*
for H.B. Robinson Unit 2 Steam Generators

a,c,e

Table 7-7. Cumulative Forces Resisting Pull Out from the TTS H.B. Robinson Unit 2
Hot Leg Normal Conditions

a,c,e

Table 7-8. Cumulative Forces Resisting Pull Out from the TTS H.B. Robinson Unit 2
Cold Leg Normal Conditions

a,c,e

Table 7-9. Cumulative Forces Resisting Pull Out from the TTS H.B. Robinson Unit 2
Faulted (SLB) Conditions (Applies to Hot Leg and Cold Leg)

a,c,e

Table 7-10. 0.25 Inch Displacement Pullout Test Data

a,c,e

Table 7-11. Summary of H* Calculations for H.B. Robinson Unit 2

a,c,e

Table 7-12. H* Summary Table		
Zone	Limiting Loading Condition	Engagement from TTS (inches)
		Hot and Cold Leg
A	1.4 SLB ΔP	4.78 [2]
B	1.4 SLB ΔP	7.12 [2]
C	1.4 SLB ΔP	8.34 [2]

Notes:
1. Seismic loads have been considered and are not significant in the tube joint region (Reference 25).
2. 0.3 inches is conservatively added to the maximum calculated H* for Zones A, B and C to account for the uncertainty in the location of the hydraulic expansion transition from the top of the tubesheet.

a,c,e

Figure 7-1. Definition of H* Zones (Reference 36)

a.c.e

Figure 7-2. Finite Element Model of Model 44F Tubesheet Region
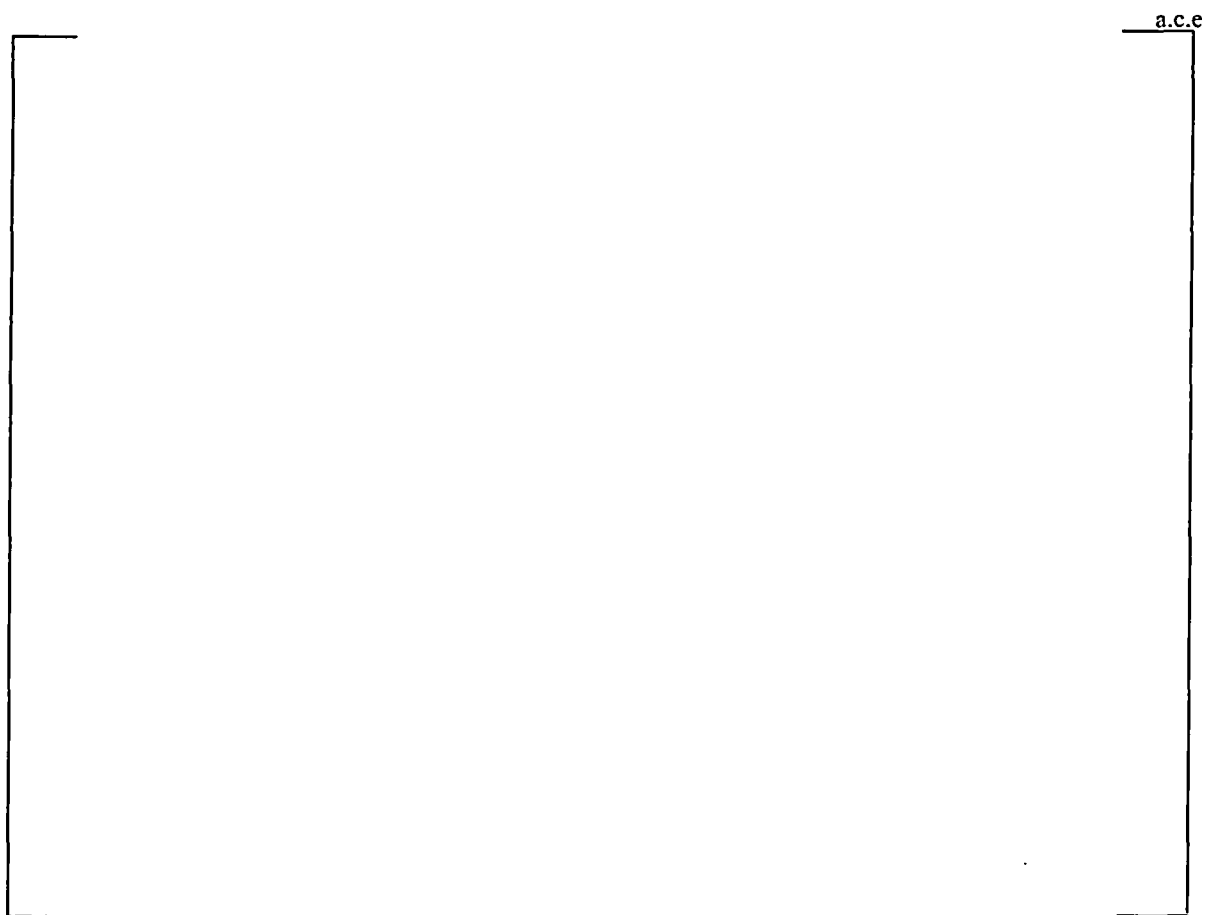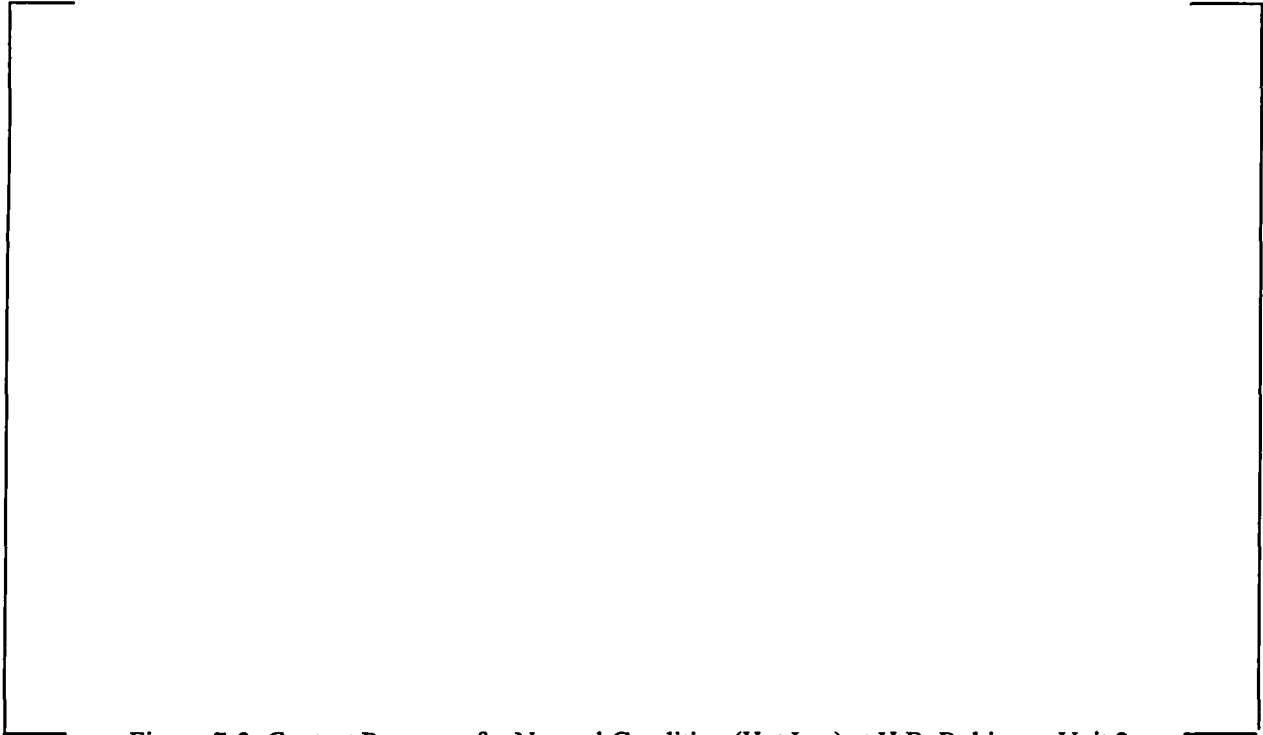
a,c,e

Figure 7-3. Contact Pressures for Normal Condition (Hot Leg) at H.B. Robinson Unit 2

a.c.e

Figure 7-4. Contact Pressures for Normal Condition (Cold Leg) at H.B. Robinson Unit 2

a,c,e

Figure 7-5. Contact Pressures for SLB Faulted Condition at H.B. Robinson Unit 2

a,c,e

Figure 7-6. Model 44F Pullout Test Results for Force/inch at 0.25 inch Displacement

8.0   LEAK RATE ANALYSIS OF CRACKED TUBE-TO-TUBESHEET JOINTS

This section of the report presents a discussion of the leak rate expectations from axial and circum-ferential cracking confined to the tube-to-tubesheet joint region, including the tack expansion region, the tube-to-tubesheet welds and areas where degradation could potentially occur due to bulges and overexpansions within the tube at a distance at or below 9 inches from the top of the tubesheet. It is noted that the methods discussed below support a permanent change to the H.B. Robinson Unit 2 Technical Specifications. With regard to the inherent conservatism embodied in the application of any predictive methods it is noted that the presence of cracking was not confirmed because removal of a tube section was not performed at Catawba 2 or Vogtle 1.

8.1   THE BELLWETHER PRINCIPLE FOR NORMAL OPERATION TO STEAM LINE BREAK LEAK RATES

From an engineering expectation standpoint, if there is no significant primary-to-secondary leakage during normal operation, there should likewise be no significant leakage during postulated accident conditions from indications located approximately below the mid-plane of the tubesheet. The rationale for this is based on consideration of the deflection of the tubesheet with attendant dilation and diminution (expansion and contraction) of the tubesheet holes. In effect, the leakage flow area depends on the contact pressure between the tube and tubesheet and would be expected to decrease during postulated accident conditions below some distance from the top of the tubesheet. The primary-to-secondary pressure difference during normal operation is on the order of 1200 to 1500 psid, while that during a postulated accident, e.g., steam line and feed line break, is on the order of 2560 to 2650 psid.[1] Above the neutral plane of the tubesheet the tube holes tend to experience a dilation due to pressure induced bow of the tubesheet. This means that the contact pressure between the tubes and the tubesheet would diminish above the neutral plane in the central region of the tubesheet at the same time as the driving potential would increase. Therefore, if there was leakage through the tube-to-tubesheet crevice during normal operation from a through-wall tube indication, that leak rate could be expected to increase during postulated accident conditions. Based on early NRC staff queries regarding the leak rate modeling code associated with calculating the expected leak rate, see Reference 33 for example, it was expected that efforts to license criteria based on estimating the actual leak rate as a function of the contact pressure during faulted conditions on a generic basis would be problematic.

As noted, the tube holes diminish in size below the neutral plane of the tubesheet because of the upward bending and the contact pressure between the tube and the tubesheet increases. When the differential pressure increases during a postulated faulted event the increased bow of the tubesheet leads to an increase in the tube-to-tubesheet contact pressure, increasing the resistance to flow. Thus, while the dilation of the tube holes above the neutral plane of the tubesheet presents additional analytic problems in estimating the leak rate for indications above the neutral plane, the diminution of the holes below the neutral plane presents definitive statements to be made with regard to the trend of the leak rate, hence, the bellwether principle. Independent consideration of the effect of the tube-to-tubesheet contact pressure

---

[1]The differential pressure could be on the order of 2405 psid if it is demonstrated that the power operated relief valves will be functional.

leads to similar conclusions with regard to the opening area of the cracks in the tubes, thus further restricting the leak rate beyond that through the interface between the tube and the tubesheet.

In order to accept the concept of normal operation being a bellwether for the postulated accident leak rate for indications above the neutral plane of the tubesheet, the change in leak rate had to be quantified using a somewhat complex, physically sound model of the thermal-hydraulics of the leak rate phenomenon. This is not necessarily the case for cracks considered to be present below the neutral plane of the tubesheet. This is because a diminution of the holes takes place during postulated accident conditions below the neutral plane relative to normal operation. For example, at a radius of 23.2 inches from the center of the SG, the contact pressure during normal operation at the bottom of the tubesheet is calculated to be 2491 to 2571 psi[2] (see the last contact pressure entry in the 23.227 inch radius columns of Table 7-8 and Table 7-7, respectively), while the contact pressure during a postulated steam line break would be on the order of 4054 psi at the bottom of the tubesheet at a radius of 23.227 inches, see Table 7-9. (Note: The radii specified in the heading of the tables are the maximum values for the respective zones analyzed, hence the contact pressures in the center column correspond to the radius specified for the left column, etc. The leftmost column lists the contact pressure values for a radius of 3.7258 inches.) The analytical model for the flow through the crevice, the Darcy equation for flow through porous media, indicates that flow would be expected to be proportional to the differential pressure. Thus, a doubling of the leak rate could be predicted if the change in contact pressure between the tube and the tubesheet were ignored. Examination of the nominal correlation in Reference 34 indicates that the resistance to flow (the loss coefficient) would increase during a postulated SLB event.

The leak rate from a crack located within the tubesheet is governed by the crack opening area, the resistance to flow through the crack, and the resistance to flow provided by the tube-to-tubesheet joint. The path through the tube-to-tubesheet joint is also frequently referred to as a crevice, but is not to be confused with the crevice left at the top of the tubesheet from the expansion process. The presence of the joint makes the flow from cracks within the tubesheet much different from the flow to be expected from cracks outside of the tubesheet. The tubesheet prevents outward deflection of the flanks of cracks, a more significant effect for axial than for circumferential cracks, which is a significant contributor to the opening area presented to the flow. In addition, the restriction provided by the tubesheet greatly restrains crack opening in the direction perpendicular to the flanks regardless of the orientation of the cracks. The net effect is a large, almost complete restriction of the leak rate when the tube cracks are within the tubesheet.

The leak path through the crack and the crevice is very tortuous. The flow must go through many turns within the crack in order to pass through the tube wall, even though the tube wall thickness is relatively small. The flow within the crevice must constantly change direction in order to follow a path that is formed between the points of hard contact between the tube and the tubesheet as a result of the differential thermal expansion and the internal pressure in the tube. There is both mechanical dispersion and molecular diffusion taking place. The net result is that the flow is best described as primary-to-secondary weepage. At its base, the expression used to predict the leak rate from tube cracks through the tube-to-tubesheet crevice is the Darcy expression for flow rate, Q, through porous media, i.e.,

---

[2] The change occurs as a result of considering various hot and cold leg operating temperatures.

$$Q = \frac{1}{K \mu} \frac{dP}{dz} \qquad (1)$$

where μ is the viscosity of the fluid, P is the driving pressure, z is the physical dimension in the direction of the flow, and K is the "loss coefficient" which can also be termed the flow resistance if the other terms are taken together as the driving potential. The loss coefficient is found from a series of experimental tests involving the geometry of the particular tube-to-tubesheet crevice being analyzed, including factors such as surface finish, and then applied to the cracked tube situation.

The calculation of the leak rate during a postulated SLB is not based on a fluid temperature of 600° F but a temperature obtained from the examination of the equipment specification curves for the transient. The SLB transient is assumed to initiate while the plant is at hot standby conditions, i.e., 547° F. The primary and secondary side temperature drop is 335° F leading to an analysis temperature of 142° F for the tubesheet, channel head and shell temperature difference. The temperature history during a postulated SLB is shown on Figure 8-5. It can be readily seen that the most limiting differential pressure, 2560 psig, occurs when the temperature is at a relative steady state value for both the hot and cold legs (212° F). The H* engagement length required to resist SLB differential with a margin of 1.4 is longer later in the transient as the pressure differential increases and temperature remains relatively constant. Also, the B* length (discussed later in this report) to restrict the SLB leak rate to a factor of 2 relative to normal operation will also be longer for the SLB condition as the transient progresses.

If the leak rate during normal operation was 0.1 gpm (about 150 gpd), the postulated accident condition leak rate would be on the order of 0.2 gpm if only the change in differential pressure were considered, however, the estimate would be reduced when the increase in contact pressure between the tube and the tubesheet was included during a postulated steam line break event. An examination of the contact pressures as a function of depth in the tubesheet from the finite element analyses of the tubesheet as reported in Table 7-7 through Table 7-9 shows that the bellwether principle applies to a significant extent to all indications below the neutral plane of the tubesheet. At the neutral plane of the tubesheet, the increase in contact pressure shown on Figure 7-3 is more on the order of 11% relative to that during normal operation for all tubes regardless of radius. Still, the fact that the contact pressure increases means that the leak rate would be expected to be bounded by a factor of two relative to normal operation. At a depth of 16.4 inches from the top of the tubesheet the contact pressure increases by about 42% at a radius of 3.73 inches relative to that during normal operation. The flow resistance would be expected to increase by about 38%, thus the increase in driving pressure would be partially offset by the increase in the resistance of the joint.

The numerical results from the finite element analyses are presented on Figure 8-1 at the bottom of the tubesheet. A comparison of the contact pressure during postulated SLB conditions relative to that during NOp is also provided for depths of 16.4, 10.9 and 5.4 inches below the top of the tubesheet. The observations are discussed in the following.

- At the bottom of the tubesheet, Figure 8-1, the contact pressure increases by 1483 psi near the center of the tubesheet and exhibits no change at a radius of approximately 52 inches.

- At 16.4 inches below the top of the tubesheet (a little over 5.4 inches from the bottom) the tubesheet the contact pressure increases by about 787 psi at the center to a minimum of approximately 100 psid at a radius of 54 inches, Figure 8-2. The contact pressure during a SLB is everywhere greater than that during NOp. The influence of the channelhead and shell at the periphery causes the deformation to become non-uniform near the periphery.

- At 10.5 inches below the top of the tubesheet, (roughly the neutral plane), Figure 8-3 shows the contact pressure during SLB being uniformly greater than that during normal operation by about 110 psi (ranging from 110 to 200 psi traversing outward).

- At a depth of 5.44 inches from the TTS, Figure 8-4, the contact pressure decreases by about 528 psi near the center of the TS to a decrease of 264 psi at a radius of 45.52 inches.

The absolute value of the contact pressure is not as important as the change in contact pressure because the parameter of interest in applying the B* criteria is the relative leak rate between NOp and SLB conditions. The analysis results indicate that there is an axial location within the tubesheet as a function of radius from the center where the contact pressure is invariant between NOp and SLB. The analysis results discussed in the next section include a plot of the invariant elevation for the H.B. Robinson Unit 2 SGs (Figure 9-11). The distribution of the contact pressure would decrease near the TTS in the central region. Thus, it would not be sufficient to simply use an arbitrary depth value and suppose that the leak rate would be relatively unchanged even if the potential difference were the same without further analysis. However, the fact that the contact pressure generally increases below that elevation indicates that leak rate would be relatively unaffected a little deeper in the tubesheet.

8.2   LIGAMENT TEARING DISCUSSION

One of the concerns to address when dealing with cracks in SG tubes is the potential for ligament tearing. Ligament tearing may occur during a postulated accident when the differential pressure is significantly greater than during normal operation. The approach to dealing with the question is the same as that for circumferential cracks, that is, what is the ligament that will not tear during NOp conditions compared to the ligament that will tear during a postulated SLB event. The stress that is applied to the crack flanks during normal operation is the 2250 psi primary pressure. The stress during a SLB event is the 2560 psi pressure associated with the set point of the relief valves. The net difference is only 310 psi, hence the affect is expected to be small.

8.2.1   Circumferential Cracking

Ligament tearing considerations for circumferential tube cracks that are located below the H* depths within the tubesheet are significantly different from those for potential cracks at other locations. The reason for this is that H* has been determined using a factor of safety of three relative to the normal operating pressure differential and 1.4 relative to the most severe accident condition pressure differential. Therefore, the internal pressure end cap loads which normally lead to an axial stress in the tube are not transmitted below about 2/3 of the H* depth. This means that the only source of stress acting to extend the crack is the primary pressure acting on the flanks of the crack. Since the tube is captured within the tubesheet, there are additional forces acting to resist opening of the crack. The contact pressure between the tube and tubesheet results in a friction induced shear stress acting opposite to the direction of crack opening, and the pressure on the flanks is compressive on the material adjacent to the plane of the crack,

hence a Poisson's ratio radial expansion of the tube material in the immediate vicinity of the crack plane is induced which also acts to restrain the opening of the crack. In addition, the differential thermal expansion of the tube is greater than that of the carbon steel tubesheet, thereby inducing a compressive stress in the tube below the H* length.

A scoping evaluation of the [

]^{a,c,e}

[

]^{a,c,e}.

In summary, considering the worst-case scenario, the likelihood of ligament tearing from radial circumferential cracks resulting from an accident pressure increase is small since at most, only 8% of the cross-sectional area is needed to maintain tube integrity. Also, since the crack face area will be less than the total cross-sectional area used above, the difference in the force applied as a result of normal operating and accident condition pressures will be less than the 43 lbs associated with the above numbers. Therefore, the potential for ligament tearing is considered to be a secondary effect of essentially negligible probability and should not affect the results and conclusions reported for the H* evaluation. The leak rate model does not include provisions for predicting ligament tearing and subsequent leakage, and increasing the complexity of the model to attempt to account for ligament tearing has been demonstrated to be not necessary (Reference 35).

8.2.2 Axial Cracking Discussion

The following evaluation considers the potential for ligament tearing of postulated axial cracks and to what extent such tearing would affect the technical basis for the LAR. This evaluation is based on a comparative study with a SG manufactured with 11/16 diameter OD tubing (Reference 42).

The tube area required to resist tearing due to an axially oriented crack can be calculated using traditional mechanics. The axial orientation of the damage in the tube means that the required area of the tube cross section to resist tearing and damage should be based on the local strength of the material around the crack. It is conservative, in this case, to neglect the forces that would act to keep a crack closed and compress the flanks in the ligament so that tensile tearing would become unlikely. This includes the far field axial stress on the tube cross section generated by internal pressure end cap loads which would act to close the ligament and any cracks below the H* depth (the depth required to prevent tube pullout). This is in contrast to the typical method used to compare what percent of the area is required to resist ligament tearing in circumferentially damaged tubes based on the amount of force applied to the damaged tube cross section.

The results shown in the table below were obtained using the ASME code minimum material properties (Reference 32) and the nominal dimensions of the steam generator tubes for another plant. The results were compared to the method used to calculate the required thickness to resist ligament tearing due to circumferential cracking (Reference 42) and the method described in the EPRI Tube Integrity Guidelines (Reference 48). [

]^{a,c,e}

$$\begin{bmatrix} & & \\ & & \\ & & \\ & & \end{bmatrix}^{a,c,e}$$

The results of the axial ligament tearing calculations detailed above are [

]^{a,c,e}

Considering the worst-case scenario, the likelihood of ligament tearing from axial cracks resulting from an accident pressure increase is [

]^{a,c,e} Therefore, the potential for axial ligament tearing is considered to be a secondary effect

of essentially negligible probability and is not expected to affect the results and conclusions reported for the B* evaluation. The leak rate model does not include provisions for predicting ligament tearing and subsequent leakage. Increasing the complexity of the model to attempt to account for axial or circumferential ligament tearing is not considered necessary.

This same conclusion applies to the H.B. Robinson Unit 2 Model 44F SGs which have 7/8 inch OD tubes.

a,c,e

Figure 8-1. Change in Contact Pressure at the Bottom of the Tubesheet

a,c,e

Figure 8-2. Change in Contact Pressure at 16.4 Inches Below the TTS

a,c,e

Figure 8-3. Change in Contact Pressure at 10.90 Inches Below the TTS

a,c,e

Figure 8-4. Change in Contact Pressure at 5.44 Inches Below the TTS

CURVE 10
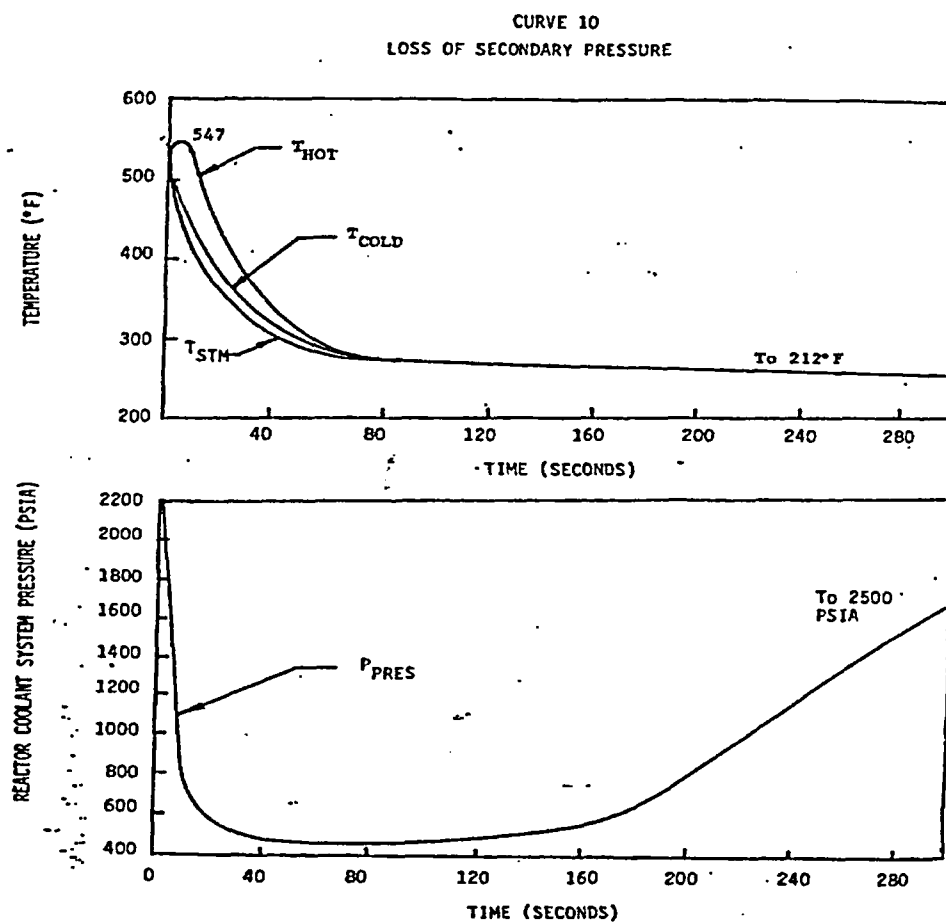LOSS OF SECONDARY PRESSURE

Figure 8-5. Loss of Secondary Pressure

9.0 DETERMINATION OF THE B* DISTANCE

B* is the length of engagement in the tubesheet needed for the leak rate during a postulated steam line break (SLB) event to be bounded by a specified multiple of the leak rate during normal operation (NOp). See Figure 9-2. The rationale for the determination of B* is that there are changes during a SLB relative to NOp that lead to the expectation of an increase in the leak rate and other changes that lead to the expectation of a higher resistance to leakage. The determination of B* is based on analyzing the contributing factors and making an estimate of the change in leak rate that would be expected. The factors that lead to an expectation of an increase in the leak rate are as follows:

1. An increase in the primary-to-secondary differential pressure induced force on the water inside a postulated tube crack and the tube-to-tubesheet interface. For H.B. Robinson Unit 2 this is a factor of 1.77.

2. A decrease in the tube-to-tubesheet contact pressure above the neutral plane of the tubesheet resulting from dilation of the tubesheet holes in response to an increase in the bending deformation from the primary-to-secondary pressure difference increase. This does not apply to the periphery of the tubesheet where the opposite effect occurs.

3. A decrease in the tube-to-tubesheet contact pressure associated with the higher coefficient of thermal expansion of the tube material relative to that of the tubesheet if the temperature of the tubesheet decreases.

The factors that lead to an expectation of a decrease in the leak rate are:

1. The increase in primary pressure within the tube expands the tube into tighter contact with the tubesheet, resulting in an increase of the resistance of the material interface to flow between the tube and the tubesheet.

2. An increase in the tube-to-tubesheet contact pressure below the neutral plane of the tubesheet resulting from diminution of the tubesheet holes in response to the increase in the bending deformation from the primary-to-secondary pressure difference increase. Again, the effect is opposite for most tubes on the periphery of the tubesheet.

3. An increase in the resistance to flow associated with an increase in the viscosity of the water in the crevice if the temperature of the tubesheet decreases.

The basis for the determination of B* is the consideration of each of the above effects using results from finite element analyses of the tubesheet and results from leak rate testing of the tube-to-tubesheet interface. The analyses and testing are described Section 6.0 of this report. In summary, the leak rate is characterized by the Darcy equation for flow through a porous medium, an equation of the same form as the Hagen-Poiseuille equation for fully developed flow. The resistance to flow was developed from test data as a function of the contact pressure between the tube and the tubesheet in accord with expectations. The finite element analysis results provide calculated results for the contact pressure as a function of tube location and depth into the tubesheet based on the NOp and postulated SLB pressure and temperature conditions of the plant.

The following are discussed: background information giving a qualitative overview supporting the development of B*, flow through a crevice formulation, tube-to-tubesheet contact pressure variation, the determination of the B* distance, and conclusions regarding the B* values.

9.1 BACKGROUND INFORMATION

A natural question regarding the development and application of the B* criterion is whether or not numerical studies were performed to verify that the reduction in leak rate resistance above the neutral surface of the tubesheet associated with tubesheet bowing was adequately bounded by the increase in resistance below the neutral surface. The following discussion is intended to provide technical insight into the behavior of the leak rate from throughwall tube indications within the tubesheet by presenting:

1) the theoretical detail that is the basis for the observations from the test data and extrapolation of the test data for leak rate as function of joint length as expressed as the flow loss coefficient, and,

2) the explanation as to why the leak rate at normal operating conditions provides a bellwether for and can be used to establish a bounding value for the leak rate during steam line break conditions.

For most of the tube locations in the tubesheet the bow is convex upwards, like a dome. The tube-to-tubesheet contact pressure is an increasing linear function of the depth from the top of the tubesheet, thus, for any specified location within the tubesheet the contact pressure increases below and decreases above that location. The resistance to leakage through the tube-to-tubesheet interface is an increasing function of the contact pressure between the tube and the tubesheet. The bellwether principle is based on considering the leak rate during a postulated steam line break (SLB) event relative to that during normal operating conditions (NOp). The primary-to-secondary differential pressure during a SLB event is greater than that during NOp so that bowing of the tubesheet increases with an associated change in the slope of the contact pressure versus depth relation as a function of tube location. For all tubes, except for the small percentage of tubes located on the periphery, the slope increases. For tubes on the periphery the slope increases in an absolute sense since there is an inflection point near the periphery. Regardless, the evaluation applies because increasing the contact pressure has a greater influence on the leak rate than decreasing the contact pressure.

Numerical studies were not initially performed because the subject was considered to be adequately addressed based on a qualitative evaluation using first principles considerations as follows:

1) In the limiting case of no dependence of the leak rate loss coefficient, i.e., the resistance per unit length, on the contact pressure, the leak rate during NOp and postulated SLB would be a function of the length of the crevice and pressure difference only. Using the Darcy equation, the leak rate is a direct function of the differential pressure and the inverse of the crevice length. Since the length remains the same and the driving pressure increases by a factor of about 2, that is, 1300 psi to 2560 psi, the leak rate change is bounded by a similar factor. Any other theoretical dependence of leak rate on pressure difference, e.g., the square root of the pressure difference à la the Bernoulli equation, results in a reduction of the bounding factor relative to the result obtained using the Darcy equation.

2) The test data have demonstrated that the resistance per unit length is a monotonically increasing, non-linear function of the contact pressure with a positive second derivative. The deflection of the TS in combination with the increase in internal pressure results in the change in the contact pressure being zero between NOp and SLB at some depth below the TTS that is above the neutral surface of the tubesheet. The net contact pressure decreases above and increases below that depth, which is a function of location within the tube bundle. Using this elevation as a reference, the increase in resistance per unit length below the zero-change location must always be more than the absolute value of the decrease in resistance per unit length above the zero-change elevation. Thus, the average resistance in going from NOp to SLB must increase and the average leak rate must decrease. This is independent of the individual leak rates involved and only depends on the trend. The latter observation is apparent by inspection of the figure relating loss coefficient to contact pressure in all submittals on the subject of leak rate through tube-to-tubesheet crevices, see Figure 6-6 in this report for example.

There are alternate approaches to proving the above statements from the observations regarding the leak rate from test specimens.

9.2 FLOW THROUGH A CREVICE (DARCY'S EQUATION)

The equation that is solved for flow through a crevice is Darcy's model for flow through a porous media, that is, the volumetric flow, Q, is a function of the differential driving pressure, ΔP, and the respective inverse values of the viscosity, μ, the loss coefficient, K, and the length of the path, L, as,

$$Q = \frac{1}{\mu K} \frac{\Delta P}{L}. \qquad (9\text{-}1)$$

The driving pressure is based on the upstream minus the downstream values, else a negative sign would be needed in front of the equation. The viscosity is a function of the temperature and pressure of the fluid. The Darcy equation is also of the same form as the Hagen-Poiseuille flow equation for fully developed, laminar, axial flow in an annular gap, i.e.,

$$Q = \frac{1}{\mu \dfrac{6}{\pi R a^3}} \frac{\Delta P}{L}. \qquad (9\text{-}2)$$

Here, R is the average radius of the gap and a is a characteristic or effective gap dimension for the rough tube-to-tubesheet interface, expected to be very small, on the order of $4 \cdot 10^{-5}$ inch. Thus, the loss coefficient would be expected to be proportional to the inverse of the cube of the effective gap. The Hagen-Poiseuille form of the leak rate equation gives insight into the relationship between the average resistance, characterized by the loss coefficient, K, and the contact pressure, i.e.,

$$K = \frac{6}{\pi R a^3}. \qquad (9\text{-}3)$$

If the characteristic gap were proportional to the contact pressure between the tube and the tubesheet, doubling the pressure would increase the leak resistance by a factor of 8, although this is not necessarily

expected to be the case because of the complex nature of the interface. In addition, it would not be unexpected that a plot of the $\ln(K)$ versus the contact pressure would approximate a straight line. For the rough tube-to-tubesheet interface, the length of the tortuous path can also be considered to be characterized as being effective because the flow does not necessarily have a straight path to follow to the TTS (top of the tubesheet). Approximation of the path as the legs of an equilateral triangle would essentially double the distance traveled from the throughwall location to the TTS. Hence, the use of the loss coefficient integrates the accounting of the effective gap and effective length.

The electrical analogy for the flow considers Q as the current flow and ΔP as the potential, hence the quantity μKL is the resistance to flow, R. Since K is a function of the contact pressure, P_c, the resistance is a function of the location within the tubesheet. The total resistance can be found as the average value of the quantity μK, the resistance per unit length, multiplied by L, or by integrating the incremental resistance, $dR = \mu K\, dL$ over the length L, i.e.,

$$R = \mu \bar{K}\left(L_2 - L_1\right) = \int_{L_1}^{L_2} \mu K\, dL, \qquad (9\text{-}4)$$

where both μ and K could be functions of location L. The viscosity is a very weak function of the pressure of the water in the crevice and can be considered to be constant for a given plant condition with negligible error, Figure 9-13, References 37 and 38. However, the viscosity is a strong function of the temperature of the water in the crevice, Figure 9-14, and the tubesheet temperature for the condition being analyzed must be considered. A decrease in the temperature can lead to a significant increase in flow resistance.

9.3 TUBE-TO-TUBESHEET CONTACT PRESSURE VARIATION

Six tubesheet radial locations for which the contact pressure as a function of depth was determined were used in calculating the length of sound tubing below the TTS required to resist the NOp and SLB axial loads, i.e., the H* depth (See Figure 9-1). The intercept, b_0, and slope, b_1, parameters for the calculation of the contact pressure as a function of length, L, into the tubesheet for the six radial locations are listed in Table 9-1. The relationships are always in linear first order form,

$$P_c = b_0 + b_1 L \qquad (9\text{-}5)$$

where the coefficients b_0 and b_1 vary as a function of the radial location of the tube in the tubesheet. This is simply a consequence of the fact that in the linear elastic stress analysis, no yielding occurs. A comparison of the FEA results with first order, linear representations is provided on Figure 9-5 for NOp and SLB conditions at a radius of 34 inches from the center of the tubesheet.

Further calculations examined the relationship between the intercept and slope of the prediction equations as a function of tube location radius. It was found that second order polynomial expressions can be used to describe the parameters almost exactly, i.e., with negligible error. A plot of the operating contact pressures, which do not include the residual contact pressure from the hydraulic expansion process, is provided on Figure 9-6 for each location during NOp and Figure 9-7 provides similar information during the postulated SLB event. The polynomial coefficients that were used to determine the values of the intercept and slope, i.e., b_0 and b_1, for any given radius, R, from the center of the tubesheet for NOp conditions are illustrated on Figure 9-8. Here, the following relationships are depicted where the g and h values were determined from the regression analyses (recall that R in the following two equations

represents radius),

Normal Operation

$$b_o = g_0 + g_1 R + g_2 R^2 \quad \text{(Intercept)}$$
$$b_1 = h_0 + h_1 R + h_2 R^2 \quad \text{(Slope)}$$

(9-6)

The coefficients, u and v, of a similar set of expressions were calculated for determining the contact pressure at all locations within the tubesheet during a SLB event, i.e.,

SLB Conditions

$$b_o = u_0 + u_1 R + u_2 R^2 \quad \text{(Intercept)}$$
$$b_1 = v_0 + v_1 R + v_2 R^2 \quad \text{(Slope)}$$

(9-7)

The polynomial coefficients that were used to determine the values of the intercept and slope for use in calculating the contact pressure during a SLB are illustrated on Figure 9-9. A comparison of the coefficients for the two conditions is provided on Figure 9-10.

9.4   DETERMINATION OF THE B* DISTANCE

The results from multiple leak rate testing programs indicate that the logarithm of the loss coefficient is a linear function of the contact pressure, i.e.,

$$\ln K = a_0 + a_1 P_c, \tag{9-8}$$

where the coefficients, a_0 and a_1 of the linear relation are found from a regression analysis of the test data; both coefficients are greater than zero. Simply put, the loss coefficient is greater than zero at the point where the contact pressure is zero and the loss coefficient increases with increasing contact pressure. Thus,

$$K = e^{a_0 + a_1 P_c}, \tag{9-9}$$

and the loss coefficient is an exponential function of the contact pressure. Combining Equation 9-9 for the loss coefficient as a function of the contact pressure with Equation 9-5 for the contact pressure as a function of length yields,

$$K = e^{a_0 + a_1 (b_0 + b_1 L)} = e^{c_0 + c_1 L} \tag{9-10}$$

where L is reckoned downward from the lower of the top of the tubesheet or the bottom of the expansion transition and the joined coefficients are given by $c_0 = a_0 + a_1 b_0$ and $c_1 = a_1 b_1$. Away from the periphery of the tubesheet, b_1 is greater than zero, hence c_1 is also greater than zero and the loss coefficient increases with depth into the tubesheet. Alternatively, the relation also means that near the periphery of the tubesheet the resistance to flow increases above any depth when the tubesheet bows upward. Since the B* distance into the tubesheet is based on finding the depth for which the resistance to leak during SLB is the same as that during NOp, the meaningful radial region of the tubesheet is away from the periphery, that is, where the resistance to leakage decreases near the top of the tubesheet. Another point to note from the above expression is that in the region of interest the second derivative of the loss coefficient with respect to depth is positive. this means that the resistance per unit length is always increasing with depth into the

tubesheet. One consequence of the relation is that the decrease in resistance for a specified distance above any reference point is balanced by the increase in resistance over a shorter distance below that reference point. The coefficients for the contact pressure as a function of location are given by Equations 9-6 and 9-7 for NOp and SLB respectively.

The B* distance is designated by L_B in the following equations and is the depth at which the resistance to leak during SLB is the same as that during NOp. Note that the product of the viscosity and the loss coefficient is the resistance per unit length for any location in the tubesheet. The resistance to leak, R, as a function of the viscosity, μ, average loss coefficient, $\overline{K}$, and length of the leak path from some uppermost location, L_0, to L_B for any condition is given by,

$$R = \mu\overline{K}\left(L_B - L_0\right) = \mu\int_{L_0}^{L_B} e^{c_0 + c_1 L}dL. \quad (9\text{-}11)$$

The limits of the integration define the range over which there is a contact pressure between the tube and the tubesheet that is greater than zero, i.e., ignoring any resistance to flow above that elevation. The lower limit is the lower of the TTS, the BET (bottom of the expansion transition), or the point where the contact pressure is zero. Carrying out the integration,

$$R = \mu\frac{e^{c_0}}{c_1}\left[e^{c_1 L_B} - e^{c_1 L_0}\right]. \quad (9\text{-}12)$$

The equation can be used directly when the point of zero contact pressure between the tube and the tubesheet is at or below the TTS or BET, whichever is lower.

In order to account for the condition wherein L_0 is < 0 (See Figure 9-3 and 9-4), i.e., at or above the TTS or BET, whichever is lower, the equation is written as,

$$R = \mu\frac{e^{c_0}}{c_1}\left[e^{c_1 L_B} - \text{if}\left(L_0 > 0, e^{c_1 L_0}, 1\right)\right]. \quad (9\text{-}13)$$

Here, the first argument of the "if" statement is the condition to be tested, the second argument is the value used if the condition is true, and the third argument is used if the condition is false, that is, when zero contact pressure is predicted above the TTS or BET (See Figure 9-4). For normal operation the resistance to leakage is given by,

$$R_N = \mu_N\frac{e^{c_{0N}}}{c_{1N}}\left[e^{c_{1N} L_B} - \text{if}\left(L_{0N} > 0, e^{c_{1N} L_{0N}}, 1\right)\right], \quad (9\text{-}14)$$

and for SLB by,

$$R_S = \mu_S\frac{e^{c_{0S}}}{c_{1S}}\left[e^{c_{1S} L_B} - \text{if}\left(L_{0S} > 0, e^{c_{1S} L_{0S}}, 1\right)\right]. \quad (9\text{-}15)$$

The B* distance is such that the resistance during SLB is the same as that during NOp, limiting the leak rate to be no more than a factor of two times that during normal operation, thus the solution is obtained for the value of L_B that makes $R_S = R_N$.

For the H.B. Robinson Unit 2 SGs the value of B* varies from a maximum of 8.01 inches at a radius of 2 inches, about row 1 at the center of the bundle, to less than 6 inches at a radius of 20 inches. Thereafter, the integrated leak resistance is always greater during a SLB event than during NOp. A plot of the calculated B* values is provided on Figure 9-15. Here, any values less than 1 inch were truncated to 1 inch. For example, the top of the tubes at the extreme periphery of the tubesheet are in compression during NOp because of contraction of the tube holes due to convex downward bending. The level of compression increases during a SLB event because the magnitude of the convex bending increases. Thus, any leak rate during NOp would bound the leak rate during SLB. While the driving pressure would increase by a factor of up to 2, the contact pressure between the tube and the tubesheet would increase toward the top of the tubesheet. A summary of the B* values is provided in Table 9-2. A plot of nominal B* values as a function of tubesheet radius where there would be no change in leak rate during a postulated SLB is provided in Figure 9-16. Figure 9-17 represents a graphical determination of B* depth based on comparing integrated resistance to depth from the top of the tubesheet at a radius of 8 inches from the center of the tube bundle.

9.5   SENSITIVITY OF THE B* CALCULATION

Additional insight into the effect of cold leg indications on the relative leak rate is illustrated by examining the plots of TTS contact pressure on Figure 9-12 for the hot leg and Figure 9-18 for the cold leg. The change in differential pressure and the change in temperature result in the contact pressure at the TTS decreasing relative to the hot leg. This means that leakage during NOp operation on the cold leg will be closer to that during a postulated SLB event and the relative increase smaller. The conclusion regarding the cold leg indications is that the application of a hot leg derived B* is conservative.

9.6   ADDITIONAL LEAKAGE SENSITIVITY STUDY FOR 17 INCH INSPECTION LENGTH CRITERIA COMPLETED FOR 11/16 OD TUBING

It is judged by Westinghouse that the sensitivity results discussed below apply equally to the 7/8 inch OD tube joint as well as 11/16 inch OD tube joint (Reference 53).

The basis for the development of the 17-inch tubesheet inspection zone with regard to leak rate is the ratio of the potential leak rate during a SLB event to that during NOp using the results of data from leak rate tests of the tube-to-tubesheet interface, a.k.a. crevice. Westinghouse had historically developed a computer model for a crevice in series with a crack using the crevice data and independent data for free-span cracks. The NRC staff has expressed concerns regarding the model because of a lack of test data from physical specimens which contained a crack in series with a crevice. Westinghouse data obtained from separate testing of the tube-to-tubesheet crevice and axial cracks within a tubesheet with a zero length crevice above the crack demonstrated the resistance of the crack to be comparable to the resistance of the crevice for a larger tube size. The implication from the latter being that an analysis that neglected the effect of the crack would be valid because the effect on the numerator and denominator of the SLB:NOp leak rates ratio would be the same. Other considerations were also made, e.g., for indications within about 56 inches from the center of the tubesheet, the effect of tubesheet bow induced crack closure

would be to increase the resistance of the crack. If the geometry resistance to flow is about constant between the two conditions (at a depth of 17 inches it would be expected to increase) and if the fluid resistance to flow is about constant (if the temperature decreases it would be expected to increase), the leak rate would behave as the SLB:NOp differential pressure ratio, or the square root of the ΔP ratio, hence the factor of 2.

It is also worth noting the expectations from the NRC requested analyses based on the crack opening area formulations and the geometries inherent in the model analysis. The opening of circumferential cracks is resisted by the stiffness of the material above and below the crack flanks and by friction on the OD of the tube. For all practical purposes the tube is infinitely long in the axial direction, although, the resistance to opening due to the shear interface increases rapidly. The geometry of the tubesheet does not restrict crack opening in the axial direction. The opening of axial cracks is more restricted owing to the geometry of the problem. For example, there is a line of symmetry 180° from the crack flanks, hence the tube is built-in at that location. There is also friction associated with the interface of the tube with the tubesheet. Finally, the confinement provided by the tubesheet means that an axial crack cannot open more than the dilation of the tubesheet hole, which ranges from compression near the center to being very small on the periphery. Thus, the effects reported from the DENTFLO analyses would be expected to indicate more effect for circumferential cracks than for axial cracks.

In trying to use the Westinghouse computer model to provide a qualitative demonstration of the veracity of the B* analysis, a significant potential shortcoming associated with the approach was recognized, although it would be conservative relative to predicting actual leak rates. The crack flow leak rate model portion of the code was based on a freespan axial crack, not a crack with flanks constrained by the tubesheet hole. Thus, the crack opening area computation could be significantly biased. In order to perform the requested studies the code was modified as follows:

1) The crack opening area model for circumferential cracks of Appendix C of WCAP-15932 was included in the DENTFLO code.

2) A crack opening area model for axial cracks constrained in the tubesheet was derived accounting for the constraints added to the problem by the presence of the tubesheet and included in the DENTFLO code.

The new model for the axial crack opening that takes into account the guidance and constraint provided by the surrounding tubesheet is described in what follows. See Figure 9-19 for a sketch of the model configuration. [

]^{a,c,e}

Using these models, a sensitivity study was performed which consisted of a series of analyses to demonstrate the conservatisms of the bellwether approach. These analyses consider the locations specified in the NRC RAI, and the conditions specified in the NRC RAI, i.e., crack only, crevice only and combined crack and crevice.

The models developed for these analyses are for qualitative comparisons only (i.e., not for absolute prediction of leak rates) and were not verified and/or validated beyond their current "information" status since they are for comparative purposes only.

Constrained Axial Crack Opening Area Calculations

A literature search of the significant fracture mechanics texts and journals (e.g. Journal of Engineering Fracture Mechanics, International Journal of Fracture Mechanics, Reference 51, etc.) did not yield any previously published models for the crack opening area for a central axial crack that is circumferentially constrained in an internally pressurized tube. A new model was developed to calculate the crack opening area of a constrained SG tube under these conditions. The general form of the equation for the crack opening area in an infinite plate is (Reference 44):

$$COA = 2\pi a^2 \frac{\sigma}{E}$$

where σ is the far-field stress resulting in the crack opening, E is the Young's Modulus of the tube and a is the half-length of the crack. In the absence of empirical evidence, the general form for the crack opening area can be modified by a functional. The functional can include the important details regarding the boundary conditions and other effects relative to the constrained and cracked tube. Let $H(F(n))$ be the modifying functional for the crack opening area, where n represents the influential parameters of the geometry and loading. Then the model for the crack opening area becomes,

$$COA = H\left(F(n)\right)2\pi a^2 \frac{\sigma}{E}$$

Given the general constitutive form for the crack opening area it remains to define the modifying functional. Based on previous work (Reference 45) it is reasonable to assume that the crack opening area for the axial crack would be affected by the interactions of the internal pressure on the crack flanks and the contact pressure between the tube and the tube sheet. The largest effect on the crack flanks that can affect the flow rate through the crack will be the bending of the flanks due to the internal pressure in the event that the contact pressure between the tube and the tube sheet decreases, although, as previously noted, the amount of opening can never be greater than the change in the circumference of the hole in the tubesheet.

Comparison against Established Methods

The resulting model for the crack opening area in an internally pressurized and constrained tube with an axial crack [

]a,c,e

where ζ is a scalar coefficient that describes the local effect of the crack in a tube on an equivalent finite flat plate area and ϕ is a parameter that accounts for the change in resistance to bending of the crack flanks due to the change in tube to tubesheet contact pressure and crack length. This model was compared against several established models for unconstrained internally pressurized tubes with axial cracks. These comparison models include published work by Zahoor (Reference 46) and empirical models employed by the American Petroleum Institute (API) and developed by Anderson (Reference 49). Figure 9-20 shows the results that each model predicts for the crack opening area for cracks ranging from 0.02 to 2.00 inch.

The comparison above shows that the results for the new model, for a constrained internally pressurized tube, are reasonable in comparison to the other established models for unconstrained tubes. Specifically, the new model predicts a smaller crack opening area as a function of crack length than the unconstrained axial cracks with a smaller rate of increase in the crack opening area. This is an expected result because the other models assume a free span for the tube with no constraining effects. Therefore it is reasonable to use the new model for further calculations to estimate the crack opening area of a constrained and internally pressurized tube with a central axial crack.

Analysis of Circumferential Cracking

A model for a constrained circumferential crack in an internally pressurized tube was developed (Reference 45). This model is appropriate to use for a circumferential crack that occurs in a tube within the tubesheet. A maximum crack half angle of 90°, or a maximum circumferential crack equal to half of the circumference of the tube, was used in this analysis as a simplifying assumption. The model for constrained circumferential cracks was implemented in the code DENTFLO to determine the trend of the leakage rate ratios for normal operating and steam line break conditions. See References 45 and 48 for more details on the model and its application.

DENTFLO Analysis Methodology

The program DENTFLO was run to determine the trend of the leak rate ratios of a damaged tube at the bottom of the tubesheet at different radii. There are 36 different cases of interest with respect to the leak rate ratio analysis. The 36 cases are comprised of: 2 thermal-hydraulic conditions (NOp and SLB), 2 crack orientations (axial and circumferential), 3 radial locations (near, mid, and peripheral) and 3 conditions of interest (crack, crevice, and combined crack and crevice). The Normal Operation – Maximum Temperature (NOp-MAX) and the Steam Line Break (SLB) were chosen for the analysis because of the largest change in temperature and pressure between the two cases. The tubesheet radii for each range are: Near (2.0774 In), Mid (33.101 In), Peripheral (60.2475 In).

The contact pressures used in the DENTFLO analysis were taken at each tubesheet radius at several elevations in the tubesheet (Reference 52). The tubesheet material below 4.00 from the bottom of the tubesheet," and any contact pressure generated by that material, was conservatively neglected. The loss coefficients for the analysis were taken as a numerically integrated average over the length of the crevice (i.e. from 4" above the bottom of the tubesheet to the top of the tubesheet) based on the contact pressure distribution in the tubesheet (Reference 50). The axial and circumferential crack orientation cases used the models discussed above. The crevice only cases use a model for an unconstrained axial crack based on the work of Paris and Tada (Reference 44) because it gives less resistance to flow through a crack than the

other models available in DENTFLO. The crack length is also large in the crevice only case in order to best represent a situation where the crack cannot contribute significantly to the flow resistance.

[

$]^{a,c,e}$

[

$]^{a,c,e}$

9.7   CONCLUSIONS RELATIVE TO B*

The resistance equations above can be used to show that the resistance is always bounded by the region through the thickness of the tubesheet where the contact pressure increases relative to the region where the contact pressure decreases. This simply means that the leak rate resistance increases during a SLB event relative to that during normal operation for similar lengths about a reference depth from the TTS, for example, B*. The resistance equations were used to calculate B* as the distance from the TTS for which the resistance during a postulated SLB event is the same as that during NOp. This means that the leak rate during SLB from any and all indications below B* will be bounded by a multiple of the leak rate during NOp based on the relative driving pressure for the two conditions. The differential pressure ratio during a SLB at H.B. Robinson Unit 2 is 1.77 for the cases described in Section 8.0, times that during NOp depending on the operating conditions considered, e.g., differences in plugging level. Hence, the leak rate during a postulated SLB event would be expected to be no more than 2 times the leak rate being experienced during normal operation. Moreover, the B* analysis did not take into consideration the effect of the increase in the contact pressure below the B* elevation on the leak rate through postulated tube cracks within the tubesheet. For axial cracks the flanks would be compressed and the leak rate through the cracks themselves would be expected to decrease. For circumferential cracks the resistance to flank displacement in the axial direction would be expected to negate the effect of the slight increase in pressure on the crack flanks. In conclusion, the use of a factor of 2 would usually be expected to be conservative.

Table 9-1. First Order Equation Coefficients for the
Variation of Contact Pressures Through Tubesheet

a,c,e

Table 9-2. B* Summary Table Leak Rate Required Engagement Lengths			
Zone	Leak Resistance Ratio R_{SLB} / R_{NOp} [1,2]	Engagement from TTS (inches)	
		Hot Leg	Cold Leg
A	1.0	< 1.0	< 1.0
B	1.0	6.76	5.18
C	1.0	8.01	6.70
Notes:			
1. Conditions for the analyses are specified in Sections 7.1.4.1 for NOp, and 7.1.4.3 for SLB.			
2. Equal resistance assures leak rate during accident conditions is not more than twice that during normal operation.			
3. H* structural summary is provided in Section 7.2.			

Table 9-3: Summary of Near Radius Leak Rate Ratio Results

$$\begin{bmatrix} & \end{bmatrix}^{a,c,e}$$

Table 9-4: Summary of Mid Radius Leak Rate Ratio Results

$$\begin{bmatrix} & \end{bmatrix}^{a,c,e}$$

Table 9-5: Summary of Peripheral Radius Leak Rate Ratio Results

$$\begin{bmatrix} & \end{bmatrix}^{a,c,e}$$

Measured from lower of the bottom of transition the or the top of the tubesheet.

Tube

End Cap Pull-Out Force

Bottom of hydraulic expansion transition.

H* is the length of engagement needed to resist pullout with a margin of 3 for NOp and 1.4 for SLB.

H*

Tubesheet

Assumed 360° sever of the tube.

Full depth hydraulic expansion.

Tack expansion transition.

Tubesheet cladding.

Tube/Tubesheet Weld.

Figure 9-1. Determination of H*
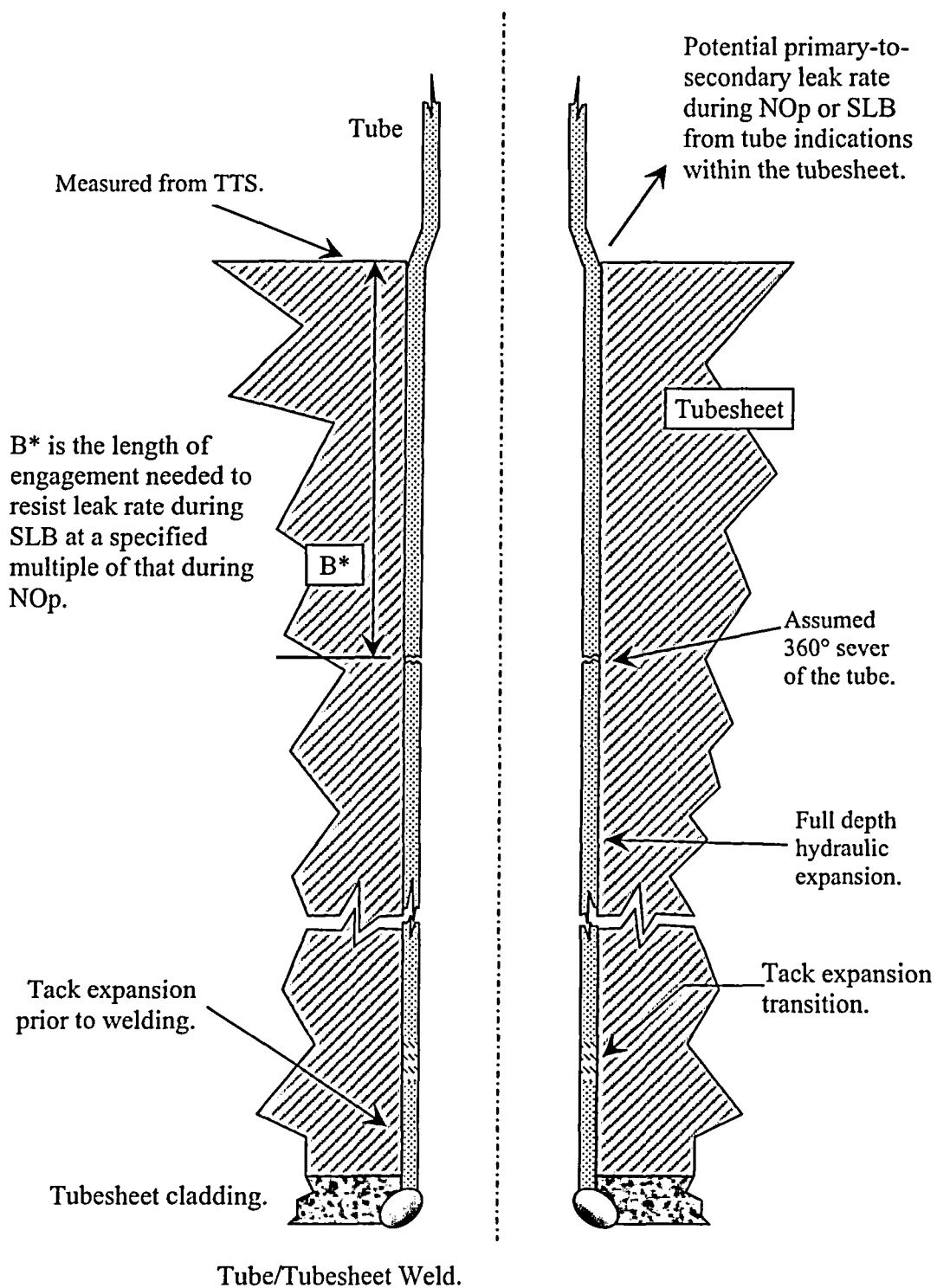
Figure 9-2. Determination of B*
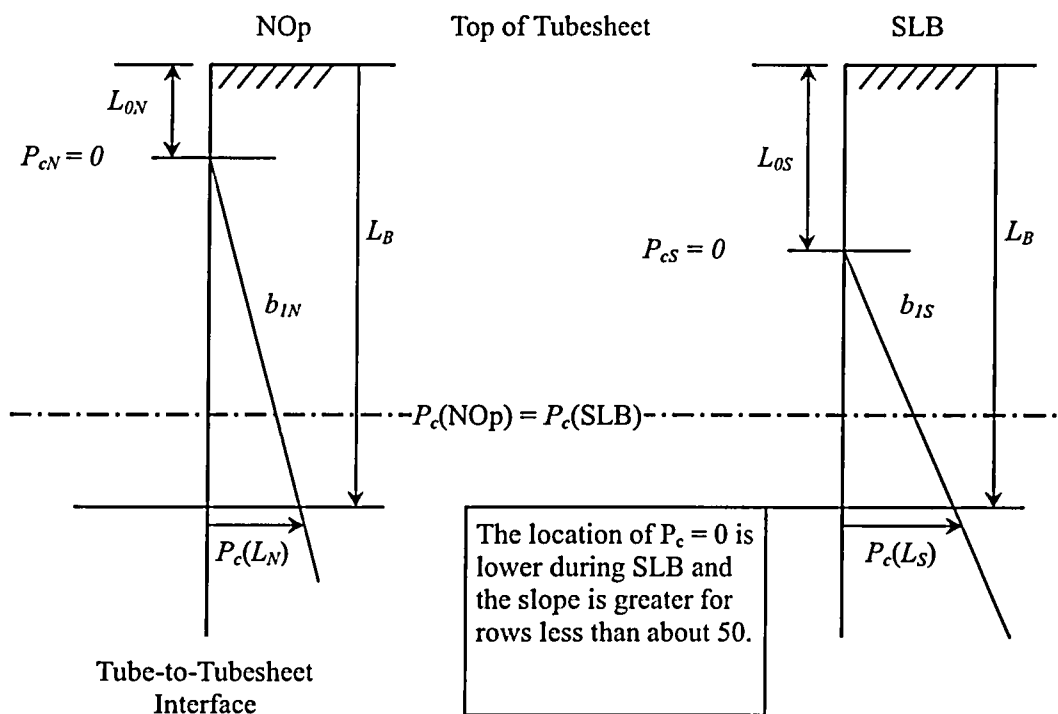
Figure 9-3. Concepts for the Determination of B*
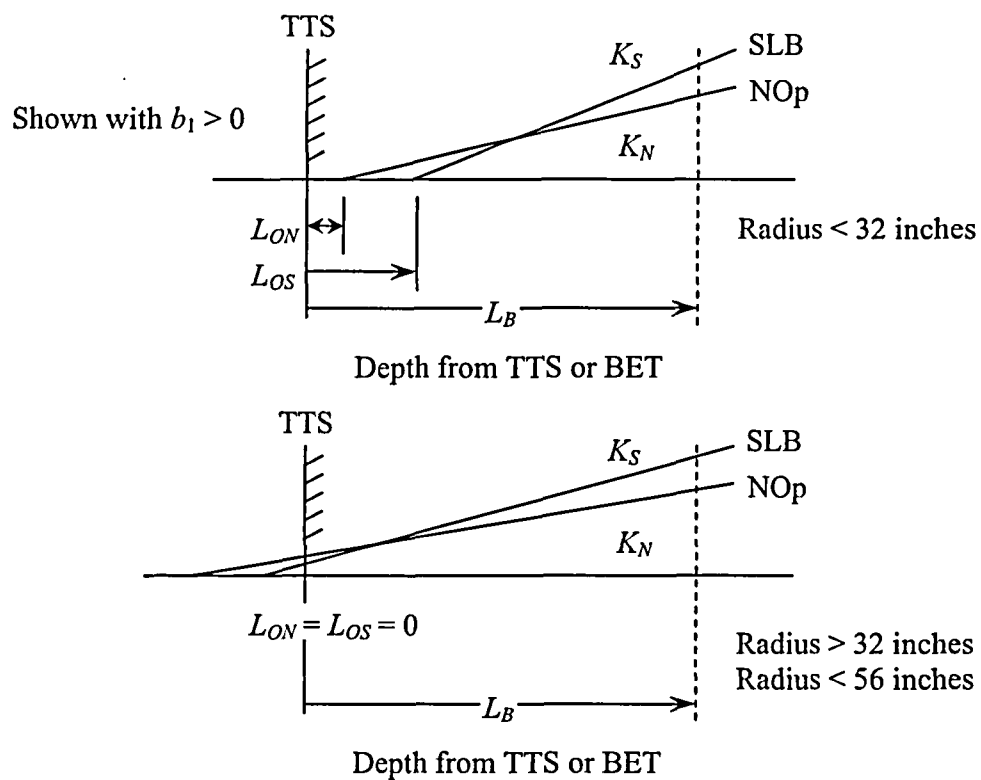
Figure 9-4. Schematic for the Determination of B* Parameters

a,c,e

Figure 9-5. First Order Linear Representation of Contact Pressure

a,c,e

Figure 9-6. Contact Pressure During Normal Operation (Model 44F)

a,c,e

Figure 9-7. Contact Pressure During SLB (2560 psi at 212°F)

NOp Contact Pressure Coefficients as Function of Radius a,c,e
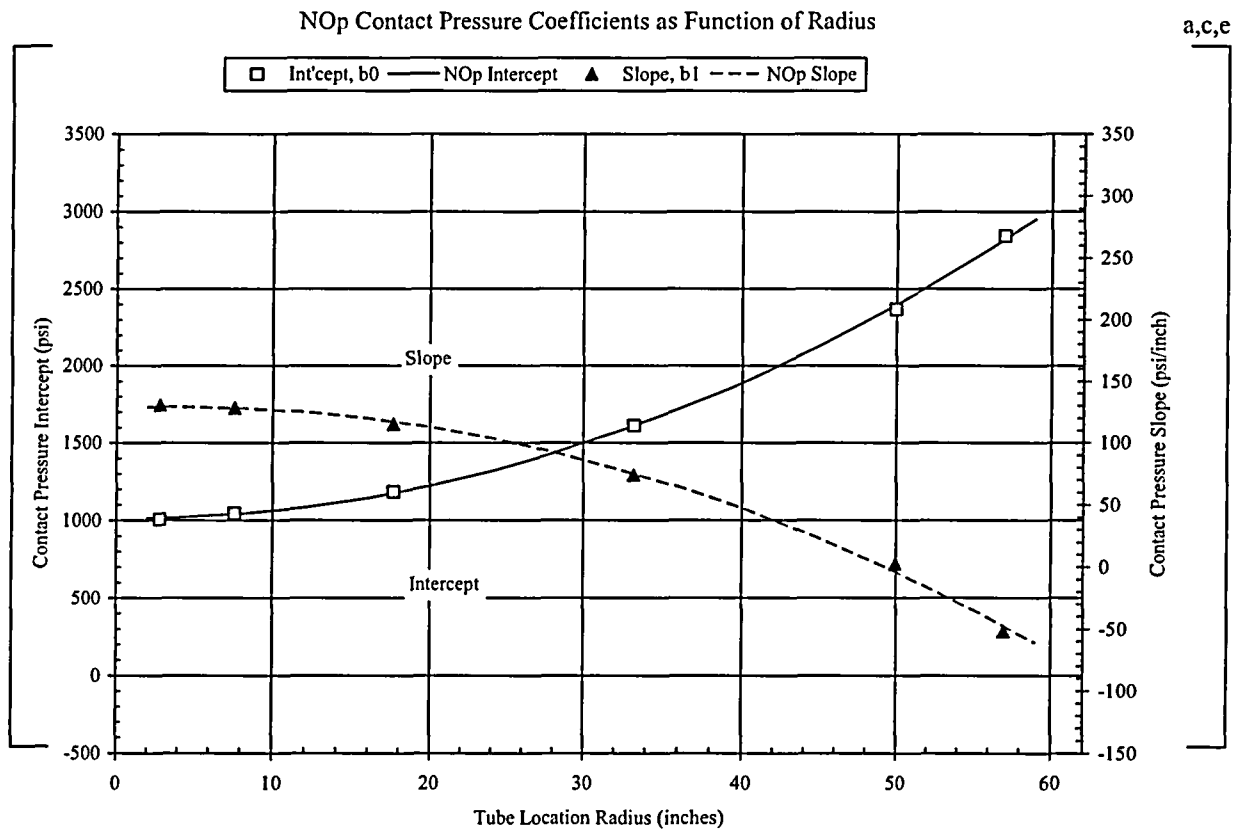
Figure 9-8. NOp Contact Pressure vs. Depth Coefficients by Radius

a,c,e

Figure 9-9. SLB Contact Pressure vs. Depth Coefficients by Radius

a,c,e

Figure 9-10. Comparison of Contact Pressure Coefficients for NOp & SLB Conditions (Hot Leg)

a,c,e

Figure 9-11. Elevation Below the TTS for Invariant Contact Pressure

a,c,e

Figure 9-12. TTS Contact Pressure for NOp & SLB Hot Leg Conditions

a,c,e

Figure 9-13. Viscosity of Water as a Function of Pressure

a,c,e

Figure 9-14. Viscosity of Water at 2560 psi as a Function of Temperature

a,c,e

Figure 9-15. Upper Bound B* for H.B. Robinson Unit 2 SGs for No Change in Resistance

a,c,e

Figure 9-16. Nominal B* for H.B. Robinson 2 SGs for No Change in Leak Rate

a,c,e

Figure 9-17. Graphical Determination of B* Depth from Flow Resistance

a,c,e

Figure 9-18. TTS Contact Pressure for NOp & SLB Cold Leg Conditions
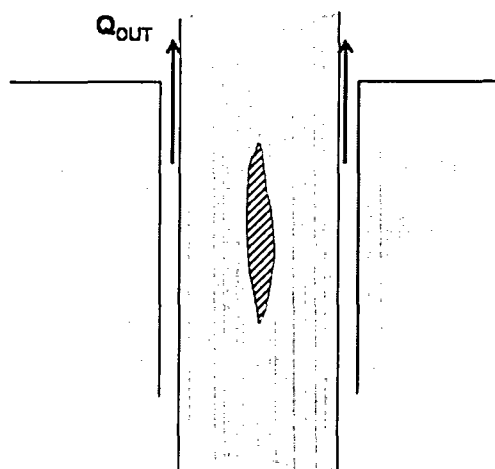
Figure 9-19. Sketch of Cracked Tube in Tubesheet leading to Leakage Flowrate, Q_{OUT}.
Note that the gap shown between the tube and the tubesheet is for illustration purposes only.
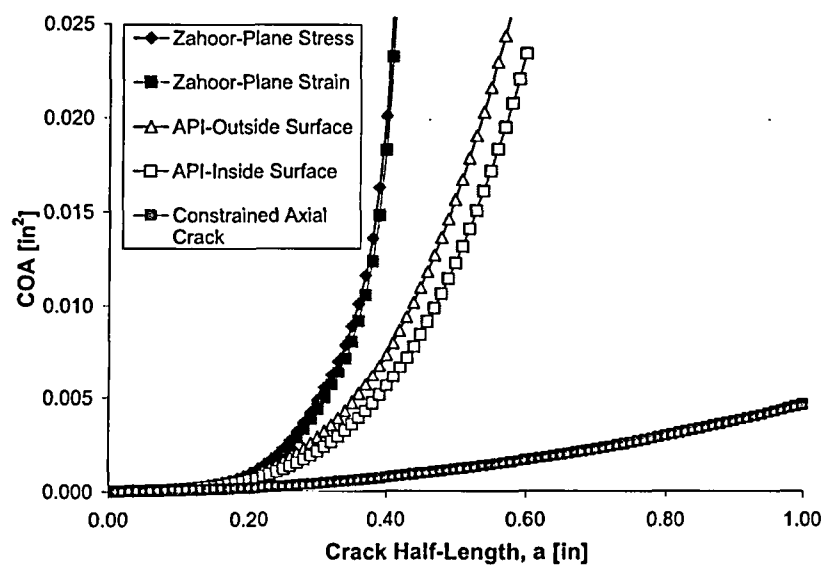
Figure 9-20. Comparison of Models for Calculating the Crack Opening Area
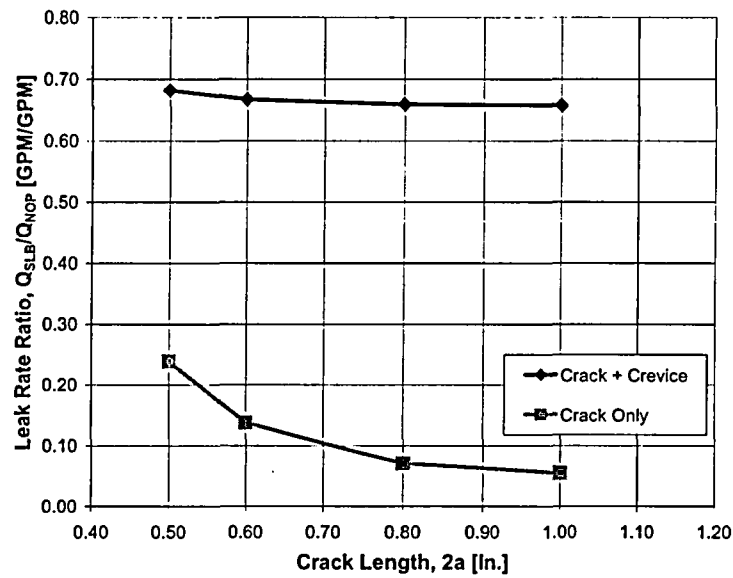
Figure 9-21. Leak Rate Ratio as a function of Axial Crack Length for a tubesheet radius of 60.248 In at the bottom of the tube sheet.
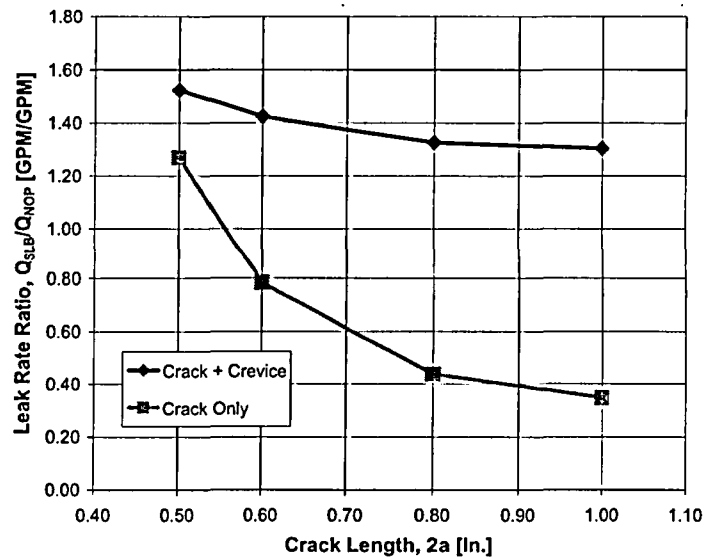
Figure 9-22. Leak Rate Ratio as a function of Circumferential Crack Length
for a tubesheet radius of 60.248 In at the bottom of the tube sheet

10.0 NRC STAFF DISCUSSION FOR ONE CYCLE APPROVAL B*
BRAIDWOOD UNIT 2

10.1 JOINT STRUCTURAL INTEGRITY DISCUSSION

As noted in Section 4.1, "Joint Structural Integrity" of Reference 13 and Section 3.1 of Reference 14, the NRC staff stated that the Westinghouse analyses that concluded that the required engagement distances that varies from 3 to 8.6 inches were not reviewed in detail and more qualitative arguments were used by the NRC staff for one time approval of the 17 inch tube joint inspection length. The qualitative arguments are stated below.

tube joint tightening associated with the radial differential thermal expansion and primary pressure inside the tube, contact pressure over at least a 6.5 inch distance should be considerably higher than the contact pressure simulated in the above mentioned pullout tests. A similar logic applied to the periphery of the tubesheet leads the staff to conclude that at the top 10.5 inches of the tubesheet region, contact pressure over at least a 6.5 inch distance should be considerably higher than the contact pressure simulated in the above mentioned pull out tests. Thus, the staff concludes that the proposed 17-inch engagement distance (or inspection zone) is acceptable to ensure the structural integrity of the tubesheet joint.

The NRC qualitative arguments are further supported on a more quantitative basis based on a study completed for the Model F steam generators for another plant (Reference 4). Moreover, similar statements were made in Reference 14 in approving a similar amendment for a plant with Model F SGs.

10.1.1 Discussion of Interference Loads

There are four source terms that must be considered relative to the determination of the interface pressure between the tube and the tubesheet. These are,

1. the initial preload from the installation of the tube,

2. internal pressure in the tube that is transmitted from the ID to the OD,

3. thermal expansion of the tube relative to the tubesheet, and

4. bowing of the tubesheet that results in dilation of the tubesheet holes.

The initial preload results from the plastic deformation of the tube material relative to that of the tubesheet. The material on the inside diameter experiences more plastic deformation than the material on the outside and thus has a deformed diameter which is incrementally greater. Equilibrium of the hoop forces and moments in the tube means that the OD is maintained in a state of hoop tension at a diameter greater than a stress free state. The model for the determination of the initial contact pressure between the tube and the tubesheet, P_c, is illustrated on Figure 10-3. Both the tube and the tubesheet behave as elastic springs after the expansion process is applied. The normal stress on the tube must be equal in magnitude to the normal stress on the tubesheet and the sum of the elastic springback values experienced by each must sum to the total interference.

As long as the tube and the tubesheet remain in contact the radial normal stresses must be in equilibrium. Thus, the problem of solving for the location of the interface and the contact pressure is determinate. The elements considered in the analysis are illustrated on Figure 9-3 for all operating and postulated accident conditions; the centerline of the tube and tubesheet hole are to the left in the figure. Each source of deformation of the tube outside surface starting from the installed equilibrium condition can be visualized starting from the top left side of the figure. The sources of deformation of the tubesheet inside surface can be visualized starting from the lower left side of the figure. As illustrated, although not to scale, the tube material has a coefficient of thermal expansion that is greater than that of the tubesheet. The radial flexibility[1], f, of the tube relative to that of the tubesheet determines how much of the pressure is actually

---

[1] Flexibility is the ratio of deformation to load and is the inverse of the stiffness.

transmitted to the interface between the tube and the tubesheet. Positive radial deformation of the tube in response to an internal pressure is found as the product of the pressure, P_p, and the tube flexibility associated with an internal pressure, discussed in the next section. Thus, the tube gets tighter in the tubesheet hole as the temperature of the tube and tubesheet increase. The deformation of the tube in response to an external pressure, P_s, is the product of the pressure times the flexibility associated with an external pressure. The normal operation contact pressure, P_N, is found from compatibility and equilibrium considerations. The deformation of the tubesheet hole in response to an internal pressure, P_s, is found as the product of the pressure and the flexibility of the tubesheet associated with an internal pressure. The opening or closing of the tubesheet hole, δr_i, resulting from bow induced by the primary-to-secondary pressure difference is in addition to the deformations associated with temperature and internal pressure. Once the tube has been installed, the deformations of the tube and tubesheet associated thermal expansion, internal pressure, and tubesheet bow remain linearly elastic.

Because of the potential for a crack to be present and the potential for the joint to be leaking, the pressure in the crevice is assumed to vary linearly from the primary pressure at the crack elevation to the secondary pressure at the top of the tubesheet. If the joint is not leaking, it would be expected that there was no significant fluid pressure in the crevice. The pressure assumption is considered to be conservative because it ignores the pressure drop through the crack, and the leak path is through the crevice will not normally be around the entire circumference of the tube. In addition, the leak path is believed to be between contacting microscopic asperities between the tube and the tubesheet, thus the pressure in the crevice would not be acting over the entire surface area of the tube and tubesheet. In any event, pressure in the crevice is always assumed to be present for the analysis.

There is no bow induced increase in the diameter of the holes during normal operation or postulated accident conditions below the mid span elevation within the tubesheet, hence most analyses concentrate on locations near the top of the tubesheet. The tubesheet bow deformation under postulated accident conditions will increase because of the larger pressure difference between the bottom and top of the tubesheet. The components remain elastic and the compatibility and equilibrium equations from the theory of elasticity remain applicable. Below the mid span elevation within the tubesheet the tubesheet holes will contract. The edges of the tubesheet are not totally free to rotate and there is some suppression of the contraction near the outside radius. This also means that the dilation at the top of the tubesheet is also suppressed near the outside radius of the tubesheet. The maximum hole dilations occur near the center of the tubesheet.

The application of the theory of elasticity means that the individual elements of the analysis can be treated as interchangeable if appropriate considerations are made. The thermal expansion of the tube can be thought of as the result of some equivalent internal pressure by ignoring Poisson effects, or that tubesheet bow could be analytically treated as an increase in temperature of the tubesheet while ignoring associated changes in material properties.

10.1.2 Flexibility Discussion

Recall flexibility, f, is defined as the ratio of deflection relative to applied force. It is the inverse of stiffness which commonly used to relate force to deformation. There are four flexibility terms associated with the radial deformation of a cylindrical member depending on the surface to which the loading is applied and the surface for which the deformation is being calculated, e.g., for transmitted internal

pressure one is interested in the radial deformation of the OD of the tube and the ID of the tubesheet. The deformation of the OD of the tube in response to external pressure is also of interest. The geometry of the tube-to-tubesheet interface is illustrated on Figure 10-1. The flexibility of the tubesheet, designated herein by the subscript c, in response to an internal pressure, P_{ci}, is found as,

$$\left[\right]^{a,c,e} \qquad \text{Tubesheet} \quad (1)$$

where, r_{ci} = inside radius of the tubesheet and outside radius of the tube,
r_{co} = outside radius of the tubesheet hole unit cell,
E_c = the elastic modulus of the carbon steel tubesheet material, and
υ = Poisson's ratio for the tubesheet material.

Here, the subscripts on the flexibility stand for the component, c for tubesheet (and later t of tube), the surface being considered, i for inside or o for outside, and the surface being loaded, again, i for inside and o for outside. The superscript designates whether the cylinder is open, o, or closed, c, of interest in dealing with the end cap load from pressure in the tube. The former case is a state of plane stress and the latter is not since a closed cylinder has an end cap load. The flexibility of the tube in response to the application of an external pressure, P_{ro}, e.g., the contact pressure within the tubesheet, is,

$$\left[\right]^{a,c,e} \qquad \text{Open Tube} \quad (2)$$

Poisson's ratio is the same for the tube and the tubesheet. When the external pressure can act on the end of the tube,

$$\left[\text{,} \right]^{a,c,e} \qquad \textit{Closed Tube} \quad (3)$$

where E_t is the elastic modulus of the tube material. The flexibility of the tube in response to an external pressure is different when the secondary side pressure is present because that pressure also acts to compress the tube in the axial direction giving rise to a Poisson expansion effect, resisting the radial compression due to the pressure.

Finally, the flexibility of the outside radius of the tube in response to an internal pressure, Pti, is,

$$\left[\right]^{a,c,e} \qquad \textit{Closed Tube} \quad (4)$$

where r_{ti} is the internal radius of the tube and the tube is assumed to be closed. For an open tube the term in parentheses in the numerator is simply 2. A closed tube expands less due to Poisson contraction associated with the end cap load from the internal pressure. A summary of the applicable flexibilities is provided in Table 10-1. Note that during normal operation there is an end cap load on the tube from the secondary pressure but not from that associated with the fluid in the crevice if the joint is leaking. Both flexibilities would then be involved in calculating the radial deformation of the outside of the tube. Only the open tube flexibility is used with the pressure in the crevice for postulated accident conditions.

When the inside of the tube is pressurized, P_{ti}, some of the pressure is absorbed by the deformation of the tube within the tubesheet and some of the pressure is transmitted to the OD of the tube, P_{to}, as a contact pressure with the ID of the tubesheet. The magnitude of the transmitted pressure is found by considering the relative flexibilities of the tube and the tubesheet as,

$$\left[\right]^{a,c,e} \tag{5}$$

Note that the tube flexibility in response to the contact pressure is for an open tube because there is no end cap load associated with the contact pressure. The denominator of the fraction is also referred to as the interaction coefficient between the tube and the tubesheet. About 85 to 90% of the pressure internal to the tube is transmitted through the tube in Westinghouse designed SGs. However, the contact pressure is not increased by that amount because the TS acts as a spring and the interface moves radially outward in response to the increase in pressure. The net increase in contact pressure is on the order of 56.4% of the increase in the internal pressure. For example, the contact pressure between the tube and the tubesheet is increased by about 1970 psi during normal operation relative to ambient conditions. Likewise, the increase in contact pressure associated with SLB conditions is about 2250 psi relative to ambient conditions.

When the temperature increases from ambient conditions to operating conditions the differential thermal expansion of the tube relative to the tubesheet increases the contact pressure between the tube and the tubesheet. The mismatch in expansion between the tube and the tubesheet, δ, is given by,

$$\delta = \left(\alpha_t \Delta T_t - \alpha_c \Delta T_c\right) r_{to} \qquad \text{Thermal Mismatch} \tag{6}$$

where: α_t, α_c = thermal expansion coefficient for the tube and tubesheet respectively,

ΔT_t, ΔT_c = the change in temperature from ambient conditions for the tube and tubesheet respectively.

During normal operation the temperature of the tube and tubesheet are effectively identical to within a very short distance from the top of the tubesheet and the individual changes in temperature can usually be replaced by ΔT_t, thus,

$$\delta = \left(\alpha_t - \alpha_c\right)\Delta T_t \, r_{to}. \tag{7}$$

The change in contact pressure due to the increase in temperature relative to ambient conditions, P_T, is given by,

$$\left[\right]^{a,c,e} \tag{8}$$

Likewise, the same equation can be used to calculate the reduction in contact pressure resulting from a postulated reduction the temperature of the tube during a postulated SLB event.

The net contact pressure, P_C, between the tube and the tubesheet during operation or accident conditions is given by,

$$\text{Net Contact Pressure } P_C = P_0 + P_P + P_T - P_B \tag{9}$$

where P_B is the loss of contact pressure due to dilation of the tubesheet holes, P_0 is the installation preload, P_P is the pressure induced load, and P_T is the thermal induced contact load. There is one additional term that could be considered as increasing the contact pressure. When the temperature increases the tube expands more in the axial direction than the tubesheet. This is resisted by the frictional interface between the tube and the tubesheet and a compressive stress is induced in the tube. This in turn results in a Poisson expansion of the tube radius, increasing the interface pressure. The effect is not considered to be significant and is essentially ignored by the analysis.

10.1.3 Analysis

From the preceding discussions it is apparent that the contact pressure during normal operation can be found by equating the total deformation of the outside radius of the tube, r_{to}, to the total deformation of the inside radius of the tubesheet hole, r_{ci}, where the net deformation of the outside of the tube, δ_{to}, is given by,

$$\text{Tube Deformation } \quad \delta_{to} = \alpha_t \Delta T_t r_{to} + P_p f_{toi}^c + P_s f_{too}^c + P_N f_{too}^o \tag{10}$$

and the net deformation of the tubesheet hole, δ_{ci}, is given by,

$$\text{TS Deformation } \quad \delta_{ci} = \alpha_c \Delta T_c r_{ci} + P_s f_{cii}^o + \delta r_i + P_N f_{cii}^o. \tag{11}$$

The inclusion of the P_N terms assures compatibility and the two net deformations must be equal. It can usually be assumed that the secondary fluid pressure does not penetrate the tubesheet hole and the terms involving P_s may be ignored. All of the terms except for the final contact pressure, P_N, are known and the tubesheet bow term, δ_{ri}, is found from the finite element model analysis of the tubesheet. The total contact pressure during operation is then found as P_N plus P_c, the installation contact pressure. For postulated SLB conditions the solution is obtained from,

$$\alpha_t \Delta T_t r_{to} + P_p f_{toi}^c + P_N f_{too}^o = \alpha_c \Delta T_c r_{ci} + \delta r_i + P_N f_{cii}^o, \tag{12}$$

or, the total contact pressure during a postulated SLB event is given by,

$$\text{SLB Contact Pres.} \quad P_T = P_c + \frac{\alpha_t \Delta T_t r_{to} - \alpha_c \Delta T_c r_{ci} + P_p f_{toi}^c - \delta r_i}{f_{cii}^o - f_{too}^o}, \tag{13}$$

where $r_{to} = r_{ci}$. A similar expression with more terms is used to obtain the contact pressure during normal operation. The denominator of the above equation is referred to as the tube-to-tubesheet influence coefficient because it related deformations associated with the interfacing components to the interface pressure. The influence coefficient for Westinghouse Model F SG tubes is calculated using the information tabulated in Table 10-1 as $3.33 \cdot 10^{-6}$ psi/inch.

By taking partial derivatives with respect to the various terms on the right the rate of change of the contact pressure as a function of changes in those parameters can be easily calculated. For example, the rate of change of the contact pressure with the internal pressure in the tube is simply,

$$\frac{\Delta P_N}{\Delta P_p} = \frac{f_{toi}^c}{f_{cii}^o - f_{too}^o}. \tag{14}$$

Thus, the rate of change of contact pressure with internal pressure in the tube is 0.564 psi/psi. Likewise, the rate of change of the contact pressure with change in the tube temperature or tubesheet temperature is given by,

$$\frac{\Delta P_N}{\Delta T_t} = \frac{\alpha_t r_{to}}{f_{cii}^o - f_{too}^o} \quad \text{and} \quad \frac{\Delta P_N}{\Delta T_c} = - \frac{\alpha_c r_{ci}}{f_{cii}^o - f_{too}^o}, \tag{15}$$

respectively. Again using the values in Table 10-1, the rate of change of contact pressure with tube temperature is 18.3 psi/°F if there is no increase in tubesheet temperature. The corresponding change with an increase in tubesheet temperature without an increase in tube temperature is -17.36 psi/°F leave a net increase in contact pressure of 0.94 psi/°F with a uniform increase in temperature of the tube and the tubesheet.

Finally, the rate of change of contact pressure with tubesheet bow is calculated as,

$$\frac{\Delta P_N}{\Delta \delta r_{ci}} = \frac{1}{f_{cii}^o - f_{too}^o}. \tag{16}$$

The effect of the dilation associated with the tubesheet bow can be calculated using the information tabulated in Table 10-1. For each 0.1 mil of diameter dilation the interface pressure is reduced on the order of 380 psi. A summary of all of the contact pressure influence factors is provided in Table 10-2. A summary of tubesheet bow induced hole dilation values is provided in Table 10-3.

10.1.4 Conclusions

Although the study was completed for a Model F SG, the results listed in Table 10-3 indicate that the effect of tubesheet bow can result in a significant average decrease in the contact pressure during postulated accident conditions above the neutral plane. However, for the most severe case in one plant, in tube R18C77, the diametral change at the worst case location is less than 0.2 mils at the H* depth during postulated accident conditions. This same type of result would be expected to be the case for the Model 44F steam generators in H.B. Robinson Unit 2. Below the neutral plane, tubesheet bow is shown not to result in any tube dilation thus supporting the NRC staff conclusion that:

> "Given the neutral axis to be at approximately the mid-point of the tubesheet thickness (i.e., 10.5 inches below the TTS to 17 inches below the TTS), tubesheet bore dilation effects would be expected to further tighten the joint from 10 inches below the TTS to 17 inches below the TTS which would be the lower limit of the proposed tubesheet region inspection zone. Combined with the effects of the tube joint tightening associated with the radial differential thermal expansion and primary pressure inside the tube, contact pressure over at least a 6.5 inch distance should be considerably higher than the contact pressure simulated in the above mentioned pullout tests."

10.2 JOINT LEAKAGE INTEGRITY DISCUSSION

As noted in Section 4.2, "Joint Leakage Integrity," of Reference 14, the NRC staff reviewed the qualitative arguments developed by Westinghouse regarding the conservatism of the conclusion that a minimum 17 inch engagement length ensures that leakage during a main steam line break (MSLB) will not exceed two times the observed leakage during normal operation. The NRC staff reviewed the qualitative arguments developed by Westinghouse regarding the conservatism of the "bellwether approach", but the NRC staff's depth of review did not permit it to credit Westinghouse's insights from leak test data that leak flow resistance is more sensitive to changes in joint contact pressure as contact pressure increases due to the log normal nature of the relationship. The staff was still able to conclude that there should be no significant reduction in leakage resistance when going from normal operating to accident conditions.

The basis for the Westinghouse conclusion that flow resistance varies as a log normal linear function of joint contact pressure is provided in detail below. The data from the worst case tube in a comparative study analytically supports the determination that there is at least an eight inch zone in the upper 17 inches of the tubesheet where there is an increase in joint contact pressure due to a higher primary pressure inside the tube and changes in tubesheet bore dilation along the length of the tubes. The NRC concurs that the factor of 2 increase in leak rate as an upper bound by Westinghouse is reasonable given the stated premise that the flow resistance between the tube and the tubesheet remains unchanged between normal operating and accident pressure differential. The NRC staff notes in Reference 4 that the assumed linear relationship between leak rate and differential pressure is conservative relative to alternative models such as the Bernoulli or orifice models, which assumes leak rate to be proportional to the square root of the differential pressure.

The comparative study supports the NRC staff conclusion that "considering the higher pressure loading when going from normal operating to accident conditions, Westinghouse estimates that contact pressures,

and, thus, leak flow resistance, always increases over at least an 8 inch distance above 17 inches below the top of the tubesheet appears reasonable to the NRC Staff."

10.2.1 Loss Coefficient Contact Pressure Correlation

For subsequent analyses, the loss coefficient of the flow through the tube-to-tubesheet crevice must be determined as a function of the contact pressure between the tube and tubesheet. The plot of loss coefficient versus contact pressure for the Model D5 and Model F steam generators is provided in Section 6.3 of this report.

Since the Model D5, Model F and Model 44F steam generators have similar geometry along the tube-to-tubesheet crevice path, the Model D5 loss coefficients that were previously calculated can be used as applicable loss coefficients for the Model 44F steam generators. However, the Model D5 steam generator tubes have an outer diameter of 0.75 inch while the Model 44F steam generator tubes have an outer diameter of 0.875 inch. Therefore, in order to apply the Model D5 loss coefficients (which includes normalized Model F test results) to the Model 44F steam generators, the Model D5 loss coefficients must be multiplied by the ratio 0.750/0.875, which is the ratio of the Model D5 SG tube circumference to the Model 44F steam generator circumference. By applying the aforementioned scaling factor to the Model D5 loss coefficients, the results obtained are considered to be the loss coefficients that would have been obtained during the Model D5 testing if the Model D5 steam generators had tubes with an 0.875 inch outer diameter rather than 0.750 inch outer diameter.

A new linear regression and an uncertainty analysis was performed for the Model 44F steam generator. Figure 10-4 provides a plot of the loss coefficient versus contact pressure with the linear regression trendline for the combined data represented as a thick, solid black line. The regression trendline is approximated by the following log-linear relation,

$$Log_{10}(K) = A\sigma_c + B$$

where A = slope of log-linear regression trendline,
        B = y-intercept of log-linear regression trendline.

Therefore, the log-linear fit to the scaled Model 44F loss coefficient data follows the equation

$$Log_{10}(K) = (2.14)\sigma_c + 12.186 \qquad \text{(Reference 34)}$$

Table 10-1. Radial Flexibilities Times Elastic Modulus (in./psi)					a,c,e

Table 10-2. Contact Pressure Influence Factors for Model F SG Tubes at 600°F		a,c,e

	Table 10-3. Tubesheet Hole Diametral Dilation for R18C77					a,c,e

Tube-to-Tubesheet Unit Cell Geometry.

r_{ti} = Inside radius of the tube.

r_{to} = Outside radius of the tube, and inside radius of TS unit cell.

r_{co} = Outside radius of TS unit cell.
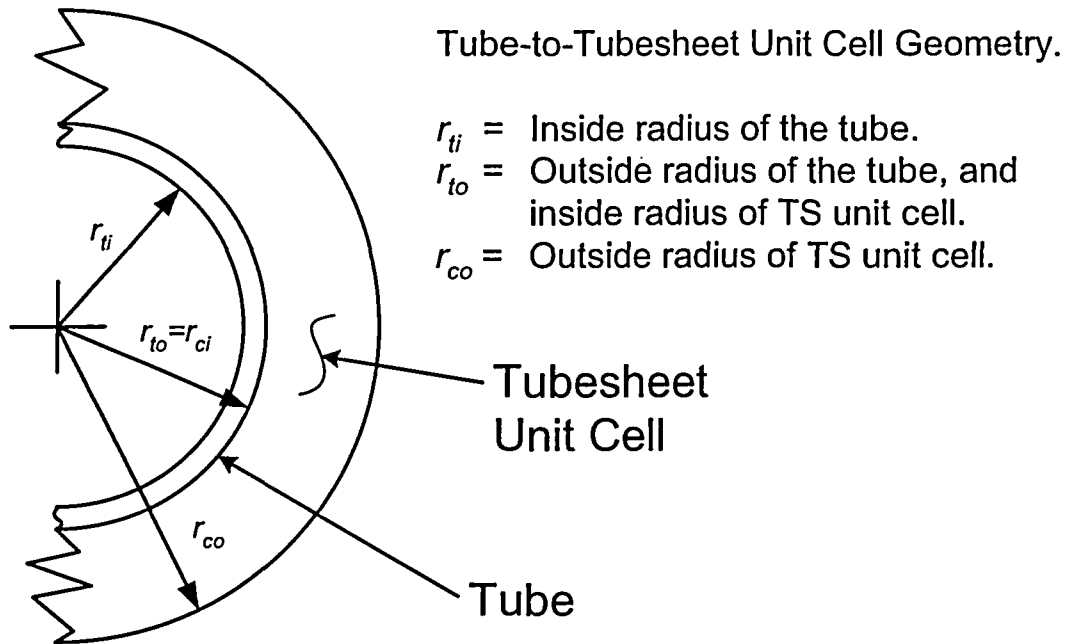
Figure 10-1. Geometry of the Tube-to-Tubesheet Interface

a,c,e

Figure 10-2. Model for Initial Contact Pressure
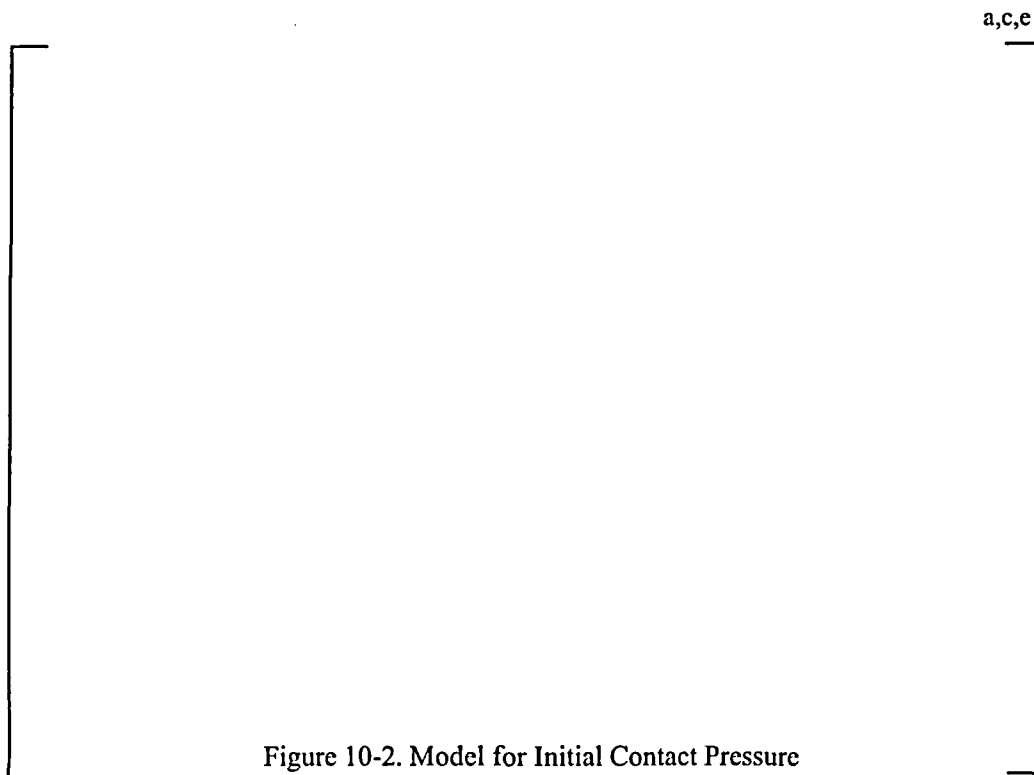
a,c,e

Figure 10-3. Determination of Contact Pressure, Normal or Accident Operation

(As illustrated, the bow does not result in a loss of contact, however, there are situations where the bow is sufficient to result in a loss of contact between the tube and the tubesheet at the top of the tubesheet.)

a,c,e

Figure 10-4. Scaled Flow Resistance Curve for Model 44F Steam Generators

11.0 CONCLUSIONS

The evaluation of Section 7.0 of this report provides a technical basis for assuring that the structural performance criteria of NEI 97-06 are inherently met for degradation of any extent below the H* depth identified in Section 7.0, i.e., depths ranging from 4.78 to 8.34 inches below the TTS (including an allowance of 0.3 inches to account for the hydraulic expansion transition) selected to be bounding for all tubes in all zones. The corresponding evaluation presented in Section 9.0 provides a technical basis for bounding the potential leak rate from non-detected indications in the tube region below about 8.01 inches from the top of the tubesheet as no more than twice the leak rate during normal operation, see Figure 9-15. A similar analysis obtained a depth of about 9.8 inches based on restricting the expected leak rate to being the same as that during normal operation, Figure 9-16. The evaluation is independent of the magnitude of any degradation that might occur because it is based solely on the resistance of the interface between the tube and the tubesheet. In other words, the tube may be nonexistent below the B* depth. The conclusion is general in that the depths determined are for the most severely affected region of the tubesheet, the central region. The conclusions also apply to any postulated indications in the tack expansion region and in the tube-to-tubesheet welds, although the level of conservatism would be significantly more. As noted in the introduction to this report, the reporting of crack-like indications in the tube-to-tubesheet welds would be expected to occur inadvertently since no structural or leak rate technical reason exists for a specific examination to take place.

A graphical summary of the findings are presented on Figure 11-1. The depths associated with H*[1] and B* are presented relative to the left ordinate while the leak rates are presented relative to the right ordinate as a function of radial location from the center of the tubesheet.

- The H* depths are bounding relative to a B* for equal leak rate resistance during NOp and SLB. This means that if the structural limits, H*, are satisfied, the leakage limit, B*, will also be satisfied.

- The SLB leak resistance is greater than that at NOp outside a radius of 4 inches, thus for a differential pressure during SLB of 2.0 times that during NOp the leak rates would be expected to be less than twice that at NOp. Beyond 4 inches the resistance to leak during SLB increases relative to that for NOp and the leak rate would be expected to decrease, becoming about a factor of 1.3 less at 45 inches and 2.9 less near the periphery.

The conclusions to be drawn from the performed analyses are that:

1) There is no structural integrity concern associated with tube or tube weld cracking of any extent provided it occurs below the H* distance as reported in Section 7.0 of this report. The pullout resistance of the tubes has been demonstrated for axial forces associated with 3 times the normal operating differential pressure and 1.4 times differential pressure associated with the most severe postulated accident.

2) Contact forces during postulated LOCA events are sufficient to resist axial motion of the tube. Also, if the tube end welds are not circumferentially cracked, the resistance of the tube-to-

---

[1]   The presented H* depths are depicted for individual radii from the center of the tubesheet rather than by zone for comparative purposes.

tubesheet hydraulic joint is not necessary to resist push-out. Moreover, the geometry of any postulated circumferential cracking of the weld would result in a configuration that would resist pushout in the event of a loss of coolant accident. In other words, the crack flanks would not form the cylindrical surface necessary such that there would be no resistance to expulsion of the tube in the downward direction.

3) The leak rate for indications below a B* depth of about 8.01 inches from the top of the tubesheet would be bounded by twice the leak rate that is present during normal operation of the plant regardless of tube location in the bundle. This is initially apparent from comparison of the contact pressures from the finite element analyses over the full range of radii from the center of the tubesheet, and ignores any increase in the leak rate resistance due to the contact pressure changes and associated tightening of the crack flanks. The expectation that this would be the case was confirmed by the detailed analysis of the relative leak rates of Section 9.0.

4) The H* depth bounds the relocation of the pressure boundary for all radial locations on the tubesheet. The B* evaluations were performed utilizing the same operating parameters that were used for the determination of the depths required to meet the structural performance criteria, that is, conservative values for the operating temperature.

In conclusion, a relocation of the pressure boundary to the deeper of the H* or B* values is acceptable from both a structural and leak rate considerations depending to the relative allowable leak rate during accident conditions. The prior conclusions rely on the inherent strength and leak rate resistance of the hydraulically expanded tube-to-tubesheet joint, a feature which was not considered or permitted to be considered for the original design of the SG. Thus, omission of the inspection of the weld constitutes a reassignment of the pressure boundary to the tube-to-tubesheet interface. Similar considerations for tube indications require NRC staff approval of a license amendment. Consideration of the allowable leak rate during accident conditions may necessitate locating the reassigned pressure boundary to a depth greater than that required for structural integrity, i.e., H*.

The analyses demonstrate that the evaluation of the conditions on the hot leg bound those for the cold leg with regard to leak rate performance. However, as previously noted, the structural results for the cold leg are bounding relative to the hot leg. The maximum difference is approximately 0.15 inch. A summary is provided in Table 7-12.

It is important to note that all of the evaluations performed considered the tube to be severed at the reassigned pressure boundary location with no resistance to flow from the leak path within the tube itself, i.e., cracks. At the specified depths the crack flanks would be restricted from opening or parting, and may be held tighter, thus reducing the accident condition leak to below that anticipated herein.

With regards to the preparation of a significant hazards determination, the results of the testing and analyses demonstrate that the relocation of the pressure boundary to a depth based on the more conservative of either H* or B* does not lead to an increase in the probability or consequences of the postulated limiting accident conditions because the margins inherent in the original design basis are maintained and the expected leak rate during the postulated accident is not expected to increase beyond the plant specific limit. In addition, the relocation of the pressure boundary does not create the potential for a new or departure from the previously evaluated accident events. Finally, since the margins inherent

in the original design bases are maintained, no significant reduction in the margin of safety would be expected.

EXAMPLE APPLICATION FOR H.B. ROBINSON UNIT 2

This document provides a technical justification for limiting the RPC inspection in the tubesheet expansion region to less than the full depth of the tubesheet (21.81 in.). The justification includes two necessary parts to satisfy both the structural requirements and the leakage requirements under normal operating conditions and under limiting accident conditions:

- H* addresses the structural requirements. H* defines the minimum length of engagement required for hydraulically expanded tubes to prevent tube pullout from the tubesheet under limiting accident conditions. The principal loads acting to pull a tube from the tubesheet are end-cap loads resulting from the primary to secondary pressure differentials. H* varies with radial position from the tubesheet centerline due to tubesheet bow resulting from the primary-to-secondary pressure differential. The bow increases during accident conditions due to a greater pressure differential across the tubesheet. Increased tubesheet bow causes tube-hole bore dilation above the neutral axis resulting in reduced interface loads between the tube and the tubesheet. Tubesheet bending varies with the radial distance from the centerline of the tubesheet as dictated by the structural constraints of the tubesheet, e.g., shell and support ring on the OD and divider plate at the centerline.

- B* addresses leakage requirements. As defined in this document, B* is the distance from the top of the tubesheet where the leakage flow resistance at SLB conditions equals the leakage flow resistance at normal operating conditions. This definition of B* is useful in that the accident leakage will be equal to the ratio of the accident pressure differential to the normal operating pressure differential times the normal operating leakage. If effect, the normal operating leakage becomes a "bellwether" for the accident leakage; therefore, if normal operating leakage is within acceptable limits, accident induced leakage will also be within acceptable limits.

The Technical Specification allowable normal operating leak rate for H.B. Robinson Unit 2 is 75 gpd (0.05 gpm) and the allowable accident induced leak rate is 150 gpd (0.1 gpm) total in the affected SG. The SLB differential pressure is a factor of 1.77 greater than the NOp differential pressure at H.B. Robinson Unit 2. Therefore, if the current NOp leakage is at its limiting value, 0.05 gpm (75 gpd), the accident induced leakage will not exceed 0.085 gpm (127.5 gpd) if the bounding values of H* and B* are applied. Recall that this does not include consideration of the reduction in flow associated with an increase in viscosity as the temperature decreases.

A summary of the H* and B* required engagement depths is provided in Table 11-1. The following observation can be made from the information in the table and on Figure 11-1 for the hot leg and on Figure 11-2 for the cold leg relative to example application. Using a maximum H* depth of 9.00 inches as the governing inspection depth is sufficient to address all hot and cold leg considerations for both structural and leak rate integrity. (8.04 inches for H* + 0.30 in. uncertainty for the distance of the BET from the top of the tubesheet + 0.28 in. eddy current uncertainty in determining the distance of an axial crack tip from the BET (maximum)+0.12 in. eddy current uncertainty in determining the length of non-degraded tube < 9.0 inches). A greater distance is required to prevent tube pullout than that is required to

achieve equal NOp and SLB flow resistances on either the hot or cold leg. It is important to note that the inspection depth of 9.0 inches has significantly increasing margin progressing from the center of the tubesheet relative to tube pullout capability and tube bundle leak tightness.

With the incorporation of responses to the NRC Seabrook RAIs into the report, it is concluded that this same report also supports the implementation of a more conservative permanent change to the H.B. Robinson Unit 2 plant Technical Specifications to incorporate a 17 inch inspection length of the SG tubes within the tubesheet using a rotating probe.

Table 11-1: Calculated H* & B* Depths by Radial Zone				
Location		H* Depths (in.)	B* Depths (in.)	
Zone	Radius (in.)	Hot and Cold Leg	Hot Leg	Cold Leg
A	≤ 57.03	4.78	< 1	< 1
B	≤34.372	7.12	6.762	5.18
C	≤23.227	8.34	8.01	6.70

a,c,e

Figure 11-1. Comparison of H* and B* Hot Leg Results

a,c,e

Figure 11-2. Comparison of H* and B* Cold Leg Results

12.0 REFERENCES

1. WCAP-11224, Rev. 1, "Tubesheet Region Plugging Criterion for the Duke Power Company McGuire Nuclear Station Units 1 and 2 Steam Generators," Westinghouse Electric Company LLC, Pittsburgh, PA, October 1986.

2. WCAP-13532, Rev. 1, "Sequoyah Units 1 and 2 W* Tube Plugging Criteria for SG Tubesheet Region of WEXTEX Expansions," Westinghouse Electric Company LLC, Pittsburgh, PA, 1992.

3. WCAP-14797, Rev. 2 "Generic W* Tube Plugging Criteria for 51 Series Steam Generator Tubesheet Region WEXTEX Expansions," Westinghouse Electric Company LLC, Pittsburgh, PA, 1997.

4. Safety Evaluation by the Office of Nuclear Reactor Regulation Related to Amendment No. 129 to Facility Operating License No. DPR-80 and Amendment No. 127 to Facility Operating License No. DPR-82 Pacific Gas and Electric Company Diablo Canyon Nuclear Power Plant, Units 1 and 2 Docket Nos. 50-275 and 50-323," United States Nuclear Regulatory Commission, Washington, DC, 1999.

5. NSD-RFK-96-015, "Vogtle 1 Tube Integrity Evaluation, Loose Part Affected SG," Westinghouse Electric Company LLC, Pittsburgh, PA, June 9, 1996.

6. NEI 97-06, Rev. 2, "Steam Generator Program Guidelines," Nuclear Energy Institute, Washington, DC, October 2005.

7. OE19662 (Restricted & Confidential), "Steam Generators (Catawba Nuclear Power Station)," Institute of Nuclear Power Operations (INPO), Atlanta, GA, USA, December 13, 2004.

8. IN 2005-09, "Indications in Thermally Treated Alloy 600 Steam Generator Tubes and Tube-to-Tubesheet Welds," United States Nuclear Regulatory Commission, Washington, DC, April 7, 2005.

9. SGMP-IL-05-01, "Catawba Unit 2 Tubesheet Degradation Issues," EPRI, Palo Alto, CA, March 4, 2005.

10. OE20339, "Vogtle Unit 1 Steam Generator Tube Crack Indications," Institute of Nuclear Power Operations (INPO), Atlanta, GA, USA, April 4, 2005.

11. ASME Boiler and Pressure Vessel Code, Section III, "Nuclear Power Plant Components," American Society of Mechanical Engineers, New York, New York, 1965, Summer 1966 Addenda

12. GL 2004-01, "Requirements for Steam Generator Tube Inspections," United States Nuclear Regulatory Commission, Washington, DC, August 30, 2004.

13. NRC Letter, "Wolf Creek Generating Station – Issuance of Exigent Amendment Re: Steam Generator (SG) Tube Surveillance Program (TAC No. MC6757)," United States Nuclear Regulatory Commission, Washington DC, April 28, 2005.

14. NRC Letter, "Braidwood Station, Units 1 and 2 – Issuance of exigent Amendments Re: Revision of the Scope of Steam Generator Inspections for Unit 2 Refueling Outage 11 – (TAC Nos. MC6686 and MC 6687)," United States Nuclear Regulatory Commission, Washington DC, April 25, 2005

15. NRC Letter, "Vogtle Electric Generating Plant, Units 1 and 2 RE: Issuance of Amendments Regarding the Steam Generator Tube Surveillance Program (TAC Nos. MC8078 and MC8079)," United States Nuclear Regulatory Commission, Washington, DC, September 21, 2005.

16. LTR-CDME-05-82, "Limited Inspection of the Steam Generator Tube Portion Wihin the Tubbesheet of the Wolf Creek Generation Station," Westinghouse Electric Company LLC, Pittsburgh, PA, April 2005.

17. PCWG-862, "PCWG Minutes (April 29, 1980 Meeting), 5/20/1980 (Original Steam Generators)

18. NSD-E-SGDA-98-3611 (Proprietary), "Transmittal of Yonggwang Unit 2 Nuclear Power Plant Steam Generator Tube-to-Tubesheet Joint Evaluation," Westinghouse Electric Company LLC, Pittsburgh, PA, November 1998.

19. WCAP-16124, "Justification of the Partial Length Rotating Pancake Coil (RPC) Inspection of the Tube Joints of the Wolf Creek Model F Steam Generators," Westinghouse Electric Company, LLC, Pittsburgh, PA, December 2003.

20. CN-SGDA-03-87 (Proprietary), "Evaluation of the Tube/Tubesheet Contact Pressures and H* for Model D5 Steam Generators at Byron, Braidwood, Catawba and Comanche Peak," Westinghouse Electric Company LLC, Pittsburgh, PA, October 2003..

21. CN-SGDA-02-152 (Proprietary), Rev. 1, "Evaluation of the Tube-to-Tubesheet Contact Pressures for Callaway Model F Steam Generators," Westinghouse Electric Company LLC, Pittsburgh, PA, March 2003.

22. NCE-88-271 (Proprietary), "Assessment of Tube-to-Tubesheet Joint Manufacturing Processes for Sizewell B Steam Generators Using Alloy 690 Tubing," Westinghouse Electric Company, LLC, Pittsburgh, PA May 2003.

23. WCAP-14871 (Proprietary), "Vogtle Electric Generating Plant (VEGP) Steam Generator Tube-to-Tubesheet Joint Evaluation," Westinghouse Electric Company, LLC, Pittsburgh, PA May 1997.

24. DP-SGDA-05-2, Rev. 0, "Data Package for H Star Pull Test of 7/8 Inch Tubing for Simulated Tubesheet, PA-MSC-0199 WOG Program", November 2005.

25. WNEP-8323 (Proprietary), "Model 44F Replacement Steam Generator Stress Report for Carolina Power and Light H.B. Robinson Unit 2", April 1984

26. CN-SGDA-05-50, "Evaluation of the Tube/Tubesheet Contact Pressures and H* for Model 44F Steam Generators at H.B. Robinson Unit 2 and Turkey Point Units 3 & 4," November 2005.

27. Porowski, J.S. and O'Donnell, W.J., "Elastic Design Methods for Perforated Plates," Transactions of the ASME Journal of Engineering for Power, Vol. 100, p. 356, 1978.

28. Slot, T., "Stress Analysis of Thick Perforated Plates," PhD Thesis, Technomic Publishing Co., Westport, CN 1972.

29. Computer Program WECAN/Plus, Users Manual," Second Edition, Revision D, Westinghouse Government Services LLC, Cheswick, PA, May 1, 2000.

30. SM-98-102 (Proprietary), Rev. 2, "Tube/Tubesheet Contact Pressures for Yonggwang 2," Westinghouse Electric Company LLC, Pittsburgh, PA, November 1998.

31. Nelson, L.A., "Reference for Model D Tubesheet Simulate of 1.800 Inch Diameter," electronic mail (Contained in Reference 31), Westinghouse Electric Company LLC, Pittsburgh, PA, August 6,2003.

32. ASME Boiler and Pressure Vessel Code Section III, "Rules for Construction of Nuclear Power Plant Components," 1989 Edition, The American Society of Mechanical Engineers, New York, NY.

33. WCAP-16932-P (Proprietary), Rev. 1, Improved Justification of Partial-Length RPC Inspection of the Tube Joints of Model F Steam Generators of Ameren-UR Callaway Plant," Westinghouse Electric Company LLC, Pittsburgh, PA, May 2003.

34. CN-SGDA-05-56, "Calculation of the Loss Coefficient for Model 44F and 51F Steam Generators", November 2005

35. CN-SGDA-05-54, "H* Ligament Tearing for Models 44F and 51F Steam Generators," November 2005 (Proprietary Report).

36. CN-SGDA-05-57, "H* Zone Boundaries Model 44F and 51F Steam Generators PA-MSC-0199 WOG Program," November 2005.

37. VBA/Excel compatible version of the steam67.dll (dynamic link library) from Winsim.com, Internet Available,

38. ChemicaLogic SteamTab Companion, "Thermodynamic and Transport Properties of Steam, Version 2.0, Based on the IAPWS – 95 Formulation," ChemicaLogic Corporation, Burlington, MA, 2003.

39. ASME Boiler and Pressure Vessel Code Section III, Rules for Construction of Nuclear Power Plant Components," 1989 Edition, The American Society of Mechanical Engineers, New York, NY.

40. Improved Justification of Partial Length RPC Inspection of Tube Joints of Model F Steam Generators of Ameren-UE Callaway Plant", WCAP-15932, Revision 1, May 2003

41. Reference Not Used.

42. LTR-SGDA-06-108, "Data and Analysis Methodology in Support of Axial Ligament Tearing Model," 6/29/06

43. NSD-RMW-91-026, "An Analytical Model for Flow Through an Axial Crack in Series with a Denting Corrosion Medium," M.J. Sredzienski. 02/05/1991

44. H. Tada, The Stress Analysis of Cracks Handbook, 2nd Ed., Del Research Corporation, 226 Woodburne Dr., St. Louis, Missouri, USA. 1985.

45. WCAP-16053-P, Revision 1, "Improved Justification of Partial Length RPC Inspection of Tube Joints of Model F Steam Generators of Seabrook Station," June 2004.

46. NP-6301-D, "Ductile Fracture Handbook," Volume 1, EPRI, 3412 Hillview Avenue, Palo Alto, CA, June 1989.

47. CN-SGDA-03-85, Revision 1, "Input Data for the H*/P* Effort pertaining to both Model D-5 and Model F Steam Generators," 09/30/2003.

48. Steam Generator Degradation Specific Management Flaw Handbook, EPRI, Palo Alto, CA, USA: 2006. 1001191.

49. T.L. Anderson, "Stress Intensity and Crack Growth Opening Area Solutions for Through-Wall Cracks in Cylinders and Spheres," WRC Bulletin 430, Welding Research Council, January, 2003.

50. TH-98-37, Revision 0, "Vogtle/Yonggwang Tubesheet Crevice Leakage," J.H. Lilly, 10/30/1998.

51. R.J. Sanford, Principles of Fracture Mechanics, Prentice Hall, Upper Saddle River, NJ, 2003.

52. CN-SGDA-03-99, Revision 0, "Evaluation of the Tube/Tubesheet Contact Pressures for Wolf Creek, Seabrook, and Vogtle 1 & 2 Model F Steam Generators," A.L. Thurman, 09/26/2003.

53. LTR-SGDA-06-107, "Data and Analysis Methodology in Support of Constrained Axial Cracking Model for DENTFLO," 6/29/06

H. B. ROBINSON STEAM ELECTRIC PLANT, UNIT NO. 2

REQUEST FOR TECHNICAL
SPECIFICATIONS CHANGE REGARDING
<u>STEAM GENERATOR ALTERNATE REPAIR CRITERIA</u>

Westinghouse Affidavit Regarding Proprietary WCAP-16627-P

Westinghouse

U.S. Nuclear Regulatory Commission
Document Control Desk
Washington, DC 20555-0001

Direct tel: (412) 374-4643
Direct fax: (412) 374-4011
e-mail: greshaja@westinghouse.com

Our ref: CAW-06-2184

August 4, 2006

APPLICATION FOR WITHHOLDING PROPRIETARY INFORMATION FROM PUBLIC DISCLOSURE

Subject: WCAP-16627-P, "Steam Generator Alternate Repair Criteria for Tube Portion Within the Tubesheet at H.B. Robinson Unit 2," August 2006 (Proprietary)

The proprietary information for which withholding is being requested in the above-referenced report is further identified in Affidavit CAW-06-2184 signed by the owner of the proprietary information, Westinghouse Electric Company LLC. The affidavit, which accompanies this letter, sets forth the basis on which the information may be withheld from public disclosure by the Commission and addresses with specificity the considerations listed in paragraph (b)(4) of 10 CFR Section 2.390 of the Commission's regulations.

Accordingly, this letter authorizes the utilization of the accompanying affidavit by Progress Energy, Inc.

Correspondence with respect to the proprietary aspects of the application for withholding or the Westinghouse affidavit should reference this letter, CAW-06-2184, and should be addressed to J. A. Gresham, Manager, Regulatory Compliance and Plant Licensing, Westinghouse Electric Company LLC, P.O. Box 355, Pittsburgh, Pennsylvania 15230-0355.

Very truly yours,

J. A. Gresham, Manager
Regulatory Compliance and Plant Licensing

Enclosures

cc: G. Shukla/NRC

bcc: J. A. Gresham (ECE 4-7) 1L
       R. Bastien, 1L (Nivelles, Belgium)
       C. Brinkman, 1L (Westinghouse Electric Co., 12300 Twinbrook Parkway, Suite 330, Rockville, MD 20852)
       RCPL Administrative Aide (ECE 4-7A) 1L, 1A (letter and affidavit only)
       G. W. Whiteman, Waltz Mill
       R. F. Keating, Waltz Mill
       H. O. Lagally Waltz Mill
       N. R. Brown, Waltz Mill
       D. C. Beddingfield, ECE 558B
       J. Gambino, ECE 557D
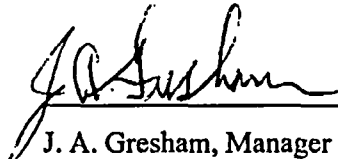   C. D. Cassino, Waltz Mill
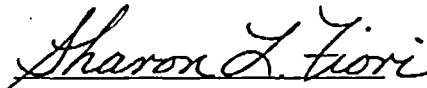
AFFIDAVIT

COMMONWEALTH OF PENNSYLVANIA:

ss

COUNTY OF ALLEGHENY:

Before me, the undersigned authority, personally appeared J. A. Gresham, who, being by me duly sworn according to law, deposes and says that he is authorized to execute this Affidavit on behalf of Westinghouse Electric Company LLC (Westinghouse), and that the averments of fact set forth in this Affidavit are true and correct to the best of his knowledge, information, and belief:
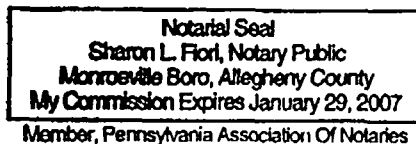
J. A. Gresham, Manager

Regulatory Compliance and Plant Licensing

Sworn to and subscribed before

me this _4th_ day of August, 2006

Notary Public

Notarial Seal
Sharon L. Fiori, Notary Public
Monroeville Boro, Allegheny County
My Commission Expires January 29, 2007
Member, Pennsylvania Association Of Notaries

(1)   I am Manager, Regulatory Compliance and Plant Licensing, Nuclear Services, Westinghouse Electric Company LLC (Westinghouse), and as such, I have been specifically delegated the function of reviewing the proprietary information sought to be withheld from public disclosure in connection with nuclear power plant licensing and rule making proceedings, and am authorized to apply for its withholding on behalf of Westinghouse.

(2)   I am making this Affidavit in conformance with the provisions of 10 CFR Section 2.390 of the Commission's regulations and in conjunction with the Westinghouse "Application for Withholding" accompanying this Affidavit.

(3)   I have personal knowledge of the criteria and procedures utilized by Westinghouse in designating information as a trade secret, privileged or as confidential commercial or financial information.

(4)   Pursuant to the provisions of paragraph (b)(4) of Section 2.390 of the Commission's regulations, the following is furnished for consideration by the Commission in determining whether the information sought to be withheld from public disclosure should be withheld.

(i)   The information sought to be withheld from public disclosure is owned and has been held in confidence by Westinghouse.

(ii)   The information is of a type customarily held in confidence by Westinghouse and not customarily disclosed to the public. Westinghouse has a rational basis for determining the types of information customarily held in confidence by it and, in that connection, utilizes a system to determine when and whether to hold certain types of information in confidence. The application of that system and the substance of that system constitutes Westinghouse policy and provides the rational basis required.

Under that system, information is held in confidence if it falls in one or more of several types, the release of which might result in the loss of an existing or potential competitive advantage, as follows:

(a)   The information reveals the distinguishing aspects of a process (or component, structure, tool, method, etc.) where prevention of its use by any of Westinghouse's competitors without license from Westinghouse constitutes a competitive economic advantage over other companies.

(b)   It consists of supporting data, including test data, relative to a process (or component, structure, tool, method, etc.), the application of which data secures a competitive economic advantage, e.g., by optimization or improved marketability.

(c)   Its use by a competitor would reduce his expenditure of resources or improve his competitive position in the design, manufacture, shipment, installation, assurance of quality, or licensing a similar product.

(d)   It reveals cost or price information, production capacities, budget levels, or commercial strategies of Westinghouse, its customers or suppliers.

(e)   It reveals aspects of past, present, or future Westinghouse or customer funded development plans and programs of potential commercial value to Westinghouse.

(f)   It contains patentable ideas, for which patent protection may be desirable.

There are sound policy reasons behind the Westinghouse system which include the following:

(a)   The use of such information by Westinghouse gives Westinghouse a competitive advantage over its competitors. It is, therefore, withheld from disclosure to protect the Westinghouse competitive position.

(b)   It is information that is marketable in many ways. The extent to which such information is available to competitors diminishes the Westinghouse ability to sell products and services involving the use of the information.

(c)   Use by our competitor would put Westinghouse at a competitive disadvantage by reducing his expenditure of resources at our expense.

(d)   Each component of proprietary information pertinent to a particular competitive advantage is potentially as valuable as the total competitive advantage. If competitors acquire components of proprietary information, any one component may be the key to the entire puzzle, thereby depriving Westinghouse of a competitive advantage.

(e)   Unrestricted disclosure would jeopardize the position of prominence of Westinghouse in the world market, and thereby give a market advantage to the competition of those countries.

(f)   The Westinghouse capacity to invest corporate assets in research and development depends upon the success in obtaining and maintaining a competitive advantage.

(iii)   The information is being transmitted to the Commission in confidence and, under the provisions of 10 CFR Section 2.390; it is to be received in confidence by the Commission.

(iv)   The information sought to be protected is not available in public sources or available information has not been previously employed in the same original manner or method to the best of our knowledge and belief.

(v)   The proprietary information sought to be withheld in this submittal is that which is appropriately marked in WCAP-16627-P, "Steam Generator Alternate Repair Criteria for Tube Portion Within the Tubesheet at H.B. Robinson Unit 2," dated August 2006 (Proprietary). The information is provided in support of a submittal to the Commission, being transmitted by Progress Energy, Inc. for Withholding Proprietary Information from Public Disclosure, to the Document Control Desk. The proprietary information as submitted for use by Westinghouse for H.B. Robinson 2 is expected to be applicable to other licensee submittals in support of implementing a limited inspection of the tube joint with a rotating probe within the tubesheet region of the steam generators.

This information is part of that which will enable Westinghouse to:

(a) Provide documentation of the analyses, methods, and testing for the implementation of an alternate repair criteria for the portion of the tubes within the tubesheet of the H.B. Robinson steam generators.

(b) Provide a primary-to-secondary side leakage evaluation for the H.B. Robinson Unit 2 steam generators during all plant conditions.

(c) Assist the customer to respond to NRC requests for information.

Further this information has substantial commercial value as follows:

(a)   Westinghouse plans to sell the use of similar information to its customers for
        purposes of meeting NRC requirements for licensing documentation.

(b)   Westinghouse can sell support and defense of this information to its customers in
        the licensing process.

(c)   The information requested to be withheld reveals the distinguishing aspects of a
        methodology which was developed by Westinghouse.

Public disclosure of this proprietary information is likely to cause substantial harm to the
competitive position of Westinghouse because it would enhance the ability of competitors
to provide similar licensing support documentation and licensing defense services for
commercial power reactors without commensurate expenses. Also, public disclosure of the
information would enable others to use the information to meet NRC requirements for
licensing documentation without purchasing the right to use the information.

The development of the technology described in part by the information is the result of
applying the results of many years of experience in an intensive Westinghouse effort and
the expenditure of a considerable sum of money.

In order for competitors of Westinghouse to duplicate this information, similar technical
programs would have to be performed and a significant manpower effort, having the
requisite talent and experience, would have to be expended.

Further the deponent sayeth not.

PROPRIETARY INFORMATION NOTICE

Transmitted herewith are proprietary and/or non-proprietary versions of documents furnished to the NRC in connection with requests for generic and/or plant-specific review and approval.

In order to conform to the requirements of 10 CFR 2.390 of the Commission's regulations concerning the protection of proprietary information so submitted to the NRC, the information which is proprietary in the proprietary versions is contained within brackets, and where the proprietary information has been deleted in the non-proprietary versions, only the brackets remain (the information that was contained within the brackets in the proprietary versions having been deleted). The justification for claiming the information so designated as proprietary is indicated in both versions by means of lower case letters (a) through (f) located as a superscript immediately following the brackets enclosing each item of information being identified as proprietary or in the margin opposite such information. These lower case letters refer to the types of information Westinghouse customarily holds in confidence identified in Sections (4)(ii)(a) through (4)(ii)(f) of the affidavit accompanying this transmittal pursuant to 10 CFR 2.390(b)(1).

COPYRIGHT NOTICE

The reports transmitted herewith each bear a Westinghouse copyright notice. The NRC is permitted to make the number of copies of the information contained in these reports which are necessary for its internal use in connection with generic and plant-specific reviews and approvals as well as the issuance, denial, amendment, transfer, renewal, modification, suspension, revocation, or violation of a license, permit, order, or regulation subject to the requirements of 10 CFR 2.390 regarding restrictions on public disclosure to the extent such information has been identified as proprietary by Westinghouse, copyright protection notwithstanding. With respect to the non-proprietary versions of these reports, the NRC is permitted to make the number of copies beyond those necessary for its internal use which are necessary in order to have one copy available for public viewing in the appropriate docket files in the public document room in Washington, DC and in local public document rooms as may be required by NRC regulations if the number of copies submitted is insufficient for this purpose. Copies made by the NRC must include the copyright notice in all instances and the proprietary notice if the original was identified as proprietary.